GEOLOGIC SETTING AND PETROLOGY OF THE PROTEROZOIC OGILVIE MOUNTAIN BRECCIAS OF THE COAL CREEK INLIER, SOUTHERN OGILVIE MOUNTAINS, YUKON TERRITORY

by

ROBERT ANDREW LANE

B.Sc., The University of British Columbia, 1984

A THESIS SUBMITTED IN PARTIAL FULFILLMENT OF
THE REQUIREMENTS FOR THE DEGREE OF
MASTER OF SCIENCE

in
THE FACULTY OF GRADUATE STUDIES
Department of Geological Sciences

We accept this thesis as conforming
to the required standard

THE UNIVERSITY OF BRITISH COLUMBIA
March, 1990

Department of Geography

The University of British Columbia
Vancouver, Canada

Date March 26/90

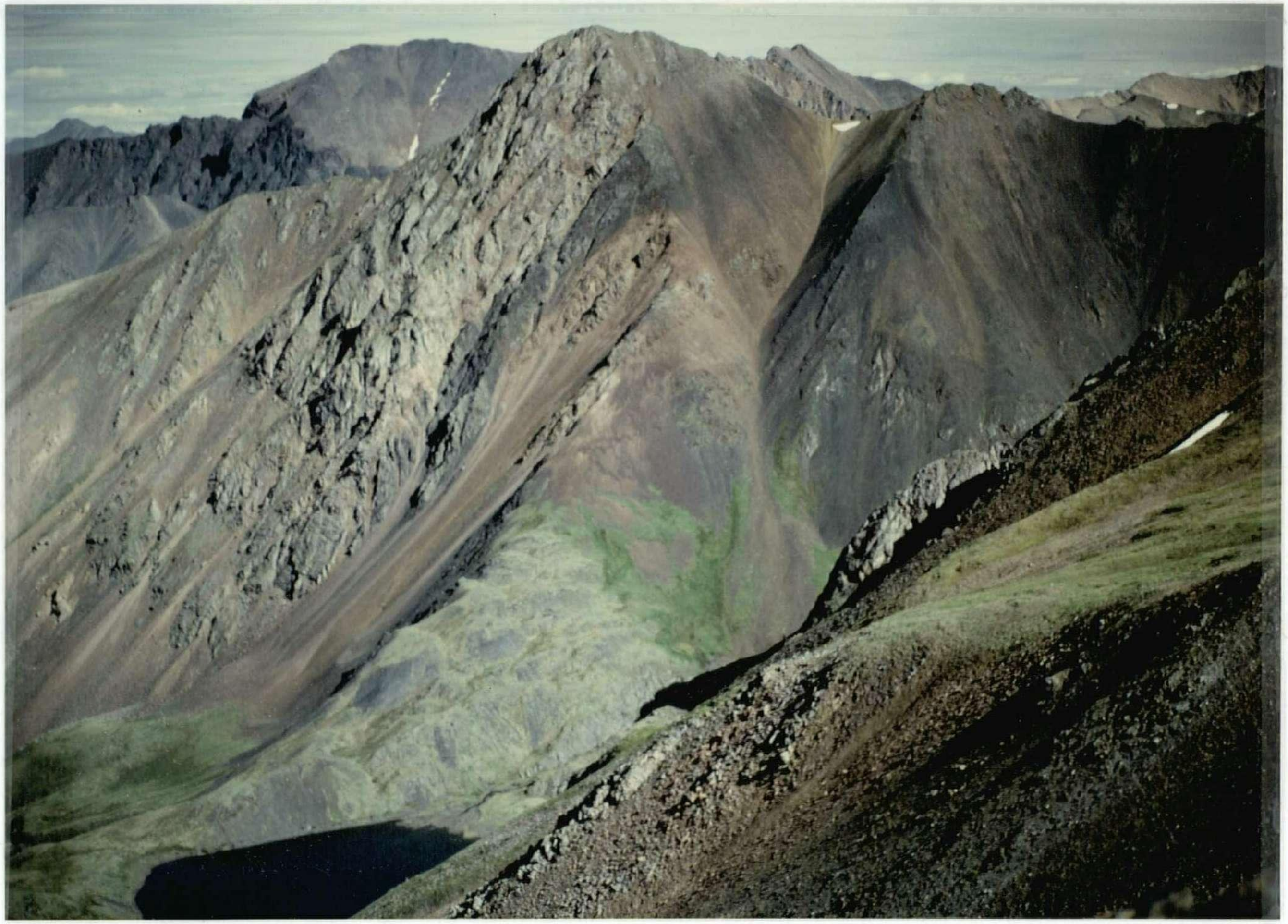

FRONTISPIECE: View looking east at resistant exposure of buff weathering Ogilvie Mountains breccia (OMB), located just east of the *DONUT* breccia locality, in contact with grey weathering Quartet Group.

ABSTRACT

Ogilvie Mountains breccia (OMB) is in Early(?) to Late Proterozoic rocks of the Coal Creek Inlier, southern Ogilvie Mountains, Yukon Territory. Host rocks are the Wernecke Supergroup (Fairchild Lake, Quartet and Gillespie Lake groups) and lower Fifteenmile group. Distribution and cross-cutting relationships of the breccia were delineated by regional mapping. OMB was classified by clast type and matrix composition.

Ogilvie Mountains breccia crops out discontinuously along two east-trending belts called the Northern Breccia Belt (NBB) and the Southern Breccia Belt (SBB). The NBB extends across approximately 40 km of the map area, and the SBB is about 15 km long. Individual bodies of OMB vary from dyke- and sill-like to pod-like. The breccia belts each coincide with a regional structure. The NBB coincides with a north side down reverse fault--an inferred ruptured anticline--called the Monster fault. The SBB coincides with a north side down fault called the Fifteenmile fault. These faults, at least in part, guided ascending breccia.

The age of OMB is constrained by field relationships and galena lead isotope data. It is younger than the Gillespie Lake Group, and is at least as old as the lower Fifteenmile group because it intrudes both of these units. A galena lead isotope model age for the Hart River stratiform massive sulphide deposit that is in Gillespie

Lake Group rocks is 1.45 Ga. Galena from veinlets cutting a dyke that cuts OMB in lower Fifteenmile group rocks is 0.90 Ga in age. Therefore the age of OMB formation is between 1.45 and 0.90 Ga.

Ogilvie Mountains breccia (OMB) has been classified into monolithic (oligomictic) and heterolithic (polymictic) lithologies. These have been further divided by major matrix components--end members are carbonate-rich, hematite-rich and chlorite-rich. Monolithic breccias with carbonate matrices dominate the NBB. Heterolithic breccias are abundant locally in the NBB, but are prevalent in the SBB. Fragments were derived mainly from the Wernecke Supergroup. In the SBB fragments from the lower Fifteenmile group are present. Uncommon mafic igneous fragments were from local dykes. OMB are generally fragment dominated. Recognized fragments are up to several 10s of metres across and grade into matrix sized grains. Hydrothermal alteration has locally overprinted OMB and introduced silica, hematite and sulphide minerals. This mineralization has received limited attention from the mineral exploration industry.

Rare earth element chemistry reflects a lack of mantle or deep-seated igneous process in the formation of OMB. However, this may be only an apparent lack because flooding by a large volume of sedimentary material could obscure a REE pattern indicative of another source.

The genesis of OMB is significantly similar to modern mud diapirs. It is proposed that OMB originated from pressurized, underconsolidated fine grained limey sediments (Fairchild Lake Group). These were trapped below and loaded by turbidites (Quartet Group) and younger units. Tectonics and the initiation of major faults apparently triggered movement of the pressurized fluid-rich medium. The resulting bodies of breccia are sill-like and diapir-like sedimentary intrusions. Fluid-rich phases may have caused hydrofracturing (brittle failure) of the surrounding rocks (especially in the hanging wall). Breccia intrusion would have increased the width of the passage way while encorporating more fragments. Iron- and oxygen-rich hydrothermal fluids apparently were associated with the diapirism. Presumably these fluids are responsible for the high contents of hematite and iron carbonate in fragments, and especially, in the matrix of the breccias. Exhalation of these fluids may have formed the sedimentary iron formations that are spatially associated with the breccias.

TABLE OF CONTENTS

Page

TITLE PAGE i
FRONTISPIECE ii
ABSTRACT iii
TABLE OF CONTENTS vi
LIST OF TABLES viii
LIST OF FIGURES ix
LIST OF PLATES xi
LIST OF MAPS xviii
ACKNOWLEDGEMENTS xix

1.0 INTRODUCTION 1
1.1 GENERAL STATEMENT 1
1.2 LOCATION AND ACCESS 4
1.3 PREVIOUS WORK 5
1.4 SCOPE OF THESIS 6

2.0 REGIONAL GEOLOGY 8
2.1 REGIONAL SETTING AND TECTONIC EVOLUTION 8
2.2 STRATIGRAPHIC SUMMMARY AND REGIONAL CORRELATION 13
2.3 GEOLOGY OF THE COAL CREEK INLIER 16
2.3.1 Introduction 16
2.3.2 Stratified Rocks 19
2.3.2.1 Wernecke Supergroup 19
2.3.2.2 Fifteenmile Assemblage 30
2.3.2.3 Harper Group 31
2.3.2.4 Paleozoic Rocks 32
2.3.3 Cross-Cutting Rocks 34
2.3.3.1 Mafic dykes 34
2.3.3.2 Ogilvie Mountains Breccia 37
2.4 STRUCTURAL GEOLOGY 41
2.4.1 Introduction 41
2.4.2 Structural Data and Interpretation 42

3.0 DETAILED GEOLOGY OF THE OGILVIE MOUNTAINS BRECCIA 51
3.1 GENERAL DESCRIPTION AND CLASSIFICATION 51
3.1.1 Distribution and Form 51
3.1.2 Contact Relations 53
3.1.3 Alteration 55
3.1.4 Textural Varieties 60
3.1.5 Classification 64
3.2 PETROGRAPHY 65
3.2.1 Monolithic Ogilvie Mountains Breccia 67
3.2.1.1 Monolithic Fairchild Lake Group OMB 67
3.2.1.2 Monolithic Quartet Group OMB 80
3.2.1.3 Monolithic Gillespie Lake Group OMB 82

Page

3.2.2 Heterolithic Ogilvie Mountains Breccia ..84
3.2.2.1 Heterolithic carbonate-rich matrix OMB 84
3.2.2.2 Heterolithic hematite-rich matrix OMB 95
3.2.2.3 Heterolithic chlorite-rich matrix OMB 105
3.3 OTHER BRECCIA BODIES IN THE COAL CREEK INLIER ..109

4.0 PETROCHEMISTRY 117
4.1 INTRODUCTION 117
4.2 SAMPLING AND ANALYTICAL METHODS 118
4.3 MAJOR AND MINOR ELEMENT OXIDE AND TRACE ELEMENT CHEMISTRY 119
4.3.1 Major Element Chemistry 119
4.3.2 Minor and Trace Elements 121
4.4 RARE EARTH ELEMENT CHEMISTRY OF THE OGILVIE MOUNTAINS BRECCIA 122
4.4.1 Data Presentation 125
4.4.2 Data Analysis 133
4.4.3 Interpretation of Data 135

5.0 ORIGIN OF THE OGILVIE MOUNTAINS BRECCIA OF THE COAL CREEK INLIER 137
5.1 WORLD EXAMPLES OF BRECCIA SIMILAR TO OGILVIE MOUNTAINS BRECCIA 137
5.2 ORIGINS PROPOSED BY OTHERS FOR OGILVIE MOUNTAINS BRECCIA 139
5.3 GEOLOGICAL CONSTRAINTS ON GENESIS OF THE OGILVIE MOUNTAINS BRECCIA 142
5.4 GENETIC MODEL PROPOSED FOR THE OGILVIE MOUNTAINS BRECCIA 145

REFERENCES 153

APPENDIX A: METALLOGENY OF THE COAL CREEK INLIER 163
APPENDIX B: POTASSIUM-ARGON PREPARATION AND ANALYTICAL PROCEDURES 178
APPENDIX C: SPECIFIC REFERENCES USED TO CONSTRUCT FIGURE 2.1 182
APPENDIX D: SUMMARY OF OGILVIE MOUNTAINS BRECCIA IN THIN SECTION 183
APPENDIX E: GEOCHEMICAL TECHNIQUES AND RESULTS 185
APPENDIX F: THE DEVELOPMENT OF RARE EARTH ELEMENT CHEMISTRY AND ITS GEOLOGICAL APPLICATIONS ...208
APPENDIX G: A REVIEW OF WORLD WIDE PROTEROZOIC BRECCIAS FROM THE LITERATURE 212

LIST OF TABLES

Page

Table 2.1 Stratigraphic units and tectonic events of the Coal Creek Inlier (adapted from Roots (1987) and Thompson and Roots (1982)). 10

TABLE 3.1 A brief description of breccia localities examined in detail (Map 1) in the Coal Creek Inlier, southern Ogilvie Mountains, west-central Yukon Territory. 54

TABLE 3.2. Classification scheme used to characterize Ogilvie Mountains breccia of the Coal Creek Inlier, southern Ogilvie Mountains, west-central Yukon Territory. 65

Table 4.1 Rare earth element abundances in chondritic meteorites (Wakita et al., 1971; in Boynton, 1984), used to normalize the raw sample data (Table E.6), and the North American shales composite (NASC; Haskin et al., 1968). 128

Table 4.2 Chondrite normalized REE data for 17 rocks from the Coal Creek Inlier, southern Ogilvie Mountains, west-central Yukon Territory. The duplicate analyses for four samples, presented in Table E.6, were averaged prior to normalizing. Normalizing standards are in Table 4.1. 129

Table 4.3 Description of anomalous REE patterns in samples of breccias from the Coal Creek Inlier, southern Ogilvie Mountains, west-central Yukon Territory. 136

Table 5.1 A comparison of the characteristics of Proterozoic breccia deposits from the Ogilvie and Wernecke Mountains to Olympic Dam and Mt. Painter, Australia, and to East Arm of Great Slave Lake and Bathurst Inlet. 140

LIST OF FIGURES

Page

Figure 1.1 Map of Yukon Territory and western Northwest Territories showing the distribution of Proterozoic rocks and the position of the field area with respect to major physiographic divisions, major highways and towns. 2

Figure 2.1 Regional stratigraphic correlation chart for Proterozoic and overlying Paleozoic rocks of the Northern Cordillera and the Purcell Mountains, southeastern B.C. 12

Figure 2.2 Geology of the Coal Creek Inlier, southern Ogilvie Mountains, west-central Yukon Territory. 18

Figure 2.3 Stereonet plots of structural data for: (a) domain 1, (b) domain 2, (c) domain 3, and (d) domain 4, Coal Creek Inlier, southern Ogilvie Mountains, west-central Yukon Territory. 46

Figure 2.4 Schematic representation of the development of structures that are related to breccia formation. Top: Folding and faulting during Proterozoic compression. Bottom: Deformation by faults along which emplacement of the Ogilvie Mountains breccia (shown as triangles) was concentrated. FLG = Fairchild Lake Group; QG = Quartet Group; GLG = Gillespie Lake Group; and the stippled pattern is the lower Fifteenmile group. Dashed wiggly line in FLG is a zone of detachment. 50

Figure 3.1 Position of Ogilvie Mountains breccia localities that were investigated and are discussed in the text. 52

Figure 4.1a Ternary plot of La-Th-Sc. Data from sample suite 3 are plotted; symbol codes are listed on the following page. UC = upper crust; TC = bulk continental crust; OC = oceanic crust (from Taylor and McLennan, 1985). Dashed line represents field of 40 shale analyses (from Taylor and McLennan, 1985). 123

Figure 4.1b List of symbols and their corresponding sample numbers and lithologic name for the La-Th-Sc diagram on Figure 4.1a. 124

page

Figure 4.2 Chondrite normalized REE plot of some host sedimentary rocks and monolithic breccias from the Coal Creek Inlier, southern Ogilvie Mountains, west-central Yukon Territory. 130

Figure 4.3 Chondrite normalized REE plot of some monolithic breccias and heterolithic breccias from the Coal Creek Inlier, southern Ogilvie Mountains, west-central Yukon Territory. 131

Figure 4.4 Chondrite normalized REE plot of heterolithic breccias, breccia matrix concentrates, a carbonatite(?) dyke, and a banded iron formation from the Coal Creek Inlier, southern Ogilvie Mountains, west-central Yukon Territory. 132

Figure 5.1 Comparison of (top) seismic reflection section across a mud diapir field from Barbados (after Brown and Westbrook, 1988) and (bottom) proposed model for formation of Ogilvie Mountains breccia (OMB). Note particularly the comparable scales, the imbricate faulting and the associated gentle folding. In the OMB model the zone of high fluid pressure would have been the FLG silty carbonate and muddy sediment. These pressures were induced by deposition of Quartet Group turbidites. The Monster and Fifteenmile faults localized emplacement and formation of OMB. FLG = Fairchild Lake Group; QG = Quartet Group; GLG = Gillespie Lake Group; and 15G = lower Fifteenmile group. SBB = Southern Breccia Belt and NBB = Northern Breccia Belt. 149

LIST OF PLATES

Page

Plate 2.1 Outcrop of ribbed weathering platy dolomitic siltstone and dolomitic limestone of Fairchild Lake Group (unit 1A; located about 1 km north of the *BEEHIVE* locality). Pen for scale. 22

Plate 2.2 Platy weathering, dolomitic siltstone-dolomitic limestone with distinctive chlorite partings of the Fairchild Lake Group (unit 1A; sample BL9-22). 23

Plate 2.3 Pink to buff weathering silty dolostone (unit 1B; sample BL87-3) of Fairchild Lake Group is best exposed in the Northern Breccia Belt area, especially north and west of the *BEEHIVE*. Weather-resistant features, most likely casts of gypsum or anhydrite, occur only locally. 24

Plate 2.4 Interbedded, fine grained quartzite and dolomite (unit 1B; sample BL4-7) of Fairchild Lake Group from the *LALA* locality. 26

Plate 2.5 Prominent exposure of grey-brown weathering turbidite sequence, interbedded fine grained sandstone and argillite, (unit 2) of Quartet Group. This typical exposure is located about 5 km north of the *BEEHIVE*. 27

Plate 2.6 Close up of crossbedding in sandstone of turbidite in Quartet Group (unit 2; sample BL87-61 located about 5 km north of the *BEEHIVE*). 29

Plate 2.7 Columnar stromatolites (*Conophyton*) in Gillespie Lake Group dolostone (unit 3A) located approximately 4.5 km west of *LALA* locality. 33

Plate 2.8 Outcrop of maroon conglomerate of Slats Creek Group (unit 6) from northeastern corner of field area (Map 1). 33

Plate 2.9 Weathered surface and cut polished surface (left, wet) of hematite stained, amygdaloidal diabase dyke (sample BL37-19) from northwest corner of field area (Map 1). 36

page

Plate 2.10 Rugged exposure of pink weathering heterolithic breccia, looking east, east of *DONUT* locality (Map 1). Breccia is discordant with Quartet Group rocks (black in foreground). Contact (dashed line) runs from lower right to middle left edge of photo. 38

Plate 2.11 Photograph of Quartet Group (unit 2) turbidites showing the relationship between bedding and axial planer cleavage. Fine grained sandstone layers define bedding that dips moderately to the south. Argillite shows steeply south dipping axial planer cleavage. This cleavage steeper than bedding relationship indicates that bedding is not overturned. Outcrop is located about 3 km southeast of *LALA* locality (Map 1). 43

Plate 3.1 Fairchild Lake Group dolostone (unit 1B; sample BL5-8 located in the northeast corner of the field area) showing typical hematitic alteration. 58

Plate 3.2 Hydrothermally altered breccia from the *LALA* mineral prospect (Map 1) displaying cockade texture (rhythmically precipitated quartz and hematite: sample BL40-11, upper left), carbonate-quartz-sericite alteration (sample BL40-27, upper right) and intense silicification (sample BL40-29, bottom). 59

Plate 3.3 Hematitic heterolithic chlorite-rich matrix breccia (unit BHcl; sample BL50-2 located in central part of Southern Breccia Belt; Map 2) displaying delicate laminations. Note varying degrees of hematite replacement of fragments (near top and right side) that indicate hematitization was secondary. 61

Plate 3.4 Heterolithic carbonate-rich matrix breccia (unit BHcb; sample BL34-5 located on ridge about 1.5 km southeast of *LALA* locality) showing well-defined layering and textures such as weakly defined graded bedding of possible sedimentary origin. 62

Plate 3.5 Monolithic breccia (unit BM1; sample BL32-5 located on ridge about 1.5 km south of *LALA* locality) showing subrounded pink quartzite fragments in a dense matrix of predominantly chlorite. The chaotic jumbled texture is common to most breccia. 63

page

Plate 3.6 Exposure of heterolithic carbonate-rich matrix breccia (unit BHcb), located about 2 km west of the *BEEHIVE* locality, displaying angular block of bedded dolostone 0.8 m in length (middle right), smaller angular blocks of argillite (lower left), and abundant subrounded fragments of several varieties. 68

Plate 3.7 View of the *SLAB* looking west. The sharp contact between overlying **OMB** (buff) and Quartet Group (grey) is the Monster fault. Truncation of bedding in Quartet Group rocks is visible at right skyline. 71

Plate 3.8 Monolithic Fairchild Lake Group breccia (unit BM1; sample BL26-2 located about 3 km east of *LALA* locality). 72

Plate 3.9 Photomicrograph of monolithic Fairchild Lake Group breccia (unit BM3; thin section BL16-2) showing subrounded quartzite fragments (several are outlined by a dashed line) in a carbonate matrix. Note growth zoned dolomite grain and other dolomite rhombs--evidence of recrystallization. 73

Plate 3.10 Photograph of monolithic Fairchild Lake Group breccia (unit BM1). A large block of semi-plastically deformed Fairchild Lake Group dolomitic siltstone (upper middle) and the centimetre sized angular fragments in a hematized carbonate matrix (lower middle) are displayed. The outcrop is located on the west ridge of the *DONUT*. Pencil for scale. 76

Plate 3.11 Cut and polished surface of crackle breccia variety of monolithic Fairchild Lake Group breccia (unit BM1; sample BL18-10 located approximately 6 km west-southwest of the *BEEHIVE* locality) from margin of breccia body. Contorted bedding and clear rotation of some fragments are conspicuous. 77

Plate 3.12 Cut and polished (wet) surface of channelway breccia variety of monolithic Fairchild Lake Group breccia (unit BM1: sample TW208 located on ridge about 1.75 km southeast of *LALA* locality). Fragments are quartzite in a quartz- and chlorite-rich matrix. 78

Plate 3.13 Crackle breccia variety of monolithic Fairchild Lake Group breccia (unit BM1 located 1.5 km southeast of *LALA* locality) from margin of breccia body. Fairchild Lake Group at this point is mainly dolostone with siltstone interbeds. 79

page

Plate 3.14 Monolithic Quartet Group breccia (unit BM2: sample BL11-7; *LALA* locality, Map 1) from Lala mineral prospect. Some fragments are breccia (angular black argillite fragments in a pale grey matrix); others are black argillite. Chalcopyrite (yellow mineral; centre of photograph) and pyrite are disseminated throughout. ...81

Plate 3.15 **a:** Photograph of cut and polished slab of hematitic monolithic Gillespie Lake Group breccia (unit BM3; sample BL87-7) from the contact between Gillespie Lake Group dolostone and OMB on the northern edge of the *DONUT*; Map 1). **b:** Microphotograph of monolithic Gillespie Lake Group breccia (unit BM3; thin section BL87-7; from *DONUT* locality) showing subangular fine grained dolostone fragments in a coarse grained dolomite cement. Minor hematite partially rims some fragments. 83

Plate 3.16 Location of breccia sill is marked by a dashed line in this view of the "*BEEHIVE*" (Map 1) looking west. Note also the band of breccia (arrow) hosted in Quartet Group sediments on flank of mountain to the left of the *BEEHIVE*. 86

Plate 3.17 Cut and polished surface of hand sample from heterolithic carbonate-rich matrix breccia (unit BHcb; sample BL10-14) from the *BEEHIVE* breccia sill. Note generally angular outline of fragments and chaotic orientation. Fragments are: hematite altered diabase (d), quartzite (q), argillite (a), dolostone (o), and siltstone (s). 87

Plate 3.18 Cut surface of hand sample from heterolithic carbonate-rich matrix breccia (unit BHcb; sample BL87-70) from the exposure of breccia to the south (to the left of *BEEHIVE* in Plate 3.16) of the *BEEHIVE*. Fragments are: diabase (d), quartzite (q), argillite (a), dolostone (o), and siltstone (s). 89

Plate 3.19 Crosscutting nature of dyke-like breccia body (outlined by a dashed line) is shown in this view of the *SLAB* locality (Map 1) looking east. 90

Plate 3.20 *DONUT* locality (Map 1) looking north-east at steeply dipping contact, in foreground, between orange weathering dolostone of Gillespie Lake Group (unit 3A, right and far left) and maroon heterolithic breccia (unit BHcb, centre). 92

page

Plate 3.21 *DONUT* locality (Map 1) looking west from the middle of the complex. Note irregular and interfingering contact between breccia (tan, above) and Quartet Group (grey, below). 93

Plate 3.22 Outcrop of heterolithic carbonate-rich matrix OMB from the northwest part of the *DONUT* locality (Map 1). Angular fragments consist of dolomitic siltstone of uppermost Quartet Group and pale green siltstone, pink silty dolostone and jasper of the Fairchild Lake Group. Mafic dyke fragments are rare. Hammer for scale. 94

Plate 3.23 Photomicrograph of core of mafic igneous fragment from sample BL35-4 (unit BHcb). Broad, green chlorite laths formed after Fe-Mg silicates. Hexagonal opaque crystals are pyrite. 97

Plate 3.24 Prominent craggy exposure of heterolithic breccia on east facing flank of *DONUT* locality (Map 1). *SLAB* locality (Map 1) is in the background across the valley. Note the moderate south dipping contact (shown by a dashed line) between breccia (upper right) and underlying Quartet Group clastic rocks. 98

Plate 3.25 Heterolithic hematite-rich-matrix breccia (unit BHh; sample BL43-7) from western edge of Southern Breccia Belt (Map 1). Note plastically deformed clasts and crudely defined layering. Clasts are: dolostone (o), quartzite (q), mudstone (m), coarse grained sandstone or grit (g), and specular hematite (h). 99

Plate 3.26 Heterolithic hematite-rich matrix breccia (unit BHh; sample BL48-3) from the (*POD* locality; Map 1), Southern Breccia Belt. Fragments are: limestone (l), hematite altered diabase (d), quartzite (q), argillite (a), dolostone (o), siltstone (s), mudstone (m), and jasper (j). Fine grained matrix consists of specularite, hematite stained carbonate and subordinate quartz. 100

Plate 3.27 Hematite-rich matrix breccia (unit BHh; sample BL24-12) from the southeast facing flank of the ridge 2 km southwest of *LALA* mineral showing (Map 1), Northern Breccia Belt. Note delicate laminations of specularite. 102

page

Plate 3.28 Photomicrograph of heterolithic hematite-rich matrix breccia (unit BHh; sample BL43-7) of broken crystals of quartz (q), dolomite (d), and hematite (opaque blades) in fine grained matrix. Note deformation lamellae and ghost zoning, outlined by hematite dust and fluid inclusions, in largest quartz grain. The broken end of this crystal and scalloped edges of other crystals attest to comminution during emplacement of this rock via a gaseous fluid. Fine grained matrix consists of muscovite, carbonate, hematite and quartz. 103

Plate 3.29 Photomicrograph of heterolithic hematite-rich matrix breccia (sample BL24-12) from area north of *LALA* locality. Note growth zones, defined by fluid inclusions, and undulose extinction in large quartz crystal (centre of photograph). Opaques grains are hematite; high birefringent minerals are carbonate. Fine grained matrix is hematite, chlorite and clay. 104

Plate 3.30 Two examples of heterolithic chlorite-rich matrix breccia (unit BHcl; sample BL35-5, above, from ridge top about 1.5 km southeast of the LALA locality, and sample BL3-25, below, about 2.5 km east-southeast of LALA locality). Fragments are: quartzite (q), silty dolostone (o), mudstone (m) and mafic dyke (d). Fine grained matrix is chlorite and subordinate dolomite. 107

Plate 3.31 Photomicrograph of heterolithic chlorite-rich matrix breccia (unit BHcl; thin section of sample BL30-6 from elongate breccia body south of *LALA* mineral showing). Subrounded fragments of quartzite are cemented by chlorite, carbonate and rock flour. 108

Plate 3.32 Photomicrograph of coarse crystalline (metasomatic) microcline and quartz fragment from a heterolithic chlorite-rich-matrix breccia (unit BHcl; thin section of sample BL50-2 from middle of Southern Breccia Belt). Large ragged, poikilitic chlorite lath and subhedral high birefringent dolomite are later forming minerals. A dashed line separates the fine grained matrix (left) from the clast. 110

Plate 3.33 Photomicrograph of heterolithic chlorite-rich-matrix breccia (unit BHcl; sample BL3-25). Subrounded silty dolostone fragment is hosted in a bimodal matrix comprised of larger quartz and carbonate grains set in a fine grained mosaic of chlorite and hematite. 111

page

Plate 3.34 Quartz-hematite breccia from Pettet mineral showing, located about 1 km southwest of the *BEEHIVE* locality. 114

Plate 3.35 Intraformational Gillespie Lake Group breccia (unit 3A) from outcrop on north bank of Beehive creek due north of *LALA* locality. This breccia forms a discontinuous zone near the base of unit 3A. 115

LIST OF MAPS

Map 1 Geology of the Ogilvie Mountains breccia, Coal Creek Inlier, southern Ogilvie Mountains, west-central Yukon Territory .... ~~in pocket~~ in Sp. Coll

Map 2 Sample Locations .... in ~~pocket~~ Sp. Coll

ACKNOWLEDGEMENTS

This study was supported by the Geological Survey of Canada (Cordilleran Division) under the direction of Dr. Bob Thompson and is part of the Dawson project. I am indebted to him for providing the opportunity to work in the Ogilvie Mountains and for introducing the Proterozoic geology of the Coal Creek Inlier. I also thank him for reviews of parts of this thesis. Additional financial support was provided by an Arctic and Alpine Research Grant and by an NSERC Grant to Dr. Colin Godwin at The University of British Columbia.

I also thank my thesis supervisor, Dr. Colin Godwin. His tireless editing of numerous drafts of the manuscript, suggestions for its improvement, and the inconceivably low interest loan of a portable personal computer, is appreciated. Other helpful advisors at the university include: Dr. W.R. Danner, who reviewed the manuscript, Dr. J.K. Russell who reviewed the petrochemistry section and provided useful comments, Dr. R. Chase who edited the rare earth element chemistry section and Dr. A.J. Sinclair who critiqued the lead isotope section.

I would also like to acknowledge a number of people at The University of British Columbia whose assistance and discussions during different parts of this project were beneficial. Janet Gabites provided excellent instruction during galena lead isotope analyses. Dita Runkle provided guidance through potassium analyses and Joe Harakal performed argon analyses. Gord Hodge provided expert drafting and photography skills and made numerous improvements to the figures and maps in this thesis. Yvonne Douma provided countless thin and polished thin sections. Brian Cranston, Ray Rodway and Doug Poulson kept the rock machinery, microscopes and photographic equipment well-tuned. I would also like to thank those people at The University of British Columbia not directly involved with this project, but who were enjoyable companions.

Dr. Charlie Roots, Geological Survey of Canada (Cordilleran Division), spent time discussing many aspects of the thesis. His critical review of parts of the manuscript and timely encouragement helped immeasurably. Dr. Murray Hitzman of Chevron Minerals Ltd. also provided stimulating discussion and REE analyses of the breccias. Craig Boyle, formerly of Newmont Exploration of Canada Ltd. provided 30 element ICP analyses of the breccias. Doug Eaton, of Archer, Cathro and Associates provided valuable discussion of Wernecke-type breccia deposits and made available a private company report on mineral occurrences in the Coal Creek Inlier.

Randy McGillivray, Dennis Burne and Kevin May provided capable and amiable assistance in the field.

Finally I would especially like to thank my wife, Wendy, for her patience and understanding and child rearing throughout the course of this project.

1.0 INTRODUCTION

1.1 GENERAL STATEMENT

Enigmatic breccia complexes are exposed in the Coal Creek Inlier, an oval-shaped, east-trending erosional window located in the southern Ogilvie Mountains, west-central Yukon Territory (Figure 1). The breccia complexes are distributed along two distinct northeast trending belts that are about 40 and 15 km long, respectively. Breccias within these belts are called the Ogilvie Mountains breccia (**OMB**). Proterozoic shelf assemblages of the Middle Proterozoic Wernecke Supergroup and lower Fifteenmile group host these breccias. These strata make up part of a discontinuous east trending belt of Proterozoic sediments that extends eastward from east-central Alaska through the Ogilvie and Wernecke Mountains into the Mackenzie Mountains, Northwest Territories.

The occurrence of Proterozoic rocks in the southern Ogilvie Mountains was originally called "Coal Creek Dome" by Green (1972). "Coal Creek Inlier", as suggested by Roots (1987), is adopted here because the exposure resulted from

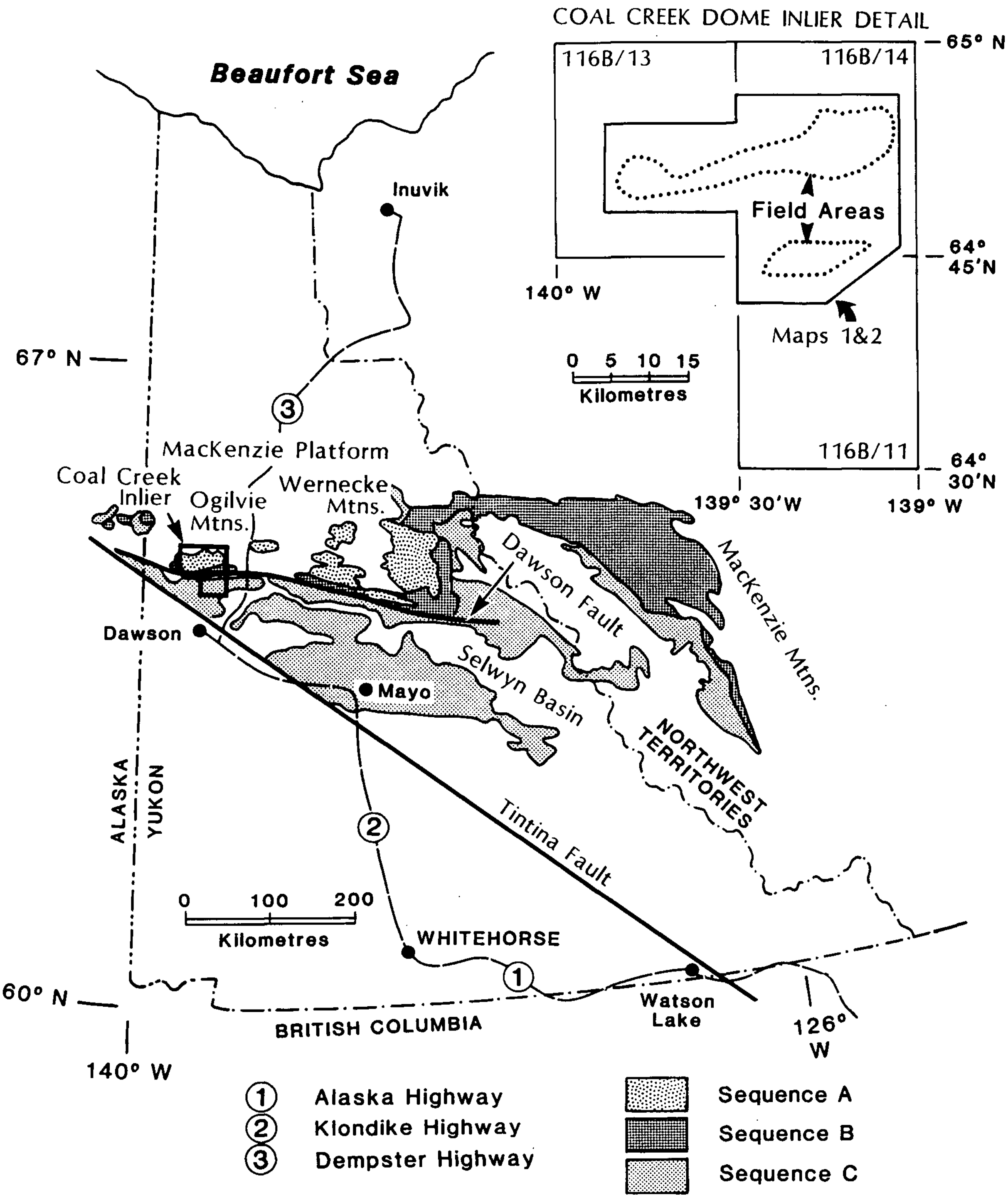

Figure 1.1 Map of Yukon Territory and western Northwest Territories showing the distribution of Proterozoic rocks (adapted from Young et al., 1979) and the position of the field areas (Map 1; inset) with respect to major physiographic divisions (Tempelman-Kluit, 1979), major highways and towns. Sequence A includes the Wernecke Supergroup; sequence B consists Fifteenmile assemblage, Pinguicula Group and Mackenzie Mountains Supergroup; and Sequence C is made up of Windermere Supergroup and its equivalents. The field areas follow the Northern Breccia Belt and the Southern Breccia Belt.

the erosion of structurally shortened and thickened shelf strata (Thompson and Roots, 1982) rather than by upward arching of the basement as the term "dome" suggests.

The Wernecke-type breccias in the Wernecke Mountains, centered about 300 km east of the Coal Creek Inlier, apparently are similar to the Ogilvie Mountains breccia. The Wernecke-type breccias have been investigated and described in detail (Archer et al., 1986; Archer and Schmidt, 1978; Bell, 1978, 1982, 1986; Bell and Delaney, 1977; Delaney, 1981; Eaton, pers. comm., 1988; Laznicka and Edwards, 1979; Thompson and Roots, 1982). They have been compared favorably by Bell (1986, 1987) with breccias that host the world class Olympic Dam gold-copper-uranium deposit north of Adelaide, Australia. Proterozoic breccia complexes of a similar nature also have been reported from the vicinity of the East Arm of Great Slave Lake (Reinhardt, 1972) and from the Bathurst Inlet area (Cecile and Campbell, 1977), Northwest Territories.

The Wernecke Mountain breccias occur in structurally complex zones and have been moderately to intensely altered (Eaton, pers. comm., 1988). They potentially host economic deposits of gold, copper, cobalt and uranium. In contrast, the Coal Creek Inlier is relatively uncomplicated by structure and little altered. Exploration, albeit limited to date, has yet to discover any mineralization of major interest.

Some breccia textures in the Ogilvie Mountains breccia resemble glacio-marine breccias of the much younger Rapitan Group (Yeo, 1981) in the Mackenzie and Wernecke Mountains to the east. The breccia complexes locally are hematite-rich. In some respects they are similar to Algoma-type banded iron formations.

Only minor base and precious metal occurrences are hosted by the breccia complexes of the Wernecke and Ogilvie Mountains. If the correlations to Olympic Dam, Australia are real and justified they may have economic potential. Consequently, investigation of these relatively undeformed and unaltered breccias in the Ogilvie Mountains was designed to elucidate types, sources and mechanism of formation of these major bodies of breccia.

1.2 LOCATION AND ACCESS

The Coal Creek Inlier is within the Omineca Belt (Wheeler and Gabrielse, 1972; Monger et al., 1972) and is about 55 km north of Tintina Trench. It is in the western portion of the southern Ogilvie Mountains, Yukon Territory. The study area (Figure 1.1) consists of two east-trending belts that cover 170 square kilometres. The northerly band, centered near 64°51′ north and 139°30′ west, is greater than

40 km in length, and of variable width up to 3 km. The southerly band, centered approximately at 64°45′ north and 139°19′ west, is 15 km long and about 10 m to 100 m wide. The area covers portions of the following 1:50,000 scale map sheets (NTS): 116B/11, 116B/12 and 116B/14.

This region of the Yukon Territory, along with parts of Alaska, were unglaciated during the Pleistocene (Bostock, 1946, 1961). The topography thus formed by subaerial erosion. The unglaciated area is composed of long ridges of low to moderate relief. In the field area altitudes range from about 975 m to over 1950 m. Outcrop, discontinuous but abundant on the crests and flanks of steep-sided ridges, is uncommon in valley bottoms.

Access to the area was by helicopter stationed, for the first half of the summer of 1986, from a base camp located just off the Dempster highway 60 km north-east of the field area. During the second half of the summer of 1986 and during July of 1987 the helicopter was based in Dawson City, about 85 km south of the field area.

1.3 PREVIOUS WORK

The earliest recorded observations in the area studied were made in 1887 by Ogilvie (1913) who led a party that surveyed the Alaska - Yukon Territory border. In 1910-1912

Cairnes (1914) mapped a 12 km wide transect along this boundary and formulated a preliminary geologic framework. Reconnaissance mapping in the region was first formally carried out by the Geological Survey of Canada in the summer of 1961 by Green and Roddick who completed three contiguous 1:250,000 scale map sheets: Dawson, Larson Creek and Nash Creek (Green and Roddick, 1962; Green, 1972). All subsequent geologists have used their work as a base.

More recently, 1:50,000 scale mapping of the Dawson map area by R.I. Thompson and C.R. Roots of the Geological Survey of Canada has been done. This work is scheduled to come out as an Open File Report in 1990. Ph.D. theses by Mercier (1985), Roots (1987), and Mustard (1990) provide more detailed descriptions of some specific areas.

1.4 SCOPE OF THESIS

This thesis investigates the nature of enigmatic breccia complexes that crop out in Coal Creek Inlier of the Ogilvie Mountains, Yukon Territory. It includes: (i) a map showing their lithologic distribution, (ii) description and interpretation of their contacts, (iii) their mineralogical and chemical characteristics, and (iv) analysis of genetic models that describe modes of breccia formation.

Assessments and brief descriptions of mineral occurrences are appended in sections describing galena lead isotopes in the Coal Creek Inlier. Two regions of known breccia crop out across portions of three 1:50,000 map sheets (NTS: 116B/11, 116B/12 and 116/14). These were investigated during the field season of 1986. Additional mapping was carried out during July of 1987.

2.0 REGIONAL GEOLOGY

2.1 REGIONAL SETTING AND TECTONIC EVOLUTION

The northern extension of the Rocky Mountain Fold and Thrust Belt forms a broad arc across central Yukon Territory. It contains a thick sedimentary sequence that was deposited on the passive continental margin of North America between Middle Proterozoic and Permian time (Price, 1964).

During the Middle to Late Proterozoic shallow water carbonate strata dominated the region. These are the oldest known rocks of the northern Cordillera (Gabrielse, 1967). They are preserved in several structural inliers surrounded by Paleozoic Selwyn Basin and Mackenzie Platform strata (Figure 1.1).

In the southern part of the southern Ogilvie Mountains, Selwyn Basin strata is underlain by the Hyland Group (Gordy, in press) of the Windermere Supergroup. Unnamed Cambro-Ordovician volcanics and Ordovician to Devonian Road River Formation overlie the clastic and carbonate rocks of the

Hyland Group.

The northern part of the southern Ogilvie Mountains consist of two laterally extensive, dominantly platform carbonate assemblages: (1) Wernecke Supergroup, that is overlain unconformably by the (2) Fifteenmile assemblage. These are dominated by shallow water carbonate rocks of Middle to Late Proterozoic age. Stratigraphy and tectonic events in the history of the Coal Creek Inlier is outlined in Table 2.1.

Thick mid-Proterozoic sections of shallow water, fine grained clastic and carbonate rocks that constitute the Wernecke Supergroup (Delaney, 1981) accumulated on the stable continental platform of western North America. During subsequent compression, a pervasive cleavage developed in Wernecke Supergroup rocks (Mercier, 1987). In the Ogilvie and Wernecke Mountains, argillaceous rocks were weakly regionally metamorphosed to lower greenshist grade (Gabrielse, 1967). Uplift and erosion of these units produced a marked erosional unconformity at the base of the Fifteenmile assemblage (informal designation; Thompson, pers. comm., 1988). This period of tectonic instability, termed the Fifteenmile Orogeny by Mercer (1989) for the southern Ogilvie Mountains region, occurred at about the same time as the Racklan Orogeny (Gabrielse, 1967; Eisbacher, 1978) or Racklan Tectonic Event (Thompson, pers.

Table 2.1 Stratigraphic units and tectonic events of the Coal Creek Inlier (adapted from Roots (1987) and Thompson and Roots (1982)).

AGE	UNIT	MAP UNIT[1]		LITHOLOGY
Early Ordovician to Devonian	**Road River Group** (165 m)	8	R	-black shale, chert
	Transgressive			
Early Cambrian to Devonian	**"CDb" formation** (>250 m)	7	C	-thick bedded, pale grey dolostone
	Conformable; local angular unconformity			
Early Cambrian	**Slats Creek group** (>30 m)	6	S	-white dolostone, purple mudstone, conglomerate pale green argillite and sandstone
Contact relations unknown-possible lateral equivalent to Harper Group(?)				
Late Proterozoic	**HARPER GROUP**			
	Upper Harper group (0-450 m)		Hu	-conglomerate, shale siltstone, mudstone
	Mount Harper Volcanic complex (0-1500 m)		Hv	-basalt flows, breccia, and minor rhyolite
	Lower Harper group (0-1100 m)		Hl	-conglomerate, pebbly sandstone, mudstone
	Hayhook Tectonic Event: disconformable; local angular unconformity; locally gradational			
Middle to Late Proterozoic	**FIFTEENMILE ASSEMBLAGE**			
	Upper Fifteenmile group (2500 m)	5	Fu	-grey finely laminated dolomitic limestone and dolostone
	Lower Fifteenmile group (1500 m)	4C	Fl	-upper member: mudstone, stromatolitic limestone, and quartz sandstone
		4B		middle member: dolostone
	Fifteenmile (Racklan) Tectonic Event: angular unconformity; locally conformable			
Early to Middle Proterozoic	**WERNECKE SUPERGROUP**			
	GILLESPIE LAKE GROUP (3500 m)	3B	Wg	-upper member: buff-weathering dolostone
		3A		lower member: orange weathering dolostone
	Conformable: local angular unconformity			
	QUARTET GROUP (>2250 m)	2	Wq	-grey sandstone, mudstone and black argillite
	Angular unconformity; locally disconformable			
	FAIRCHILD LAKE GROUP (>650 m)	1B	Wf	-pink-weathering silty dolostone, mudstone and quartzite
		1A		greenish-grey to purple dolomitic siltstone and dolomitic limestone

1 Numbers are units used on Map 1 (in pocket); letters designate units used on Figure 2.1

comm., 1988). In the Ogilvie Mountains, folding accompanied by cleavage development, was followed by syndepositional growth faulting associated with the initiation of Fifteenmile assemblage deposition (Thompson, pers. comm., 1987). The Upper Fifteenmile group consists of several kilometers of shallow water shelf dolostone that overlies Lower Fifteenmile group rocks conformably.

The Hayhook Orogeny (Eisbacher, 1981; Devlin, 1988), a 750 Ma extensional event followed the deposition of the upper Fifteenmile group. In the southern Ogilvie Mountains it is called the Harper rift event (Roots, 1987). This event resulted in uplift, erosion and the subsequent development of a significant angular unconformity at the base of the overlying rift assemblage that called the Harper group (Roots, 1987, 1982). In localities south of Coal Creek Inlier, the Dawson Fault (Figure 2.1) physically separates upper Fifteenmile group from the Harper group.

Clastic sediments and volcanics of the Harper group are the youngest Proterozoic rocks preserved in the Coal Creek Inlier. Basal clastics of the Harper group were deposited into a northwest-trending half graben.

Cambrian (and older?) coarse clastics and carbonates of the Slats Creek group and overlying Cambrian to Devonian carbonates of the "CDb" formation (Norris and Hopkins, 1977)

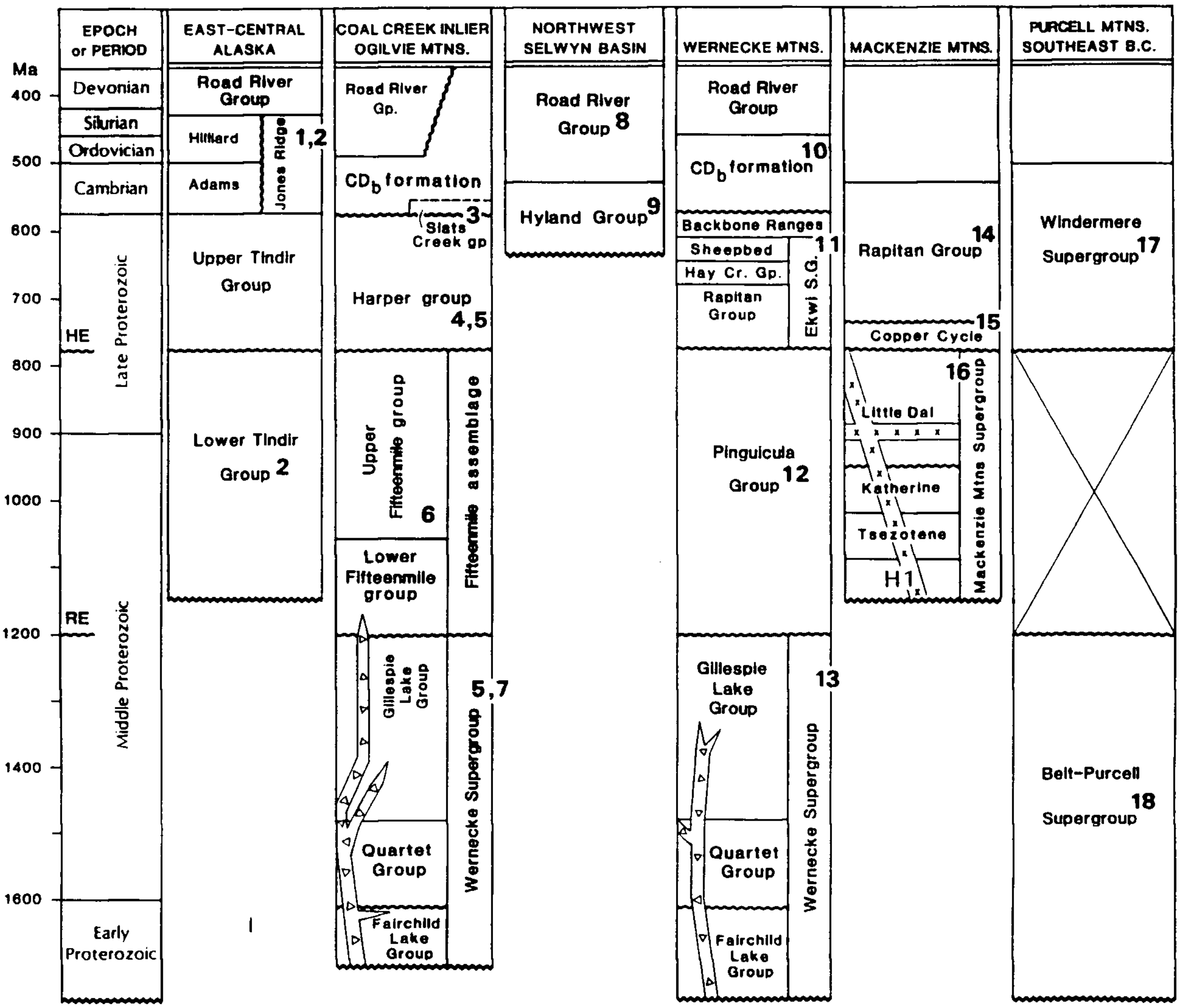

Figure 2.1 Regional stratigraphic correlation chart for Proterozoic and overlying Paleozoic rocks of the Northern Cordillera and the Purcell Mountains, south eastern B.C. Adapted from Eisbacher (1981) and Roots (1987). Additional references (superscripted numbers) are in Appendix C. HE = Hayhook tectonic event; RE = Rackla tectonic event. Dykes and sills in the Mackenzie Mountains were emplaced at approximately 770 Ma (Armstrong et al., 1982).

rest unconformably on Proterozoic strata and represent a return to stable shelf conditions. The entire Proterozoic and Phanerozoic successions were folded and faulted during Mesozoic thrusting (Thompson and Roots, 1982) when a complex volcanic - plutonic arc was welded to the continental margin (Templeman-Kluit, 1979). Remnants of this arc comprise the Yukon Tanana Terrane (Templeman-Kluit, 1979) that lies to the southwest of Selwyn basin and Tintina Fault.

2.2 STRATIGRAPHIC SUMMARY AND REGIONAL CORRELATION

The following summary is detailed in the correlation chart of Figure 2.1. Figure 1.1 shows the distribution of Proterozoic rocks across the northern Cordillera.

Similarity between Wernecke Supergroup rocks and the Belt-Purcell Supergroup of southeastern British Columbia, southwestern Alberta and adjoining Montana was noted by Cairnes (1914) and Mertie (1937); stratigraphic correlation is supported by more recent studies (Gabrielse, 1967; Young, 1978; Young et al., 1979) of Wernecke and Belt-Purcell Supergroup strata with the lower part of the Tindir Group in east-central Alaska. Subsequently, Young (1982) has argued that the Lower Tindir Group is Late Proterozoic and is a stratigraphic equivalent of the Pinguicula Group in the Wernecke Mountains and therefore not correlative with the Wernecke Supergroup. The correlation of Pinguicula Group

(Eisbacher, 1981) with the Mackenzie Mountains Supergroup in the Mackenzie Mountains is tentatively supported by Young et al. (1979) and Eisbacher (1981), but disputed by Aitken (1986). Conclusive evidence is, however, lacking (Gabrielse and Campbell, in press).

Fifteenmile assemblage rests unconformably on Wernecke Supergroup strata. It occurs at the same stratigraphic horizon as does the Pinguicula Group in the Wernecke Mountains, and appears to be a time stratigraphic equivalent (Thompson, pers. comm., 1987).

The age of the Belt - Purcell Supergroup in the southern Cordillera is known only approximately. Preserved basal sections that overlie crystalline basement have a minimum age of more than 1.6 Ga (Burwash, Baagsgaard and Peterman, 1962). In the northwestern part of the Canadian Shield a period of widespread mafic igneous activity occurred at about 1.2 Ga (Stockwell et al., 1970). This signifies an important period of crustal extension (Young et al., 1979).

Proterozoic stratigraphy of the northern Cordillera were grouped into three major divisions, Sequence A, Sequence B and Sequence C, separated from each other by a regional unconformity (Young et al., 1979). Sequence A includes the Wernecke Supergroup; Sequence B consists of the

Pinguicula Group and Mackenzie Mountains Supergroup; and Sequence C is made up of the Ekwi Supergroup and Rapitan Group (or Windermere Supergroup; Eisbacher, 1981). Belt - Purcell rocks are therefore equivalent to sequences A and B. Sequence C correlates with the Windermere Supergroup of southeastern British Columbia.

The oldest rocks exposed in the core of the Coal Creek Inlier are correlated with the Middle Proterozoic Wernecke Supergroup of the Wernecke Mountains. They are correlative on the basis of equivalent stratigraphic position, lithologic similarity (Delaney, 1981, 1985) and the presence of breccias. This stratigraphy forms an essentially continuous outcrop belt from the Southern Ogilvie Mountains into the Wernecke Mountains.

The age of the Mackenzie Mountains Supergroup has been established between 1.2 Ga and 770 Ma (Rb-Sr radiometric ages from Barager in Wanless and Loveridge, 1972, and Armstrong et al., 1981; Gabrielse and Campbell, 1990). In turn, radiometric age data and lithologic similarities support the correlation of the Mackenzie Mountains Supergroup with upper Belt-Purcell Supergroup (Missoula Group) rocks (Young et al., 1978).

Harper group basal clastics in the southern Ogilvie Mountains represent the onset of Windermere sedimentation.

Possible correlatives of the Harper rift assemblage are the upper Tindir Group (Young, 1982), the Coates Lake Group (Jefferson and Parrish, 1989), and part of the Rapitan Group (Eisbacher, 1981). Uppermost Harper group may be correlative with the Hyland Group of the Mackenzie Mountains.

"CDb" formation unconformably overlies all older rocks of the Coal Creek Inlier. It was deposited on a shallow platform that extended from east-central Alaska (Jones Ridge Formation) eastward into the Mackenzie Mountains, Northwest Territories. South of the platform was the Selwyn Basin, that contained an offshelf succession consisting of the Road River Formation. This is a prevalent unit forming recessive outcrops that can be traced from the Ogilvie Mountains eastward to the Mackenzie Mountains. "CDb" formation is in part a time-stratigraphic equivalent to the Road River Formation.

2.3 GEOLOGY OF COAL CREEK INLIER

2.3.1 Introduction

Coal Creek Inlier contains three Proterozoic successions (Figures 2.1 and 2.2, and Table 2.1). From oldest to youngest they are: Wernecke Supergroup, Fifteenmile assemblage (informal) and Harper group (informal). Each succession generally forms east trending belts across the inlier. The geology of the Coal Creek Inlier is shown in Figure 2.2.

Wernecke Supergroup consists of three parts. In ascending order they are: Fairchild Lake Group, Quartet Group, and Gillespie Lake Group (Table 2.1). The Fifteenmile assemblage is divided into the lower Fifteenmile group and the upper Fifteenmile group. The Harper group consists of three divisions. In ascending order, they are: Lower Harper group, Mount Harper volcanic complex, and Upper Harper group.

Ogilvie Mountains breccia (**OMB**) contact all divisions of the Wernecke Supergroup and the lower Fifteenmile group. They are spatially associated with mafic dykes, and crop out along two east trending belts called: (i) the Northern Breccia Belt, and (ii) the Southern Breccia Belt. The Northern Breccia Belt coincides with a steeply south dipping reverse fault called the Monster fault. The Southern Breccia Belt coincides with a steeply dipping north-side-down fault called the Fifteenmile fault. This fault juxtaposes lower Fifteenmile group against Quartet Group.

Early Paleozoic Slats Creek group (Fritz, 1980), "CDb" formation, and its off-shelf correlative the Road River Formation unconformably overlie the Proterozoic rocks.

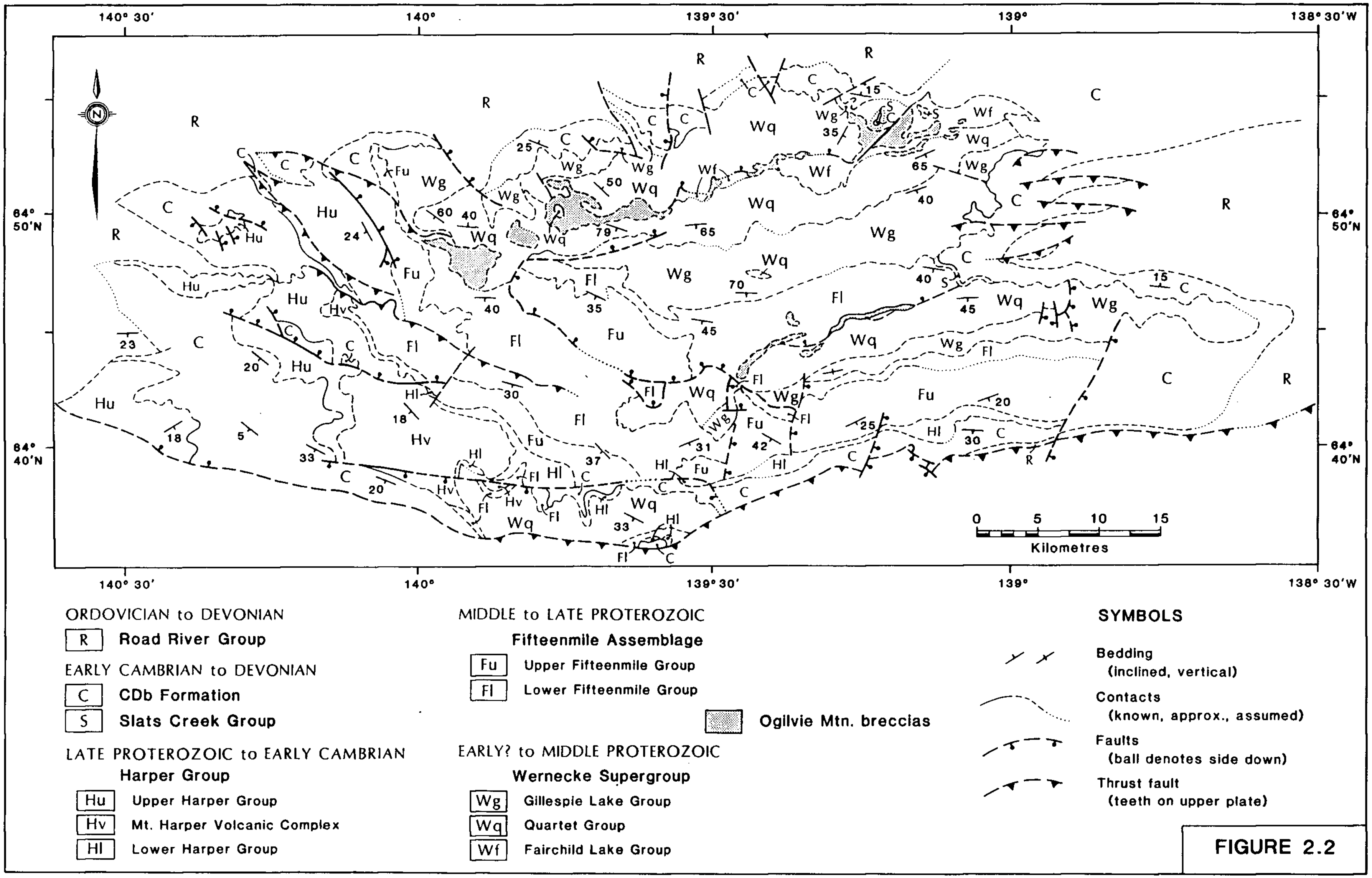

Figure 2.2 Geology of the Coal Creek Inlier, southern Ogilvie Mountains, west-central Yukon Territory. (See Map 1, in pocket, for detail.)

Their contact outlines the Coal Creek Inlier.

2.3.2 Stratified Rocks

2.3.2.1 Wernecke Supergroup

Wernecke Supergroup in the Coal Creek Inlier, southern Ogilvie Mountains consists of three mappable units. The base of the Wernecke Supergroup is not exposed; therefore total thickness is not known. The oldest unit is tentatively correlated with the Fairchild Lake Group (Delaney, 1981) because it underlies Quartet Group rocks and its lithologies (silty dolomite, dolomitic siltstone, mudstone and quartzite) are similar to those reported in the type area--the Wernecke Mountains. In the Wernecke Mountains, Delaney (1985) reported a minimum thickness of 4 km for the Fairchild Lake Group.

Quartet Group in the Coal Creek Inlier, consists of interbedded fine grained grey sandstone to siltstone and black argillite. It forms a distinctively dull succession approximately 3.5 km thick (thickness estimate from cross-sections; see Map 1). Quartet Group in the Wernecke Mountains type area is at least 5 km thick (Delaney, 1981) and represents a turbidite succession (Delaney, 1981; 1985).

Gillespie Lake Group in the Coal Creek Inlier is a thick succession of predominantly and characteristically orange weathering dolostone. It is about 3 km thick (thickness estimate from cross-sections; see Map 1). The thickness of the Gillespie Lake Group in the Wernecke Mountains is greater than 4 km (Delaney, 1981, 1985).

Aggregate thickness for the Quartet and Gillespie Lake groups, estimated from cross-sections of the field area (Map 1), is about 6.5 km. This is considerably less than the more than 9 km reported by Delaney (1981; 1985) for the combined thickness of Quartet Group (5 km). This may represent a regional westward thinning of the succession. Alternatively, structural thickening of Quartet and Gillespie Lake group strata in the Wernecke Mountains may have occurred. Recent mapping in the southern Wernecke Mountains identified thrust faults that repeated sections of Gillespie Lake Group stratigraphy (Mustard et al., 1990).

Fairchild Lake Group (Units 1a and 1b; Map 1)

The base of the Fairchild Lake Group is not exposed and not all of the informal subdivisions reported by Delaney (1981) for the Wernecke Mountains were observed. Fairchild Lake Group rocks crop out discontinuously along the south side or "hanging wall" of the Monster fault and are intimately associated with **OMB** (Map 1).

Unit 1a is the lowest exposed unit of the Wernecke Supergroup in the Coal Creek Inlier. It consists of dolomitic siltstone and dolomitic limestone that has a distinctively ribbed weathering profile (Plate 2.1). Stromatolites occur locally in an otherwise platy greenish-grey to purple succession. The platy limestone changes composition toward the east-southeast to a pale grey dolomitic limestone with distinctive chlorite partings (Plate 2.2). Unit 1a generally dips to the north, is locally disrupted, has stratigraphic continuity along strike, and is 500 to 600 m thick.

Unit 1b overlies Unit 1a with apparent conformity. It is a resistant pink to grey silty dolomite (Plate 2.3) and dolomitic mudstone that weathers pink to brown. Occasional beds of grey to purple quartzite and jaspillite are also present. Unit 1b is laminated and medium to thick bedded. At the east end of the inlier, measured sections thicker than 100 metres consist of interbedded quartzite and dolostone (Plate 2.4), quartzite and mudstone, and mudstone and dolostone.

The ratio of quartzite to dolomite in the interbedded quartzite and dolostone unit varies rapidly (5 to 15 m) along and across strike. As the quartzite content increases, bedding disappears and the succession becomes massive. This field evidence suggests that the quartzite

Plate 2.1 Outcrop of ribbed weathering platy dolomitic siltstone and dolomitic limestone of Fairchild Lake Group (unit 1A; located about 1 km north of the *BEEHIVE* locality). Pen for scale.

Plate 2.2 Platy weathering, dolomitic siltstone-dolomitic limestone with distinctive chlorite partings of the Fairchild Lake Group (unit 1A; sample BL9-22).

Plate 2.3 Pink to buff weathering silty dolostone (unit 1B; sample BL87-3) of Fairchild Lake Group is best exposed in the Northern Breccia Belt area, especially north and west of the *BEEHIVE*. Weather-resistant features, most likely casts of gypsum or anhydrite, occur only locally.

may be recrystallized jasperoid--originally fine grained silica replacement of limestone--petrographic examination of samples was inconclusive.

Stratigraphic continuity of Unit 1b is disrupted by irregular zones of brecciation. Bedding within individual segments is internally coherent but differs from nearby ones. This suggests the unit has been broken apart by the brecciation process. Widespread development of Ogilvie Mountains breccia coincides with this stratigraphic level.

Quartet Group (Unit 2; Map 1)

Quartet Group, Unit 2, overlies the Fairchild Lake Group with angular discordance in some areas and disconformably in others. It is a monotonous, grey to brown weathering, medium to thick bedded fine grained succession of sandstone, siltstone, dolomitic siltstone and mudstone. Locally there are rare quartzite pebble and cobble conglomerate. In the Wernecke Mountains Delaney (1981) divided the succession into two units of informal designation. For the purpose of this study the Quartet Group was not subdivided.

The dominant Quartet Group lithology in the study area is interbedded fine grained sandstone, siltstone and phyllitic argillite (Plate 2.5). Beds of laminated and

Plate 2.4 Interbedded, fine grained quartzite and dolomite (unit 1B; sample BL4-7) of Fairchild Lake Group from the *LALA* locality.

Plate 2.5 Prominant exposure of grey-brown weathering turbidite sequence, interbedded fine grained sandstone and argillite, (unit 2) of Quartet Group. This typical exposure is located about 5 km north of the *BEEHIVE*.

cross-laminated sandstone and siltstone, typically 30 cm thick, are separated by thin layers of argillite that mark the top of each composite turbidite (cf. Bouma, 1962). Locally, within this succession, there are thick pale red and green clay-rich beds. Sedimentary features displayed by this unit include: slump textures, interference ripple marks and trough cross-beds (Plate 2.6). At the top of the succession are thin interbeds of rusty weathering dolomite; their presence marks the transition into the overlying platform carbonate sequence.

Gillespie Lake Group (Unit 3a and 3b; Map 1)

Gillespie Lake Group conformably overlies the Quartet Group in the northern part of the Coal Creek Inlier. The contact is transitional (Thompson and Roots, 1982). In the type area in the Wernecke Mountains, Delaney (1981) noted a transitional relationship between Gillespie Lake and Quartet group rocks. He subdivided the Gillespie Lake Group into seven informal units. In the Coal Creek Inlier two units are recognized: a basal unit (Unit 3a) consisting of orange weathering grey dolostone, and an upper unit (Unit 3b) made of grey to buff weathering silty dolostone. The basal unit is laminated suggesting it accumulated in quiet water below a wave base, possibly as algal accumulations. Intraformational breccia (see section 3.3 for detailed description) occurs locally near the base of Unit 3a. The

Plate 2.6 Close up of crossbedding in sandstone of turbidite in Quartet Group (unit 2; sample BL87-61 located about 5 km north of the *BEEHIVE*).

upper unit contains colonies of the distinctive, columnar stromatolite *Conophyton* (cf. Donaldson, 1976) that are 5 to 10 cm in diameter (Plate 2.7) and 10 to 15 cm tall.

2.3.2.2 Fifteenmile Assemblage

Fifteenmile assemblage unconformably overlies Wernecke Supergroup rocks. It consists of two lithologically distinct successions: the lower Fifteenmile group, composed primarily of clastic rocks with minor dolostone; and the upper Fifteenmile group, consisting of shallow water platformal dolostone.

Lower Fifteenmile Group (Units 4a, 4b and 4c; Map 1)

Lower Fifteenmile group is informally divided into lower, middle, and upper members. Contacts between members are gradational. The middle and upper members are, in part, time-stratigraphic equivalents (Roots, pers. comm., 1988). Only the lower member (Unit 4a) crops out in the field area. It is composed dominantly of black, fine grained to medium grained sandstone, shale and black limestone; grey dolostone olistoliths, tens of metres in diameter, are an outstanding feature. Unit 4a forms an east-trending outcrop belt across the centre of the Coal Creek Inlier (Map 1). It is approximately 1,500 m thick. The middle (Unit 4b) and upper (Unit 4c) members, crop out south of the field area. Unit

4b consists mainly of thick bedded dolostone and dolostone breccia. Unit 4c consists of mudstone, stromatolitic limestone and quartz sandstone.

Upper Fifteenmile Group (Unit 5; Map 1)

Upper Fifteenmile group consists of massive, pale grey, craggy weathering sugary dolostone (Thompson and Roots, 1982). There are occasional thin bands of black shale. In localities north and east of Mount Harper, conglomerate dominated by clasts of upper Fifteenmile group grades upward into basal conglomerates of Harper group (Roots, 1988; Mustard, 1990). However, the contact between the upper Fifteenmile and Harper groups is generally an angular unconformity. upper Fifteenmile group rocks do not crop out in the field area.

2.3.2.3 Harper Group (Units Hl, Hv and Hu; Figure 2.2)

Harper group consists of clastic and volcanic rocks that disconformably overly upper Fifteenmile group and rest unconformably on older units in the southern part of the inlier. It is divided into two clastic successions called the lower Harper group and upper Harper group. A middle member is called the Mount Harper volcanic complex (MHVC). MHVC is a bimodal suite of primarily tholeiitic basalt and minor felsic flows and dykes (Roots, 1987). It is conformable with the underlying Lower Harper group. The Upper Harper group has been interpreted by Mustard (pers. comm., 1987) to have formed in a half-graben during deposition of the Windermere Supergroup (Roots, 1987). Harper group rocks crop out south and east of the map area (see Figure 2.2).

2.3.2.4 Paleozoic Rocks

Slats Creek Group (Unit 6; Map 1)

Slats Creek group (Unit 6) is exposed beneath dolostone of the CDb formation in the north and east parts of the Coal Creek Inlier. It is made up of pale grey weathering dolostone, purple graded conglomerates and pale green argillaceous sandstone (Plate 2.8). The stratigraphic position is similar to that of the uppermost Harper Group (along the west and south sides of the inlier), but Slats Creek group is Lower Cambrian (Fritz, 1980).

CDb Formation (Unit 7; Map 1)

CDb formation (informal designation; Norris, 1982) consists of thick bedded, pale grey weathering crystalline dolostone of Cambrian to Devonian age. It disconformably overlies Slats Creek group and older Proterozoic units around the margin of the Coal Creek Inlier. It also forms

Plate 2.7 Columnar stromatolites *(Conophyton)* in Gillespie Lake Group dolostone (unit 3A) located approximately 4.5 km west of *LALA* locality.

Plate 2.8 Outcrop of maroon conglomerate of Slats Creek Group (unit 6) from northeastern corner of field area (Map 1).

isolated caps on ridge tops in the eastern part of the field area (Map 1).

Road River Group (Unit 8; Map 1)

Road River Group (Unit 8) consists of Ordovician to Devonian black, carbonaceous shale that forms a transgressive sequence over the CDb formation (Unit 7). It outcrops in the northern part of Map 1.

2.3.3 Cross-cutting Rocks

2.3.3.1 Mafic Dykes

Numerous dark green to brown weathering dykes of diabase intrude Wernecke Supergroup strata. The dykes generally are 1 to 5 m thick and are dominantly east or north-northwest trending and steeply dipping. Where they cut Quartet Group rocks, dykes are difficult to observe because of their similar weathering characteristics in outcrop. However, the dykes are distinct where they cut Fairchild Lake Group and Gillespie Lake Group dolostones. This is because of their contrasting dark green weathering and greater resistance to erosion. Alteration zones adjacent to the dykes are thin and weakly developed in the Fairchild Lake Group; in the Gillespie Lake Group they are bounded by bleached zones up to several metres wide. The dykes are moderately to strongly fractured and locally brecciated. Fractures and joints are commonly lined with specular hematite, and less commonly, chalcopyrite.

Cross-cutting stratigraphic relationships indicate that the dykes are of several ages. Angular fragments of diabase occur locally in the **OMB** bodies. Dykes of similar diabase also cut **OMB** complexes in several localities and form extensions along the trend of linear **OMB** bodies. The ages of these dykes are constrained by several factors: (i) they crosscut and therefore postdate the Wernecke Supergroup; (ii) they were intruded both before and after breccia formation; (iii) they predate (are truncated by) deposition of upper Fifteenmile group, "CDb" Formation and Slats Creek Group; and (iv) a galena lead isotope date (Appendix A: Showing-10190) of associated mineralization--presumably about the same age as the dykes--is about 0.9 Ga.

These mafic intrusions are medium to dark green and are generally medium to coarse grained. In several localities, where dykes come into contact with breccia bodies, the dykes are amygdaloidal or possibly variolitic (Figure 2.9). This texture may have resulted from: (i) the exsolution of volatiles by the magma close to the surface (Best, 1982) or (ii) the presence of immiscible liquid blebs. Specimens from the vicinity of **OMB** bodies display irregular pink to red stained blotches indicative of hematization associated

Plate 2.9 Weathered surface and cut polished surface (left, wet) of hematite stained, amygdaloidal diabase dyke (sample BL37-19) from northwest corner of field area (Map 1).

with the breccias. Thin sections of 12 different dykes were studied to determine if they were suitable for dating. All but two were pervasively chlorite-altered; amphiboles in the two remaining samples were actinolite (a mineral unsuitable for K-Ar dating) intergrown with appreciable amounts of chlorite. Plagioclase is almost entirely sausuritized. Euhedral iron oxides, likely magnetite, replace intergrown actinolite and chlorite.

2.3.3.2 Ogilvie Mountains breccia (**OMB**)

Ogilvie Mountains breccia (**OMB**; Plate 2.10) is a significant and mappable unit. It crops out discontinuously along two east-trending belts. The Northern Breccia Belt in the northern part of the field area (Map 1) is about 35 kilometers in length. The Southern Breccia Belt in the southern part of the field area is approximately 15 km long. The linear distribution of these fragmental rocks (Map 1) coincides with prominent structures informally called the Monster fault (northern part of Map 1), and the Fifteenmile fault (southern part of Map 1). Breccias both intrude and cross-cut the faults. The breccias therefore are probably contemporaneous, but may be younger than these structures.

Ogilvie Mountains breccia are exposed at different stratigraphic levels: (i) within Fairchild Lake Group strata, (ii) at the Fairchild Lake Group - Quartet Group

Plate 2.10 Rugged exposure of pink weathering heterolithic breccia, looking east, east of *DONUT* locality (Map 1). Breccia is discordant with Quartet Group rocks (black in foreground). Contact (dashed line) runs from lower right to middle left edge of photo.

contact, (iii) at the top of the Quartet Group near the Quartet Group - Gillespie Lake Group contact, and (iv) within lower Fifteenmile group rocks.

Breccia bodies are both conformable and discordant with respect to bedding. Conformable breccia bodies or breccia sills generally display gradational contacts. Discordant breccias commonly exhibit steeply dipping to vertical contacts, are locally associated with diabase dykes, and are sometimes parallel to and may occupy faults.

The breccia bodies vary in composition. This is reflected in the overall colour of outcrops. Cream-coloured breccias have a carbonate-rich matrix with commonly subrounded clasts of green argillite and pink silty dolostone. Hematite-rich matrix breccias are commonly red to maroon. Breccias with a chlorite-rich matrix are dark green and commonly include mafic intrusive rock fragments. In places this breccia is mottled from abundant pink clasts. Breccia fragments are generally from Fairchild Lake Group. They are common sub-angular and probably have not travelled far from their source. However, breccia fragments derived from Quartet Group, Gillespie Lake Group and Lower Fifteenmile group are common locally. A lack of significant fragment rotation, in some instances, indicates that the breccias are represented commonly by crackled country rock.

The absolute age of the Ogilvie Mountains breccia is not known. However, stratigraphic relationships constrain **OMB** to be post-Wernecke Supergroup and approximately syn-lower Fifteenmile group in age (see galena lead data below). The upper extent of the breccias is in rocks affected by the Racklan Tectonic Event (lower Fifteenmile group).

A study of Proterozoic hosted, galena-bearing mineral occurrences that occur in and around the Coal Creek Inlier (Appendix A) have helped to constrain the age of **OMB** emplacement. The Hart River stratiform volcanigenic massive sulphide deposit, located about 150 km east of the Coal Creek Inlier, is hosted in Gillespie Lake Group argillites. It has a galena lead isotope model age of about 1.35 to 1.45 Ga. This date therefore is the age of part of the Gillespie Lake Group. In addition, the Tart Pb-Zn breccia prospect is hosted in Gillespie Lake Group dolostone. It has a galena lead model age of about 1.3 Ga; although it might be epigenetic, a syngenetic origin would give an upper age estimate for the Gillespie Lake Group. Therefore the **OMB** that cross-cuts Gillespie Lake Group is younger than 1.45 Ga--it might be younger than 1.3 Ga.

Galena from calcite veinlets in an altered mafic dyke that cross-cuts **OMB** that is hosted in Lower Fifteenmile group was dated at about 0.9 Ga. This provides a minimum age for the emplacement of **OMB**.

Two samples of chlorite-rich matrix were dated using K-Ar whole rock methods (Appendix B). However, no relevant age information was produced. Both are apparently reset ages: one age (360 Ma) happens to coincide with a Devono-Mississippian metallogenic event that was extensive throughout the northern Canadian Cordillera.

Chapter 3 describes the Ogilvie Mountains breccia in detail. A classification scheme, that divides the breccias into **monolithic** and **heterolithic** varieties, is introduced. Petrochemistry of Ogilvie Mountains breccia follows in Chapter 4.

2.4 STRUCTURAL GEOLOGY

2.4.1 Introduction

The thick Proterozoic succession of Wernecke Supergroup carbonate and clastic sedimentary rocks in the Coal Creek Inlier have been deformed, probably at several times. The Northern Breccia Belt divides Map 1 into northern and southern parts with opposing bedding attitudes. North of the Northern Breccia Belt beds dip moderately north; south of the Northern Breccia Belt beds dip moderately south. However, attitudes adjacent to the Northern Breccia Belt are irregular in strike and dip. Thus, the elongate eastern trend of the Northern Breccia Belt coincides with both: (i) an axial trace of an anticline, and (ii) a zone of faulting that resulted in regional rotation of large segments north and south of the Northern Breccia Belt. Steep, east-trending axial plane foliation supports the presence of an anticline, but imbricate reverse faulting along the Northern Breccia Belt (see cross-sections, Map 1) indicate that faulting has an important role also.

Several hundred structural attitudes of bedding and foliation were measured over Map 1 (in pocket). Additional structural field data were obtained from R.I. Thompson and C.R. Roots of the Geological Survey of Canada, and E. Mercer (1986) who performed regional mapping both in and around the field area. These data have been compiled into four pi diagrams. Each represent a structural domain (Figures 2.3a through 2.3b). One domain is north of NBB; three domains are south of the NBB. Interpretation of the structural data follows.

2.4.2 Structural Data and Interpretation

Sedimentary bedding is generally well defined in most major units in the Coal Creek Inlier. However, Fairchild Lake Group rocks show abrupt changes between areas of consistent bedding. These sudden changes suggest that large blocks of strata have been rotated with respect to each

Plate 2.11 Photograph of Quartet Group (unit 2) turbidites showing the relationship between bedding and axial planer cleavage. Fine grained sandstone layers define bedding that dips moderately to the south. Argillite shows steeply south dipping axial planer cleavage. This cleavage steeper than bedding relationship indicates that bedding is not overturned. Outcrop is located about 3 km southeast of *LALA* locality (Map 1).

other. Therefore the internal structural complexity exhibited by the Fairchild Lake Group, and its close spatial association with Ogilvie Mountains breccia, prohibit its interpretation using structural (bedding and foliation) data. The unconformity that occurs between Fairchild Lake Group and overlying Quartet Group may reflect an event that predates the Racklan Tectonic Event. Above this unconformity, Quartet, Gillespie Lake and lower Fifteenmile group rocks have been separated into the following four structural domains:

(1) Domain 1 (Figure 2.3a) covers Quartet and Gillespie Lake Group rocks that occur north of the Northern Breccia Belt.

(2) Domain 2 (Figure 2.3b) is occupied by Quartet and Gillespie Lake Group rocks that lie south of Northern Breccia Belt and north of lower Fifteenmile group strata.

(3) Domain 3 (Figure 2.3c) occurs south of domain 2 and covers lower Fifteenmile group rocks north of the Southern Breccia Belt.

(4) Domain 4 (Figure 2.3d) includes the area of Quartet and Gillespie Lake Group rocks that occur south of the Southern Breccia Belt.

Figure 2.3a, the pi diagram of domain 1, includes 72 bedding and 15 foliation measurements. Poles to bedding and foliation define east-striking bedding and foliation with dips to both the north and south. Younging directions in

Quartet Group are consistently tops up. Criteria observed in Quartet Group rocks include: ripple marks with trough cross-beds, graded fine grained sandstone laminae, load casts and rare slump features. Stratigraphic tops in Gillespie Lake Group rocks are also consistently tops up. Criteria include morphology of columnar stromatolites, which locally are abundant in some sections of dolostone.

Plotted data for structural domains 2, 3 and 4 are shown in Figures 2.3b, 2.3c and 2.3d, respectively. In domain 2 (Figure 2.3b) poles to bedding define shallowly eastern plunging, generally east-striking folds. Axial planes dip steeply south-southeast. The _pi_ diagram for domain 3 (Figure 2.3c) reflects open east trending folds of almost no plunge. The data from domain 4 (Figure 2.3d) shows an east trend to bedding and foliation. Most beds dip southerly but foliation is highly variable suggesting either more than one period of deformation or chaotic disruption to the dips in a north-south sense.

Minor folds in Quartet Group interbedded argillite-sandstone sequences, locally accompanied by well-developed axial planar cleavage, define a regional scale east-trending anticline. The axial trace of the fold is located along the occurrence of breccia and Fairchild Lake Group rocks that are east-trending and crop out between the opposing dips in structural domains 1 and 2. Domain 1 comprises north

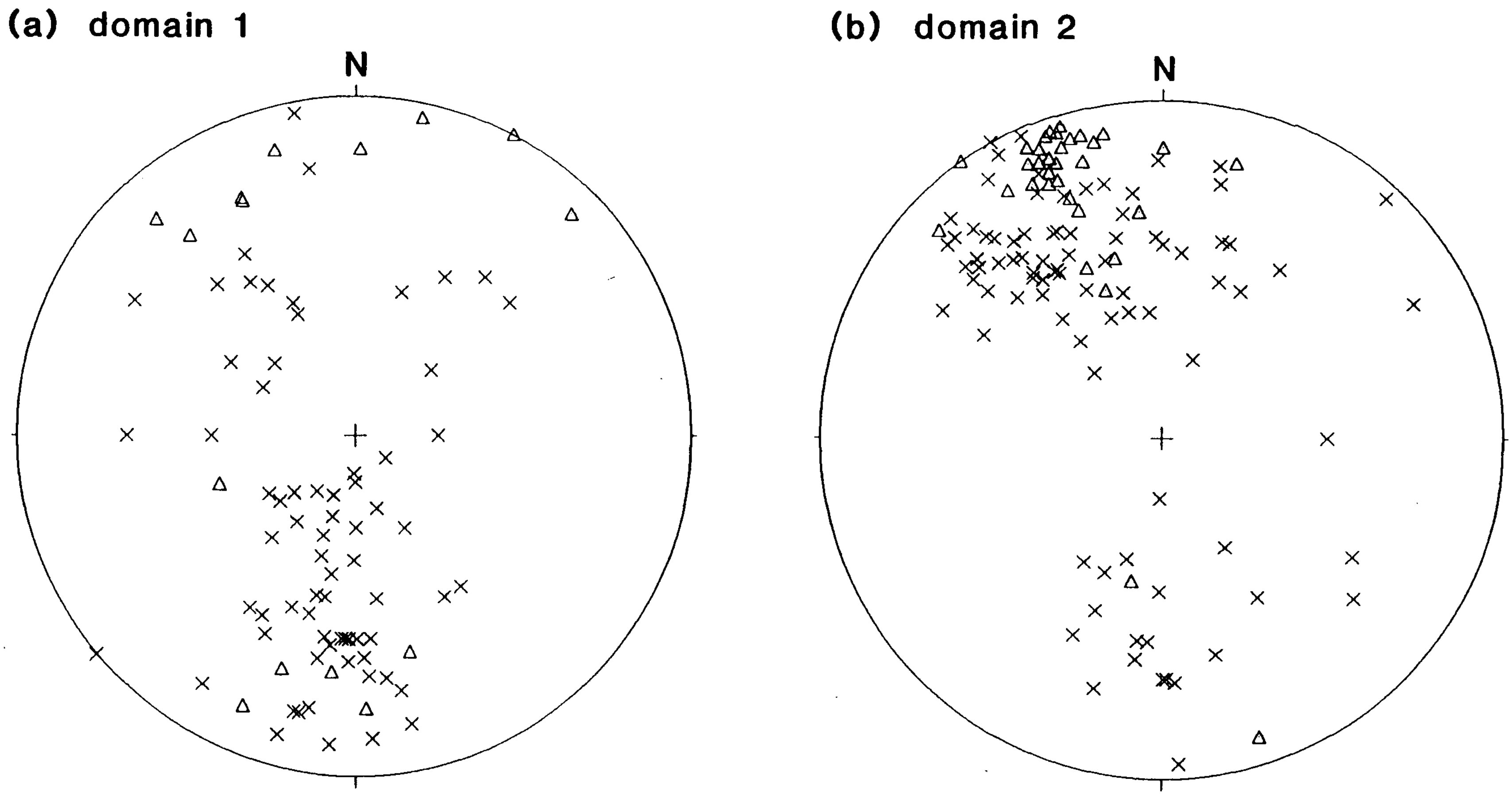

Figure 2.3 Stereonet plots of structural data for (a) domain 1, (b) domain 2, (c) domain 3, and (d) domain 4. The stereonets depict poles to bedding (x's) and poles to axial planar cleavage (triangles).

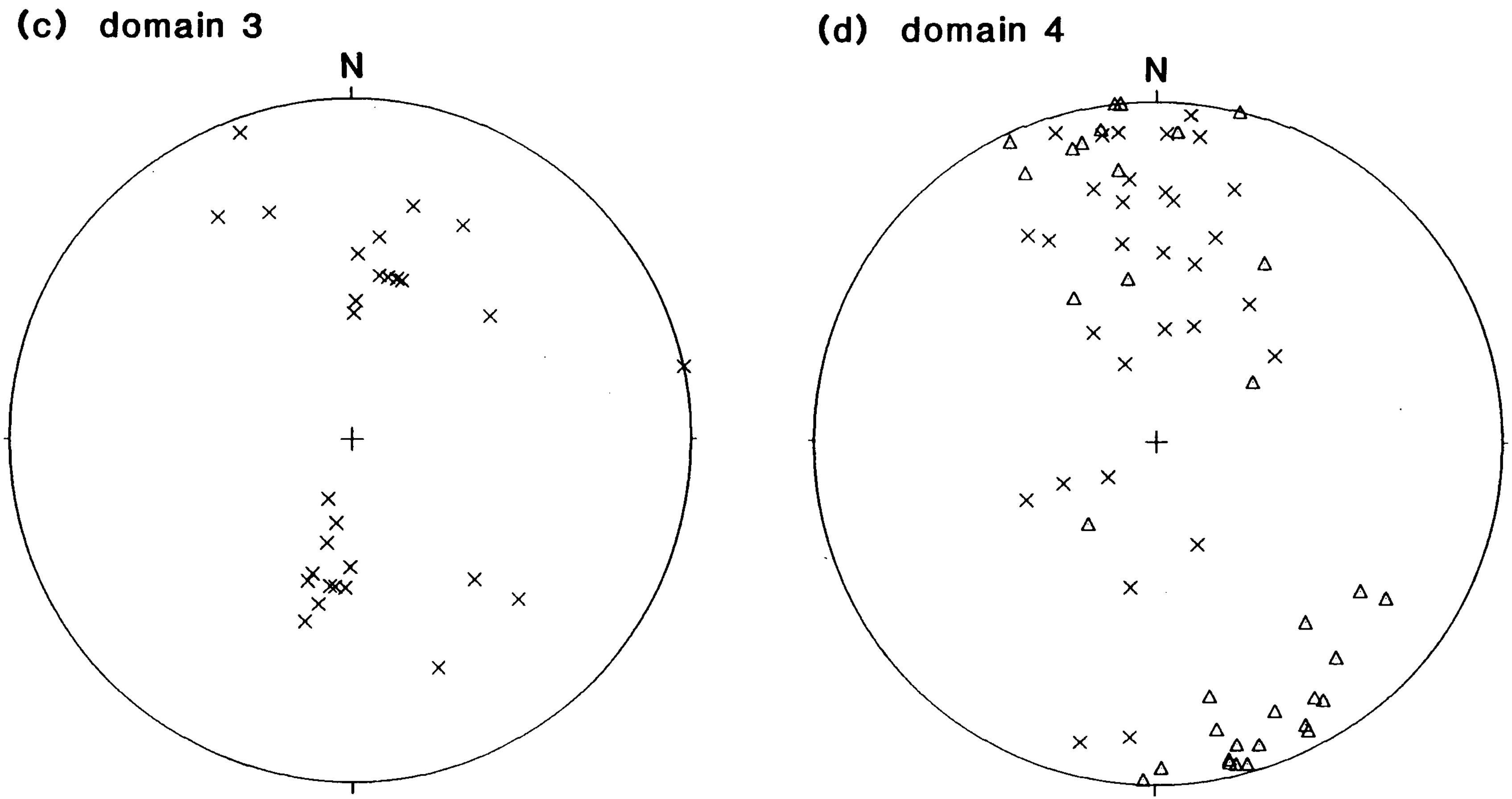

Figure 2.3 Continued

dipping strata--the north limb of the anticline which defines an east-trending fold axis that lies to the south. Domain 2 comprises south-dipping strata, or the south limb of the anticline that define an east-trending fold axis that lies to the north. The variation in dips of axial planar cleavage could be related to local rotation of blocks within each structural domain.

Lower Fifteenmile group rocks above the unconformity show similar structural poles to the Gillespie Lake Group below, indicating that no deformation occurred between deposition of these two units. Therefore domains 2 and 3 are grouped together.

The Southern Breccia Belt is situated along a major regional structure (the Fifteenmile fault) and divides domains 3 and 4. Domain 4 is similar to domain 2 and represents the south limb of the regional anticline. This indicates that the fault between them is planar. There is little evidence to suggest the style of faulting, but the north side is down based on stratigraphic relationships.

Structural data, above, strongly supports the presence of an anticlinal axis that is approximately coincident with the elongate east-west trend of the Northern Breccia Belt. However, constraints imposed by mapping (Map 1) define faults (the Fifteenmile and Monster faults) that are more readily understood in cross-section. (Note in Map 1 the fault-breccia association, and the repeated occurrence of Fairchild Lake Group along the trend of the Northern Breccia Belt and Monster fault.) The Fifteenmile and Monster faults likely had their soles in Fairchild Lake Group--a unit that, at the time of faulting, was probably only semi-consolidated (see sections 5.3 and 5.4). Faults acted as guides for much of the breccia emplacement.

The relationships of folding and faulting are shown diagramatically in Figure 2.4. This model indicates that the unit most likely responsible for decollement is the Fairchild Lake Group. Major imbricate, reverse faults mark the North and South Breccia Belts and imply a compressional regime at the time of breccia emplacement.

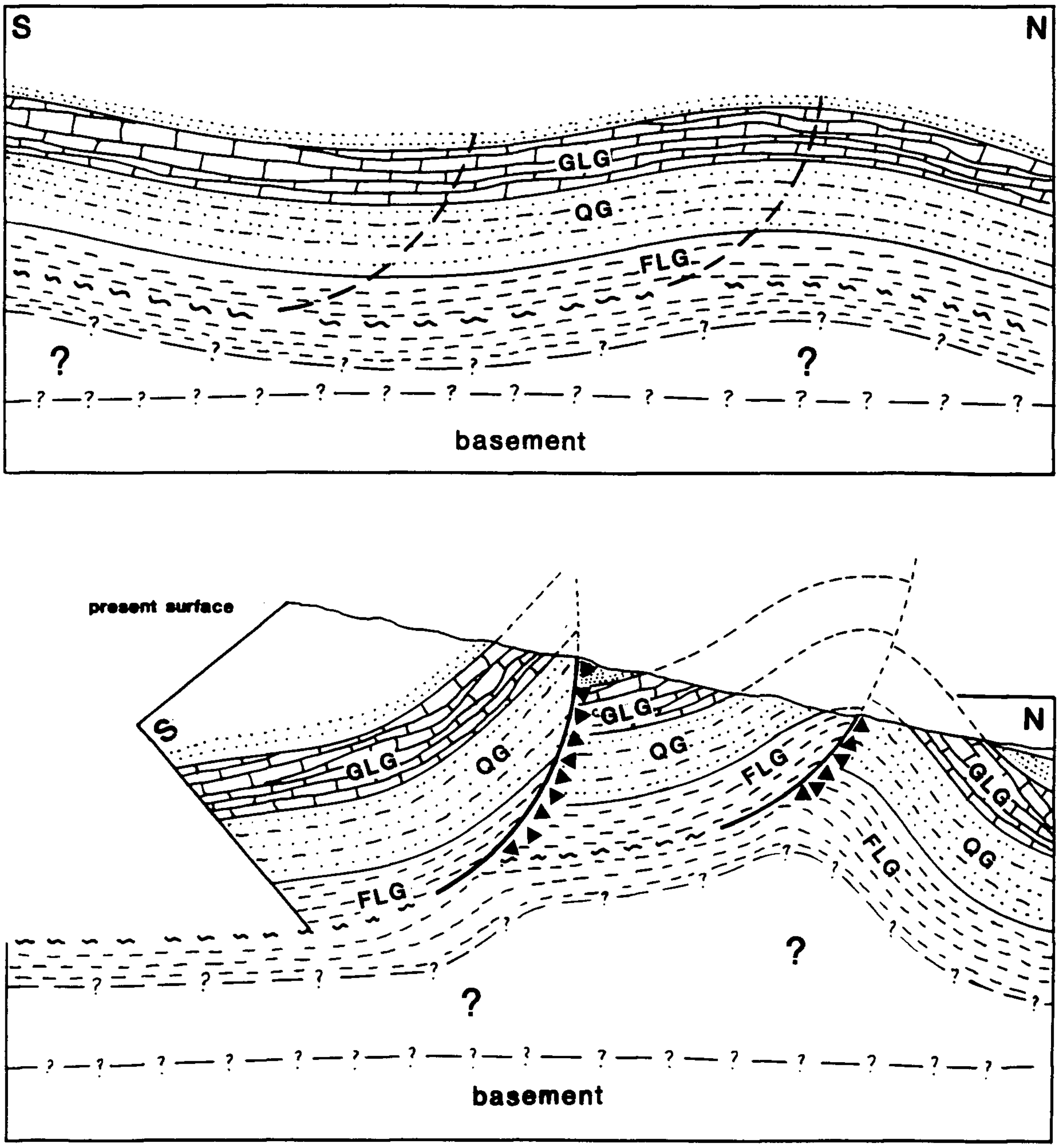

Figure 2.4 Schematic representation of the development of structures that are related to breccia formation. Top: Folding and faulting during Proterozoic compression. Bottom: Deformation by faults along which emplacement of the Ogilvie Mountain breccia (shown as triangles) was concentrated. FLG = Fairchild Lake Group; QG = Quartet Group; GLG = Gillespie Lake Group; and the stipled pattern is the lower Fifteenmile group. Dashed wiggley line in FLG is a zone of detachment.

3.0 DETAILED GEOLOGY OF THE OGILVIE MOUNTAINS BRECCIA

3.1 GENERAL DESCRIPTION AND CLASSIFICATION

3.1.1 Distribution and Form

The Ogilvie Mountains breccia (**OMB**) of the Coal Creek Inlier are exposed discontinuously along two east trending belts, namely the Northern Breccia Belt and the Southern Breccia Belt (see section 2.3.2.2). The total area of exposed breccia on Map 1 (in pocket) is 55 square km: it accounts for about seven percent of the total map area of 770 square km. Individual **OMB** bodies vary in size and extent. Widths of breccia at surface range from 2 m to more than 1,000 m.

The Northern Breccia Belt (NBB) coincides with the **Monster fault** (Map 1), a steep to moderately south dipping reverse fault. In the eastern half of the NBB the breccias occur within the only large exposure of Fairchild Lake Group in the southern Ogilvie Mountains. In the western part of this belt they occur near and along the contacts between Quartet Group and Gillespie Lake Group rocks, or wholly

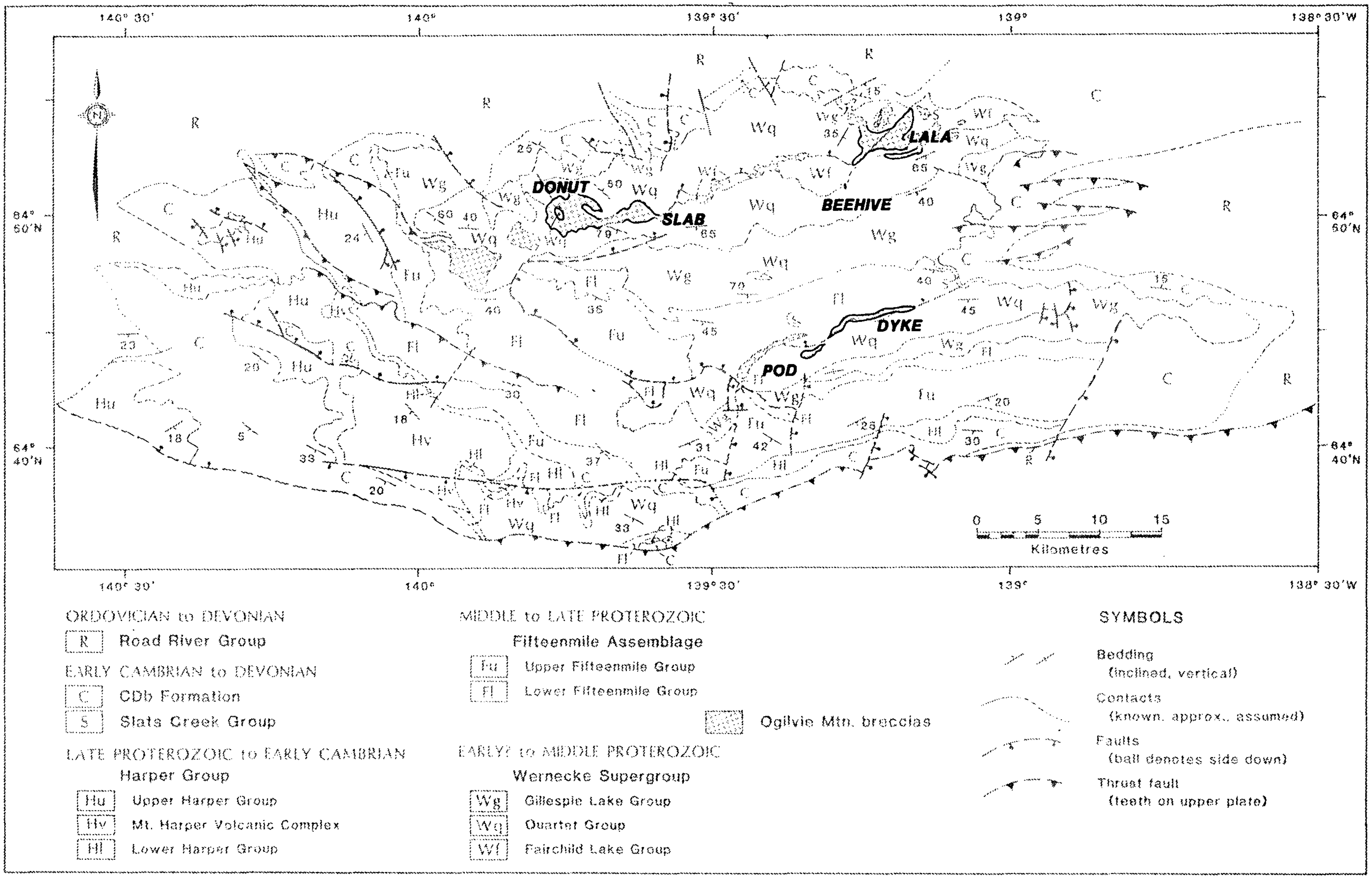

Figure 3.1 Position of Ogilvie Mountain breccia localities that are discussed in the text.

within rocks of the Quartet Group. Contrasting bedding attitudes in Quartet strata on either side of the breccia suggest that the faulting is coincident with the location of the breccia. The thickness of the breccia bodies varies considerably ranging from occurrences less than 2 metres wide to large exposures over a kilometre across.

The Southern Breccia Belt coincides with the **Fifteenmile fault** (Map 1), a sub-vertical north side down fault. It juxtaposes Quartet Group clastic sediments (on the south) against carbonate and clastic sediments of the lower Fifteenmile group to the north. From east to west the thin dyke-like form of the breccia, varying from 10 to 200 m wide, changes to elliptical bodies that range from 50 to 2,000 m in diameter. Isolated pods of **OMB** occur solely within Quartet Group and lower Fifteenmile group strata (Map 1).

Six localities along the trend of the breccias were investigated in detail. These areas are listed in Table 3.1 and labelled on Map 1.

3.1.2 Contact Relations

Contacts between breccia and host rock material are either sharp or gradational. Breccia bodies that display gradational contacts have a core of well-mixed

TABLE 3.1 A brief description of breccia localities examined in detail (Map 1) in the Coal Creek Inlier, southern Ogilvie Mountains, west-central Yukon Territory.

BRECCIA LOCALITY	**DESCRIPTION**
DONUT	A circular breccia body, about 3 km wide, flanked by Gillespie Lake and Quartet Group, and cored by Quartet Group.
SLAB	A south-dipping breccia body, up to 1.5 km in maximum dimension, that contains massive blocks of Quartet Group and truncates Quartet Group.
BEEHIVE	A conformable wedge of breccia, 60 m thick, with gradational contacts of fractured Fairchild Lake Group.
LALA	A complex area of approximately 45 ha consisting of irregularly shaped breccia bodies accompanied by hydrothermal alteration and significant copper mineralization.
DYKE	A thin and discontinuous, snake-like body of breccia, 15 km long and averaging about 75 m in width, that occupies a fault between Quartet Group and lower Fifteenmile group.
POD	A half km wide, tadpole-shaped breccia body encapsulated in Quartet Group rocks.

heterolithic breccia, and or margin of weakly to moderately altered monolithic breccia which grades outward into to crackled rock. The matrix to fragment ratio and the degree of rotation of fragments decreases toward the margin of the breccia. The width of the zone appears to depend on the host lithology and its tendency to fracture: Fairchild Lake Group rocks are particularly susceptible to "crackling", in part because of a competency contrast between dolomite and argillite layers.

Sharp or abrupt contacts are more common than gradational contacts. This is especially true where the breccia bodies are elongate or dyke-like. Sharp-walled contacts are interpreted to be either intrusive or faulted. Host rock is commonly moderately fractured within tens of metres of the contact, and fractures are mineralized with iron carbonate, quartz or hematite. In several localities strata have been warped or dragged upwards to steeply dipping attitudes, apparently by injection of the breccia.

3.1.3 Alteration

Several types of alteration are associated with the Ogilvie Mountains breccia: hematitization, carbonatization, chloritization and silicification. These four styles of alteration variably affect the breccias and their host rocks. Weak to moderate host rock alteration is typical. It is generally more extensive than the less common and limited zones of intense alteration. Albitization was not observed in the field area.

Ogilvie Mountains breccia and host rock contact zones generally are weak to moderately hematite altered. The breccias are commonly and characteristically hematized. This alteration varies from pale pink to blood-red stained carbonate matrix to local massive specularite. These breccia bodies commonly form resistant craggy towers and pinnacles that can be recognized from a distance by their pink to maroon colour. Fairchild Lake Group rocks are, in general, regionally weakly hematitic. However, adjacent to breccia bodies the degree of hematitization is commonly more intense. The permeable beds are stained to deep reds and maroons (Plate 3.1), and contain local jasper. The more intensely altered zones are a few tens of metres across and are typically accompanied by fractures that have been healed with blood-red carbonate and specularite. Quartet Group rocks in contact with breccia bodies are generally only weakly altered, displaying minor discolouration to pale greys, greens and reds. However in some cases wallrock is pervasively hematized to a deep red, and red earthy hematite dust is disseminated throughout the host rock. Gillespie Lake Group dolostone displays minor hematitic staining, but typically shows little alteration. Bedding at contact margins is commonly disrupted to densely fractured. Veins and fracture fillings near the contact consist of brown iron carbonate that is generally devoid of specular hematite.

Carbonate alteration is common throughout the Ogilvie Mountains breccia. Most noticeably, it occurs as ferruginous dolomite with rhombs 1 to 3 mm in diameter that replace the primary mineralogy of clasts and original matrix constituents. Carbonatization of host rocks is not conspicuous because of their primary carbonate mineralogy. However, thin sections of breccia from the contact zones show carbonate replacing fine grained groundmass. Carbonate overgrowths on original grains are also common.

Chlorite occurs as medium to coarse grained platy masses and isolated elongate laths in the matrix of the breccias, sometimes accounting for 80% of the matrix at hand sample scale. Although deemed an alteration mineral, no precursor mineral, such as biotite, was observed in any of the breccia specimens. Chlorite is also abundant in altered mafic dykes, where it formed after Fe-Mg silicates as a result of lower greenshist grade metamorphism.

Silicification in **OMB** is locally intense and replaces silty to sandy dolomite-rich sedimentary fragments. Textural features common to silicified breccias include clouding of fragment-matrix boundaries and general bleaching of the altered rock.

Limited quartz ± hematite stockwork zones occur locally in moderately to densely brittle fractured Quartet sediments at breccia margins. Weak silicification is shown by silica replacement of the more permeable layers in interbedded argillite-siltstone units. The *LALA* locality (Map 1), an area of some mineral exploration activity in the 1970s, has silicified fragments and exhibits features of open space filling, such as cockade and cockscomb textures (Plate 3.2). Sericitization is generally present in minor amounts. Later

Plate 3.1 Fairchild Lake Group dolostone (unit 1B; sample BL5-8 located in the northeast corner of the field area) showing typical hematitic alteration.

Plate 3.2 Hydrothermally altered breccia from the *LALA* mineral prospect (Map 1) displaying cockade texture (rythmically precipitated quartz and hematite: sample BL40-11, upper left), carbonate-quartz-sericite alteration (sample BL40-27, upper right) and intense silicification (sample BL40-29, bottom).

carbonate has filled the remaining cavities. Disseminated and late stage vein-hosted sulphide mineralization, consisting of pyrite, chalcopyrite and bornite, is present locally in amounts less than 1%.

3.1.4 Textural Varieties

Ogilvie Mountains breccia are generally matrix-supported, but both matrix- and fragment-supported varieties are common and generally occur in the same outcrop. Fragments make up 30 to 80% of the rock. Roundness of fragments range widely from angular to rounded, but is generally subangular to subrounded. Shapes range from plates and blocks with sharp edges to well rounded spherical clasts. Rare fragments form wavy, irregular shapes with serrate terminations. Fragments range in size from less than 1 cm to greater than 5 m.

On fresh surfaces **OMB** is commonly mottled pink and green, or maroon to purple in colour. Weathered surfaces of outcrops, usually pink to maroon and rusty brown, are knobby and pitted due to the contrast between weather-resistant fragments and recessive weathering matrix. Delicately laminated (Plate 3.3) and coarse grained clastic-looking layered textures (Plate 3.4) are common locally, but a chaotic jumble of mixed clasts (Plate 3.5) is the norm.

Plate 3.3 Hematitic heterolithic chlorite-rich matrix breccia (unit BHcl; sample BL50-2 located in central part of Southern Breccia Belt; Map 2) displaying delicate laminations. Note varying degrees of hematite replacement of fragments (near top and right side) that indicate hematitization was secondary.

Plate 3.4 Heterolithic carbonate-rich matrix breccia (unit BHcb; sample BL34-5 located on ridge about 1.5 km southeast of *LALA* locality) showing well-defined layering and textures such as weakly defined graded bedding of possible sedimentary origin.

Plate 3.5 Monolithic breccia (unit BM1; sample BL32-5 located on ridge about 1.5 km south of *LALA* locality) showing subrounded pink quartzite fragments in a dense matrix of predominantly chlorite. The chaotic jumbled texture is common to most breccia.

Each of the three units of the Wernecke Supergroup are represented as fragments in the breccias, but Fairchild Lake Group lithologies are the most common. Rare fragments derived from the lower Fifteenmile group occur locally in the Southern Breccia Belt. Minor mafic igneous fragments are likely derived from diabase dykes that crop out nearby.

3.1.5 Classification

Ogilvie Mountains breccia (OMB) were divided into two groups in the field:

(1) **monolithic**--(i.e. oligomictic) breccia fragments are of one lithology, and

(2) **heterolithic**--(i.e. polymictic) breccia fragments are of many lithologies.

These terms are commonly used for describing breccias and are consistent with the terminology presented by Laznicka (1989).

Both the monolithic and heterolithic breccia groups were divided into three sub-units based on fragment lithologies and type of matrix. Alteration complicates the identification and classification of these breccias. Specifically, silica flooding and pervasive hematitization alter the original textures and mineralogy of the fragments that would otherwise enable them to be more easily identified. Table 3.2 summarizes the classification scheme used.

The following section describes the characteristics of some of the breccia bodies, within the labelled areas on Map 1.

TABLE 3.2. Classification scheme used to characterize Ogilvie Mountains breccia of the Coal Creek Inlier, southern Ogilvie Mountains, west-central Yukon Territory.

Breccia variety	Fragment lithology[1]	Dominant matrix component[1] carb	chlr	hem	sil
Monolithic	GLG	*			
	QG				*
	FLG	*	*		
Heterolithic					
	mixture of GLG+QG+FLG ±FMG	*	*	*	*

1. Abbreviations are as follows: GLG = Gillespie Lake Group; QG = Quartet Group; FLG = Fairchild Lake Group; FMG = Fifteenmile Group; carb = mainly dolomite and ferruginous dolomite; chlr = chlorite; hem = specularite and red opaque hematite "dust"; sil = quartz.

3.2 PETROGRAPHY

Greater than 99% of all fragments have been derived from the Wernecke Supergroup. The other <1% consists of mafic igneous fragments, quartz and carbonate vein material, lower Fifteenmile group sediments and specularite aggregates. The breccias are commonly fragment supported. Fragments are dominantly subangular to subrounded, range in size from <1 cm to rare fragments larger than 20 by 50 m. Average size is in the 1 to 2 cm diameter range. Observed textures include: clast alignment, foliation, banding or layering, chaotic from jumbled mixtures of fragment types, milled or abraded fragment margins, and crackled fragments.

Matrix is composed of finely fragmented material that is locally gradational in size with fragments. The proportion of matrix varies appreciably over distances of less than two metres. Colour of the matrix covers a wide spectrum from pale greens, pinks and browns to dark greens, reds and greys. Where matrix is well developed it is generally darker than fragments. Alternatively, the matrix component of some breccias (especially carbonate-rich breccias) is sparse and less obvious.

Dominant alteration minerals consist of carbonate, iron carbonate, chlorite and hematite. Carbonate alteration is widespread as is hematitization. Chloritization occurs most commonly in mafic dykes cutting breccias, where it has almost entirely replaced original mafic grains. On the margins of the dykes, radiating sprays of chlorite has formed at the expense of all other constituents. Local silicification is moderate to intense and is commonly associated with weak sericitic alteration.

Mapped features of the breccia included: (i) proportion of fragments vs. matrix, (ii) proportion of each fragment type, (iii) fragment size: average and range, (iv) roundness and sphericity, (v) percent of each matrix type, (vi) textures, and (vii) alteration.

3.2.1 Monolithic Ogilvie Mountains Breccia

Monolithic **OMB** were subdivided based on their fragment lithology. Four fragment varieties were observed: (i) Fairchild Lake Group, (ii) Quartet Group, and (iii) Gillespie Lake Group, and (iv) lower Fifteenmile group. Fragments from the lower Fifteenmile group rocks were rare--only one such occurrence was observed. Composition of the matrix was not used to classify monolithic breccias, but was noted and is discussed below.

3.2.1.1 Monolithic Fairchild Lake Group Ogilvie Mountains Breccia (unit B_{M1})

Monolithic Fairchild Lake Group **OMB** (B_{M1}), with fragments derived entirely from Fairchild Lake Group lithologies, are the most common breccia in the field area. The best exposures, outlined below, occur on ridge tops where outcrops form blocky, hummocky zones that locally include spires up to 2 m high. The weathered surface of

Plate 3.6 Exposure of heterolithic carbonate-rich matrix breccia (unit BHcb), located about 2 km west of the *BEEHIVE* locality, displaying angular block of bedded dolostone 0.8 m in length (middle right), smaller angular blocks of argillite (lower left), and abundant subrounded fragments of several varieties.

outcrops, commonly knobby and pitted, display the generally chaotic nature of the rock (Plate 3.6). Typically the breccias are mottled pink or buff to rusty brown or, less commonly, pale green. All lithologies of Fairchild Lake Group are represented in the breccias, but the dominant fragment type is pink-weathering silty dolostone. Fragment size ranges widely from greater than 3 m to less than 0.5 cm, but dominantly about 3 cm. Matrix is typically carbonate (dolomite and minor iron carbonate) with minor specular hematite, chlorite and crushed rock material. The size and shape of fragments varies according to the characteristics of the rocks from which they originated. For instance, thinly bedded, brittle layers fractured easily and formed platy sharp-cornered breccia fragments.

Unit B_{M1} has two textural end members, they are: (i) disrupted or block breccia with restricted, generally small pod- and dyke-like zones that have vertical expression (channelway breccia; cf. Delaney, 1981), and (ii) crackle breccia, that forms on the margins of the more intensely brecciated and mixed zones.

Disrupted or block breccia is exposed in the northwestern part of the map area (Map 1) on the prominant sub-circular ridges in the *SLAB* and *DONUT* localities and on the ridge northwest of the *BEEHIVE* (Map 1, Figure 3.1). The main breccia mass at the *SLAB* locality is a tablet-shaped section that has developed on the hanging wall of the Monster fault. It truncates north-dipping strata of the Quartet Group (Plate 3.7). The southern margin of this breccia body is overlain by south-dipping Quartet Group rocks. The bulk of the breccia consists of blocks of pink- to brown-weathering silty dolostone whose boundaries commonly are indistinguishable. However, the chaotic nature of strike and dip of this unit over short distances (in the range of 5-10 m) discloses its disrupted nature. Where edges of individual breccia blocks are evident, matrix is not well developed; it consists generally of dolomitic rock flour, minor white calcite carbonate and subrounded fragments of sedimentary rock less than 2 cm in diameter (Plate 3.8).

In thin section, specimen BL16-2 displays a matrix including 90-95% subhedral dolomite that cements angular to subangular fragments of silty dolostone (Plate 3.9). Minor quartz and hematite, and traces of muscovite and chlorite make up the remaining 5-10%.

Local zones of breccia are called conduit breccia. These are relatively matrix-rich and normally contain fragments 5 to 20 cm across (although blocks greater than 3 metres in length do occur). These breccia bodies crosscut the block breccia. The exposures are commonly no larger than 10 m across, are bounded by zones of disrupted block

Plate 3.7 View of the *SLAB* looking west. The sharp contact between overlying **OMB** (buff) and Quartet Group (grey) is the Monster fault. Truncation of bedding in Quartet Group rocks is visible at right skyline.

Plate 3.8 Monolithic Fairchild Lake Group breccia (unit BM1; sample BL26-2 located about 3 km east of *LALA* locality).

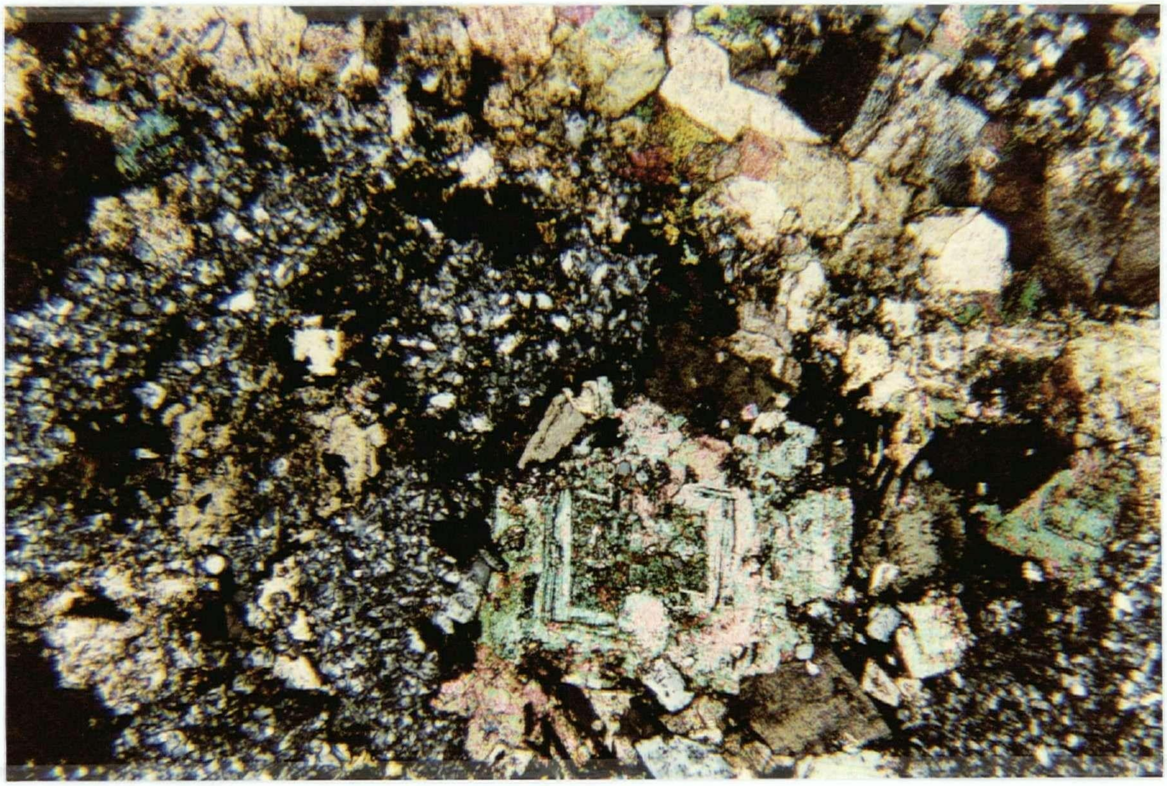

Plate 3.9 Photomicrograph of monolithic Fairchild Lake Group breccia (unit BM3; thin section BL16-2) showing subrounded quartzite fragments (several are outlined by a dashed line) in a carbonate matrix. Note growth zoned dolomite grain and other dolomite rhombs--evidence of recrystallization.

breccia, and occur as weather-resistant jagged knobs on ridge crests. Prominant exposures are located in the centre of the northern breccia band (Map 1 and Figure 3.1) north of the *BEEHIVE*).

Conduit breccia characteristically displays a well-mixed or "churned" texture where fragments have been rotated and stratigraphically mixed. The angular and sub-angular to sub-rounded fragments are set in a matrix typically consisting of pink, pervasively hematized dolomite (Plates 3.10 and 3.11). Minor matrix components consist of iron carbonate, chlorite, hematite and quartz.

However, hydrothermal alteration can significantly mask the original character of the rock (Plate 3.12). In rare cases hematite and/or chlorite comprise most of the matrix. These rocks locally display weak to strongly developed aligned textures. These textures can be defined by the subparallel arrangement of platy hematite blades and chlorite laths up to several millimeters in length. Dolomite rhombs up to 2 mm across, are minor, but occur disseminated throughout the matrix where they are locally concentrated on fragment boundaries.

Matrix usually accounts for 25 to 35% of the rock, and generally contains a mixture of minerals: carbonate is most abundant and typically accounts for between about 25 and

60%, quartz accounts for 15-40% and chlorite makes up 5-15%. Blades of hematite (<1-10%), irregular patches of clay (trace to about 5%), fine grained muscovite in trace amounts and fragments less than 1 mm in diameter comprise the remainder of the matrix.

Matrix supported varieties are uncommon, but may resemble coarse grained clastic sedimentary rocks. Subangular to subrounded, commonly gravel sized clasts, are set in a matrix consisting of broken grains of quartz and feldspar, irregular patches of carbonate and clay, radiating masses of chlorite, randomly oriented blades of hematite that rim larger grains, and minor fine grained flakes of muscovite. Chlorite and carbonate contain numerous inclusions and appear to replace quartz.

Crackle breccia forms along the margins of some breccia bodies. A good exposure of this breccia occurs on the southern margin of the irregularly shaped body that crops out on the ridges south of the old *LALA* locality (Map 1). At this locality crackle breccia (Plate 3.13) consists of platy, angular grey to pale green fragments of siltstone set in a pink matrix of dolomite. The arrangement of platy fragments, from 1 to 10 cm across and 0.5 to 3 cm thick, define a weak layering that becomes more pronounced away from the centre of the breccia body. Outer margins of the crackle breccia grade into coherent, interbedded siltstone

Plate 3.10 Photograph of monolithic Fairchild Lake Group breccia (unit BM1). A large block of semi-plastically deformed Fairchild Lake Group dolomitic siltstone (upper middle) and the centimetre sized angular fragments in a hematized carbonate matrix (lower middle) are displayed. The outcrop is located on the west ridge of the *DONUT*. Pencil for scale.

Plate 3.11 Cut and polished surface of crackle breccia variety of monolithic Fairchild Lake Group breccia (unit BM1; sample BL18-10 located approximately 6 km west-southwest of the *BEEHIVE* locality) from margin of breccia body. Contorted bedding and clear rotation of some fragments are conspicuous.

Plate 3.12 Cut and polished (wet) surface of channelway breccia variety of monolithic Fairchild Lake Group breccia (unit BM1: sample TW208 located on ridge about 1.75 km southeast of *LALA* locality). Fragments are quartzite in a quartz- and chlorite-rich matrix.

Plate 3.13 Crackle breccia variety of monolithic Fairchild Lake Group breccia (unit BM1 located 1.5 km southeast of *LALA* locality) from margin of breccia body. Fairchild Lake Group at this point is mainly dolostone with siltstone interbeds.

and dolostone. There has been little or no addition of material in the formation of this breccia. The matrix consists of remobilized carbonate derived from the carbonate-rich layers.

3.2.1.2 Monolithic Quartet Group Ogilvie Mountains Breccia (unit B_{M2})

Monolithic Quartet Group **OMB** (B_{M2}) is uncommon. It is limited to faulted contacts between stratified Quartet Group and either heterolithic breccia or Fairchild Lake Group or Gillespie Lake Group strata. It occurs only in the northern part of Map 1. Outcrops are pale to dark grey. Fragments are typically angular to sub-angular and range from 0.5 cm to 8 cm in length. Most occurrences contain appreciable amounts of secondary white silica as intricate stockworks or fracture fillings. An excellent exposure of monolithic Quartet breccia occurs on the north bank of "Beehive" creek about 200 m west of the *LALA* prospect (Figure 3.1, Map 1). This exposure, about 2 m high and 20 m long, is notable because several stages of brecciation are recognized in hand sample (Plate 3.14; sample BL-11-7). Fresh-looking angular black phyllitic argillite fragments several centimetres in diameter occur next to pale grey, bleached, silica flooded composite fragments. The latter phase of brecciation is marked by the addition of abundant quartz, carbonate and minor sulphides. These minerals are likely part of the

Plate 3.14 Monolithic Quartet Group breccia (unit BM2: sample BL11-7; *LALA* locality, Map 1) from Lala mineral prospect. Some fragments are breccia (angular black argillite fragments in a pale grey matrix); others are black argillite. Chalcopyrite (yellow mineral; centre of photograph) and pyrite are disseminated throughout.

hydrothermal alteration event related to the nearby *LALA* mineral prospect (Map 1). Multistage brecciation is defined by fragments that are made up of fragments.

3.2.1.3 Monolithic Gillespie Lake Group Ogilvie Mountains Breccia (unit B_{M3})

Monolithic Gillespie Lake Group **OMB** are rare. Only a single example is known. It occurs in the northwest corner of Map 1 on the northern margin of the *DONUT* locality (Figure 3.1, Map1). The fragment supported breccia consists of angular fragments of fine grained, pale grey dolostone (unit 3a) up to several metres in diameter. Weakly fractured Gillespie Lake Group rocks grade into intensely fractured and brecciated versions adjacent to heterolithic breccia. The contact between the breccias is well exposed near and on a north-trending ridge. The sub-vertical contact is sharp; it is likely a fault.

In thin section angular fragments of very fine grained dolostone are cemented by coarse grained (up to 7 mm across), anhedral to subhedral, intergrown dolomite or iron carbonate and quartz (Plate 3.15). Rare fine grained sprays of chlorite and anhedral opaques, likely hematite, are accessories. Fragments are commonly rimmed by a thin veneer of limonite. Commonly exhibited dilational textures indicate that some of the breccias formed by injection of

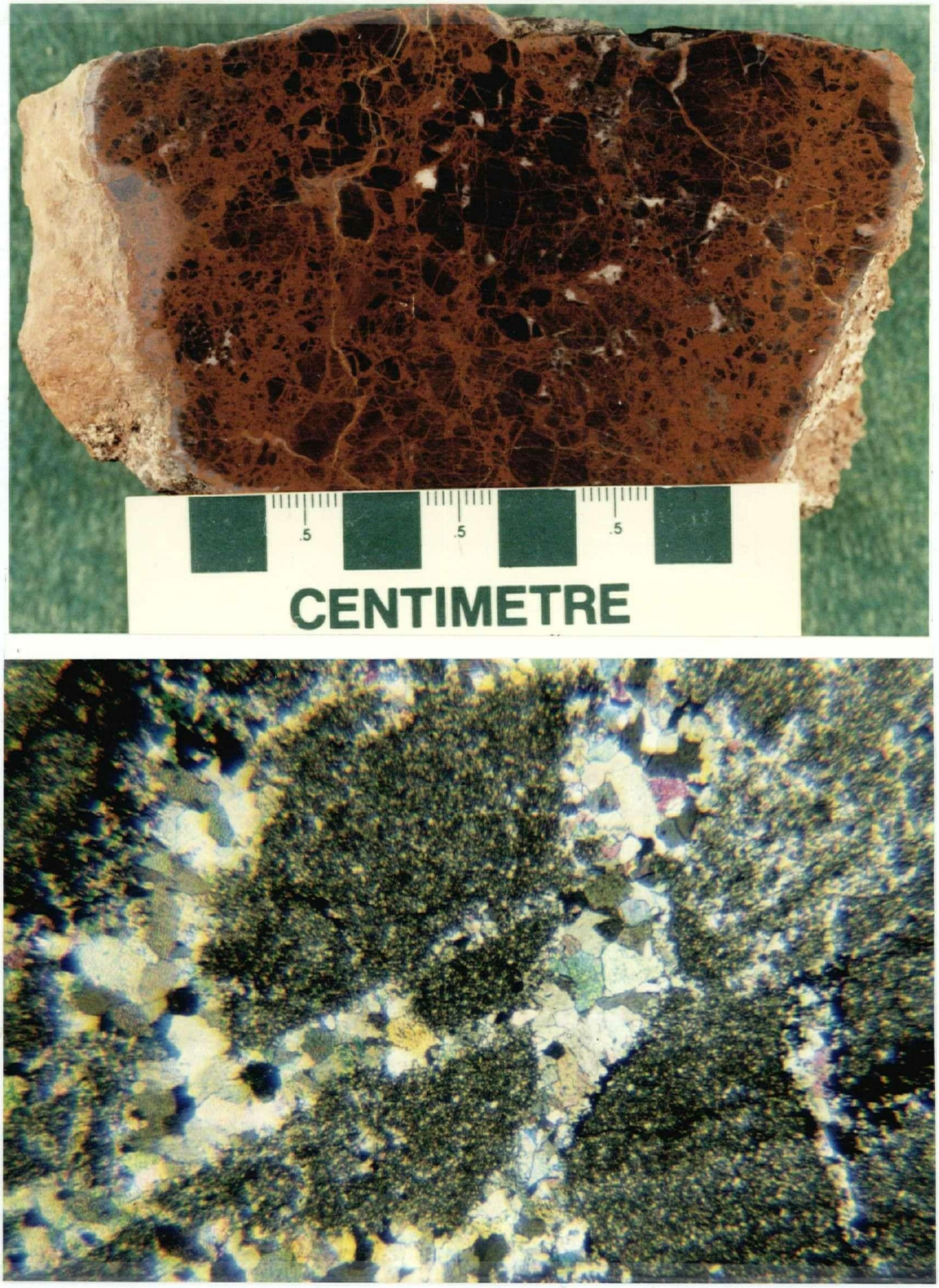

Plate 3.15 a: Photograph of cut and polished slab of hematitic monolithic Gillespie Lake Group breccia (unit BM3; sample BL87-7) from the contact between Gillespie Lake Group dolostone and OMB on the northern edge of the *DONUT*; Map 1). **b:** Photomicrograph of monolithic Gillespie Lake Group breccia (unit BM3; thin section BL87-7; from *DONUT* locality) showing subangular fine grained dolostone fragments in a coarse grained dolomite cement. Minor hematite partially rims some fragments.

carbonate- and quartz-rich material.

3.2.2 Heterolithic Ogilvie Mountains breccia

Fragments in heterolithic **OMB** are derived from the lowermost stratigraphic package of the Coal Creek Inlier. The sources, in order of most common fragment type, are: Fairchild Lake Group, Quartet Group, Gillespie Lake Group, lower Fifteenmile group, and mafic igneous material from associated diabase dykes. Lithologic heterogeneity of the breccias reflects, for the most part, the diversity of thinly interbedded units within the Fairchild Lake and Quartet Groups. Locally intense alteration or metasomatism has caused different fragment types to resemble one another so that the breccia appears to be monolithic.

Heterolithic Ogilvie Mountains breccia have been subdivided on the basis of major matrix components into, in order of abundance: (i) carbonate-rich, (ii) hematite-rich, and (iii) chlorite-rich end members. These types are detailed below.

3.2.2.1 Heterolithic carbonate-rich matrix Ogilvie Mountains breccia (unit B_{Hcb})

Heterolithic carbonate-rich matrix Ogilvie Mountains breccia (B_{Hcb}) occurs most prominently at the *BEEHIVE*

(Figure 3.1, Map 1 and Plate 3.16), a 170 m high hill of partly rubble-covered outcrop. It is situated in the western end of the broad, U-shaped, informally named "Beehive" valley. It consists of well-bedded and thinly bedded pink, silty dolostone and green argillite, gritty dolomitic sandstone, and brown weathering dolostone. A heterolithic breccia sill, 60 m in true thickness, dips shallowly and cuts through the hill about halfway up. The contacts at the margins of the breccia sill are gradational with the host rock: the core of heterolithic breccia grades outward to monolithic zones at the margin and into crackled, intensely fractured host rock. Fracture intensity decreases away from the margin. The lower contact of the breccia sill is marked by a pale green intensely chloritized mafic dyke. This dyke displays porphyroblasts of pyrite and zoned amygdules with thick siderite or ankerite rims and calcite cores. Fine grains of bladed specular hematite are minor. This brown-green mottled breccia contains Quartet Group, Fairchild Lake Group and mafic igneous fragments (Plate 3.17; sample BL10-14). Subangular fragments average about 2 cm in diameter, but rare large fragments range up to 4 m across. The matrix consists dominantly of dolomite with accessory chlorite and hematite.

A small lens-shaped exposure of breccia, 180 m by 30 m crops out 400 m south of the *BEEHIVE*. It occurs as an isolated lense-shaped body hosted in Quartet Group rocks

Plate 3.16 . Location of breccia sill is marked by a dashed line in this view of the "*BEEHIVE*" (Map 1) looking west. Note also the lens of breccia (arrow) hosted in Quartet Group sediments on flank of mountain to the left of the *BEEHIVE*.

Plate 3.17 Cut and polished surface of hand sample from heterolithic carbonate-rich matrix breccia (unit BHcb; sample BL10-14) from the *BEEHIVE* breccia sill. Note generally angular outline of fragments and chaotic orientation. Fragments are: hematite altered diabase (d), quartzite (q), argillite (a), dolostone (o), and siltstone (s).

and, when viewed from a distance, is identified by its buff-weathering that contrasts with the dark grey Quartet Group rocks (see Plate 3.16). In hand sample the orangey-pink matrix is studded with fragments of bleached silty dolostone, pale green and black argillite, white and green siliceous material, and pale green mafic igneous rock (Plate 3.18).

The *SLAB* locality (Figure 3.1 and Map 1) has two excellent exposures of variegated heterolithic breccia bodies that cut a host of Monolithic Fairchild Lake Group **OMB** (B_{M1}). One exposure is an east-trending, thin elongate body of breccia. It follows the trace of the Monster fault that divides north-dipping Quartet Group sedimentary rocks on the north from monolithic Fairchild Lake Group **OMB** (B_{M1}) to the south. The other is a north-trending zone that pinches out to the north as it cuts across and through Quartet Group rocks (Plates 3.19). The latter breccia body apparently squeezed between sections (mega blocks ?) of Quartet Group argillites. It has clasts that are dominantly subrounded to subangular pink dolostone, and interbedded argillite and dolostone up to 40 cm in diameter. Angular to subangular black argillite fragments up to 75 cm in length are abundant. White sparry calcite crystals and blebs of specular hematite are common as matrix constituents. Pock-marked weathered surfaces indicate solution of coarse-grained (0.5 to 2 mm) carbonate crystals. Carbonate also

Plate 3.18 Cut surface of hand sample from heterolithic carbonate-rich matrix breccia (unit BHcb; sample BL87-70) from the exposure of breccia to the south (to the left of Beehive in Plate 3.16) of the *BEEHIVE*. Fragments are: diabase (d), quartzite (q), argillite (a), dolostone (o), and siltstone (s).

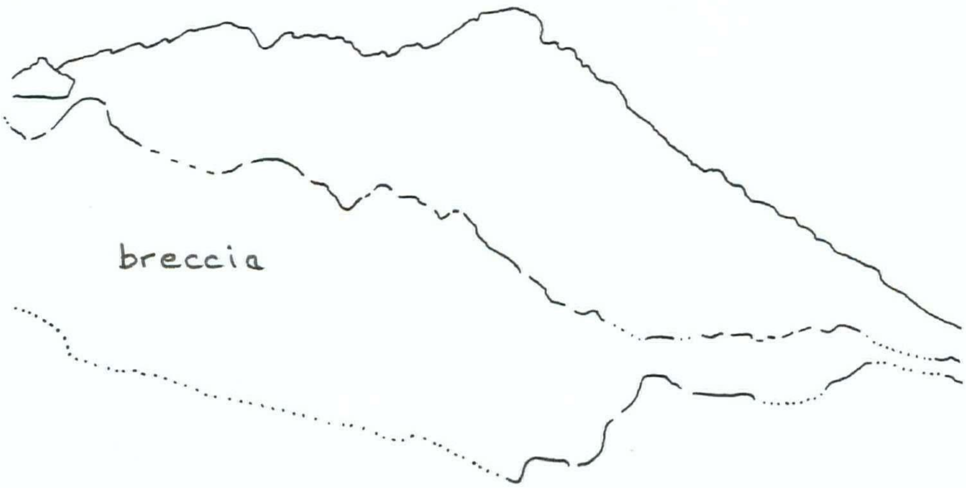

Plate 3.19 Crosscutting nature of dyke-like breccia body (shown in sketch above) is shown in this view of the *SLAB* locality (Map 1, looking east).

rims clasts.

The *DONUT* area (Figure 3.1 and Map 1) is another example locality for the carbonate-rich matrix breccia (B_{Hcb}). At this locality the gradational, brecciated contact between breccia and Gillespie Lake Group on the north-northeast side of the *DONUT* is well exposed (Plate 3.20). Bedding is steeply truncated; strata adjacent to the contact has been ruptured into rotated blocks 3-5 m across. On the northwest side of the *DONUT* subvertical cross-cutting contacts between Quartet Group and **OMB** are well displayed (Plate 3.21). There, heterolithic carbonate-rich matrix **OMB** includes fragments from Fairchild Lake Group and uppermost Quartet Group (Plate 3.22).

In thin section medium to coarse grained anhedral, commonly poikilitic, (iron) carbonate, or dolomite, comprises from 45 to 70% the matrix. Anhedral to subhedral quartz, 0.1 to 2.4 mm in diameter, account for between 15 and 35% of the matrix. Weakly developed foam texture is evidence of recrystallization. Rare quartz grains exhibit multiple stages of quartz overgrowth. Lithic fragments (comminuted sedimentary rock), less than approximately 1 mm in diameter, are classified as matrix and make up to 10% it. Opaques consist mainly of bladed hematite (ranging from trace amounts to 8%), that rims fragments; rare pyrite and limonite also occurs. Chlorite is present in minor amounts.

Plate 3.20 *DONUT* locality (Map 1) looking north-east at steeply dipping contact, in foreground, between orange weathering dolostone of Gillespie Lake Group (unit 3A, right and far left) and maroon heterolithic breccia (unit BHcb, centre).

Plate 3.21 *DONUT* locality (Map 1) looking west from the middle of the complex. Irregular and interfingering contact between breccia (buff, above) and Quartet Group (grey, below) is shown in sketch above.

Plate 3.22 Outcrop of heterolithic carbonate-rich matrix OMB from the northwest part of the *DONUT* locality (Map 1). Angular fragments consist of dolomitic siltstone of uppermost Quartet Group and pale green siltstone, pink silty dolostone and jasper of the Fairchild Lake Group. Mafic dyke fragments are rare. Hammer for scale.

Accessory components of the matrix, that occur in trace amounts, are actinolite/tremolite and epidote.

Specimen BL35-4 contains several subrounded to rounded fragments of strongly carbonate altered igneous intrusive rock. The cores of these fragments consist of a coarse grained mesh of actinolite/tremolite, carbonate, chlorite and quartz 0.2 to 2 mm in length (Plate 3.23). Masses of rusty iron oxide and coarse grained iron carbonate comprise the altered rims, which are typically 1 to 3 mm wide. Common pyrite euhedra range in size from 0.6 to 1.7 mm.

3.2.2.2 Heterolithic hematite-rich matrix Ogilvie Mountains Breccia (unit B_{Hh})

Heterolithic hematite-rich matrix **OMB** (B_{Hh}) are relatively common, but exposures are limited in extent. Outcrops have been observed mainly on ridge crests where they form prominent, often jagged, craggy towers (Plate 3.24). Good exposures occur in the Southern Breccia Belt at the eastern-most edge of the *DYKE* locality (Map 1), and at the tadpole shaped breccia body (*POD* locality; Figure 3.1 and Map 1) located in the middle of the southern part of SBB. One occurrence at the former locality is a narrow, dyke-like exposure of heterolithic breccia of largely hematite-rich matrix breccia. Layering in this breccia dips 75 degrees to the south and is weakly defined by the orientation of elongate clasts and whispy discontinuous laminae of specular hematite (Plate 3.25). These breccias are matrix supported. Fragments, subangular to subrounded, are locally plastically deformed and range up to 8 cm in diameter. Fragment lithologies consist of grey to black laminated argillite, pink silty dolostone, white to purple quartzite, "balls" of specular hematite and uncommon jasper. Hematite, both specular and earthy varieties, is the dominant matrix constituent. Less common matrix components include dolomite, chlorite, quartz and comminuted host rock.

Heterolithic hematite-rich matrix breccia also occurs at the "tail end" of the *POD* locality (Figure 3.1 and Map 1). This breccia body appears to be generally weakly zoned from chlorite-rich in the east to hematite-rich in the west. The contact between the zones is not well exposed and is assumed to be irregular and transitional. However the "tail" end is made up dominantly of hematite-rich matrix breccia that is purple-maroon to pink in outcrop. The breccia includes subrounded clasts averaging about 4 mm in diameter that consist of grey dolomite, dark grey to black argillite, red mudstone, pink silty dolomite and aggregates of specular hematite. These clasts are set in a matrix of specularite, minor carbonate, quartz and chlorite (Plate 3.26). Layering is absent. Contacts between breccia and host rock, where well exposed, are sharp and subvertical.

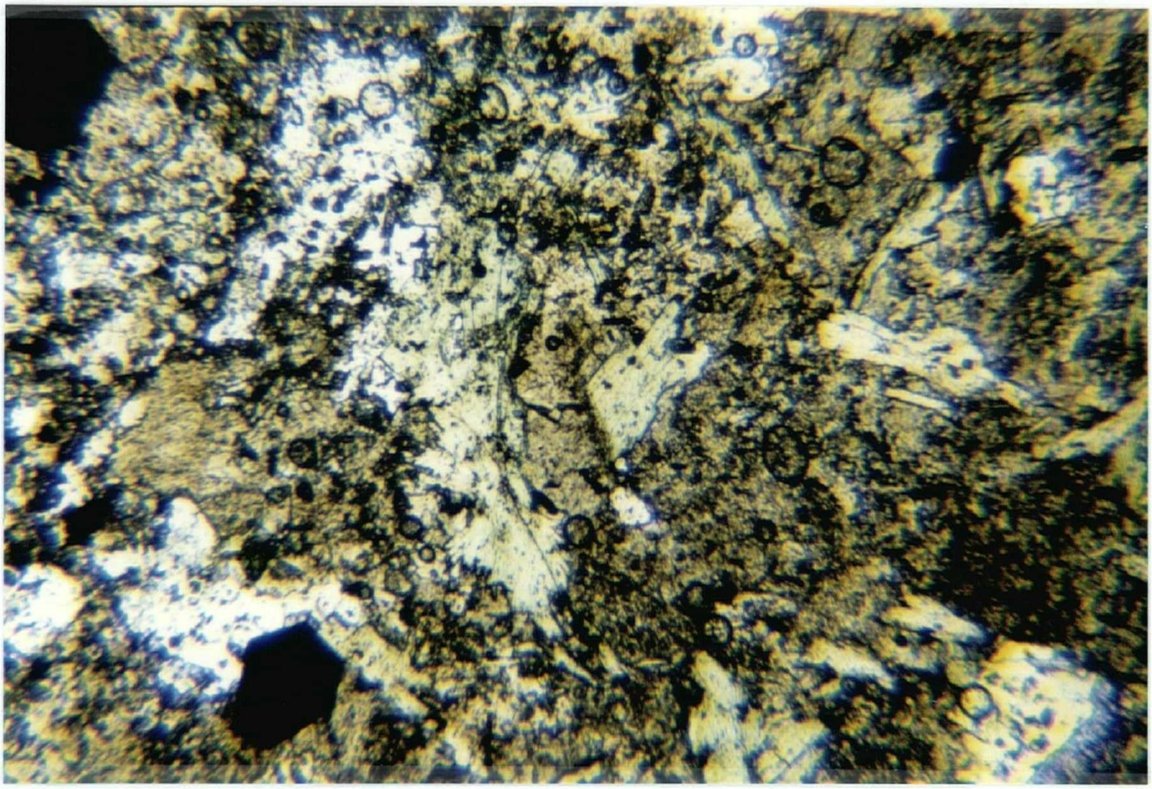

Plate 3.23 Photomicrograph of core of mafic igneous fragment from sample BL35-4 (unit BHcb). Broad, green chlorite laths formed after Fe-Mg silicates. Hexagonal opaque crystals are pyrite.

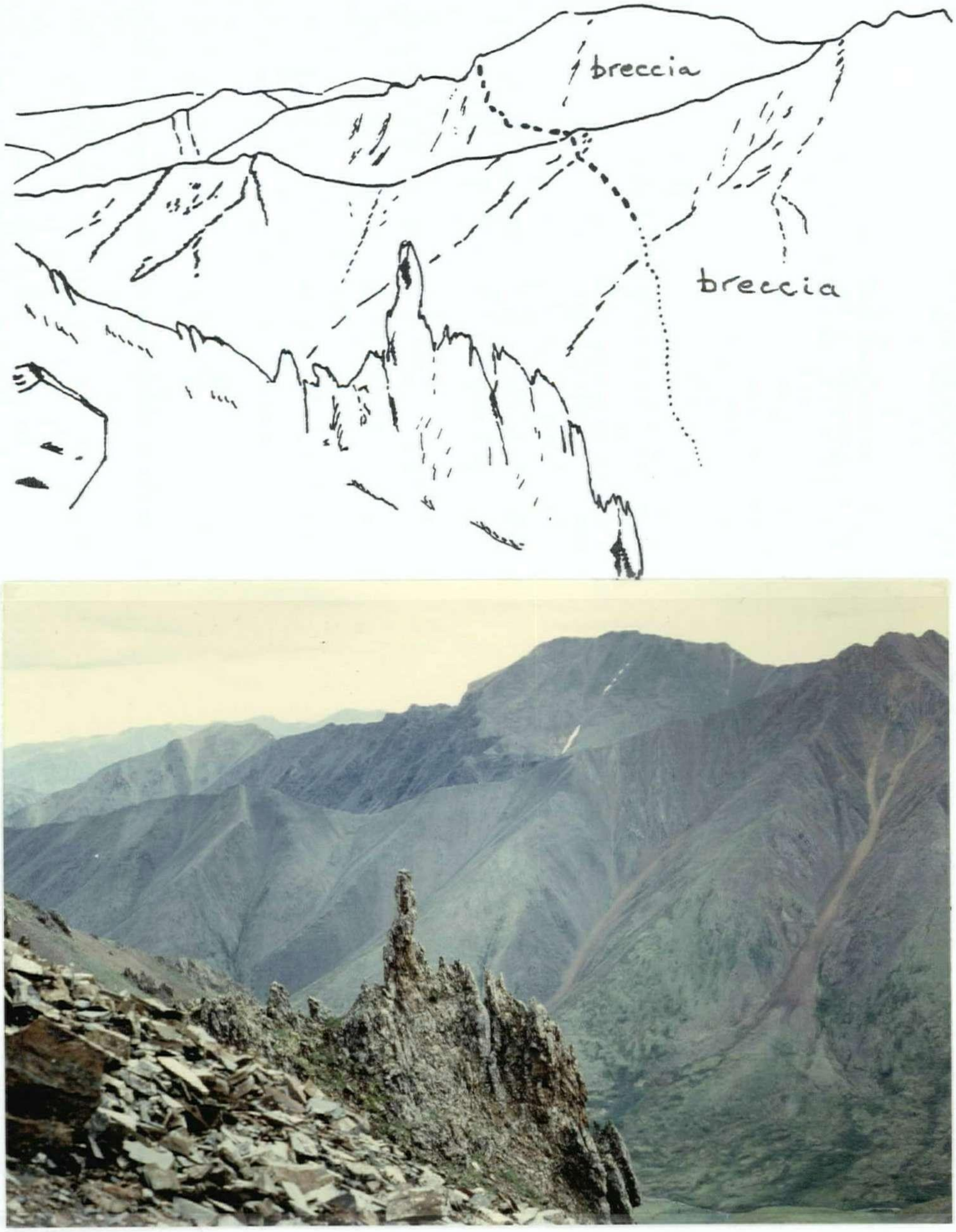

Plate 3.24 Prominant craggy exposure of heterolithic breccia on east facing flank of *DONUT* locality (Map 1). *SLAB* locality (Map 1) is in background across the valley. The south dipping contact (shown in sketch above) between breccia (upper right) and underlying Quartet Group clastic rocks.

Plate 3.25 Heterolithic hematite-rich-matrix breccia (unit BHh; sample BL43-7) from western edge of Southern Breccia Belt (Map 1). Note plastically deformed clasts and crudely defined layering. Clasts are: dolostone (o), quartzite (q), mudstone (m), coarse grained sandstone or grit (g), and specular hematite (h).

Plate 3.26 Heterolithic hematite-rich matrix breccia (unit BHh; sample BL48-3) from the (*POD* locality; Map 1), Southern Breccia Belt. Fragments are: limestone (l), hematite altered diabase (d), quartzite (q), argillite (a), dolostone (o), siltstone (s), mudstone (m), and jasper (j). Fine grained matrix comprises specularite, hematite stained carbonate and subordinate quartz.

Hematite-rich matrix **OMB** also occur at the Northern Breccia Belt north of the *LALA* locality (Figure 3.1 and Map 1). Numerous outcrops of breccia are cut by a 3 m wide west-trending diabase dyke on the south facing slope of the ridge. These characteristically layered fragmental rocks are between 50 and 75% hematite (Plate 3.27). Fragments make up to about 60% of the rock and are derived from Fairchild Lake Group and Quartet Group rocks. Rocks from this occurrence may be sedimentary iron formation.

Matrices of these rocks are characterized in thin section by thick to thin tabular plates and elongate laths of hematite up to 4 mm long that typically comprises between 25 and 75% of the rock. Lesser matrix components consist of: subhedral quartz (0.03 mm to 1.4 mm in diameter; 20-45%); poikilitic anhedral patches, and less common euhedral rhombs of iron carbonate (10-25%) up to 5 mm across; minor chlorite, clay and small lithic fragments; traces of potassium feldspar and fine grained euhedral tourmaline; local sericite; and rare pyrite and chalcopyrite. Quartz overgrowths on quartz and carbonate overgrowths on carbonate grains are common. Poorly developed foam texture in some fragments and growth of euhedral crystals are evidence of recrystallization (Plates 3.28 and 3.29). The fragments in these rocks are generally rimmed with hematite or coarse grained carbonate. Microscopic layering is defined by discrete bands of aligned hematite blades. Aggregates of

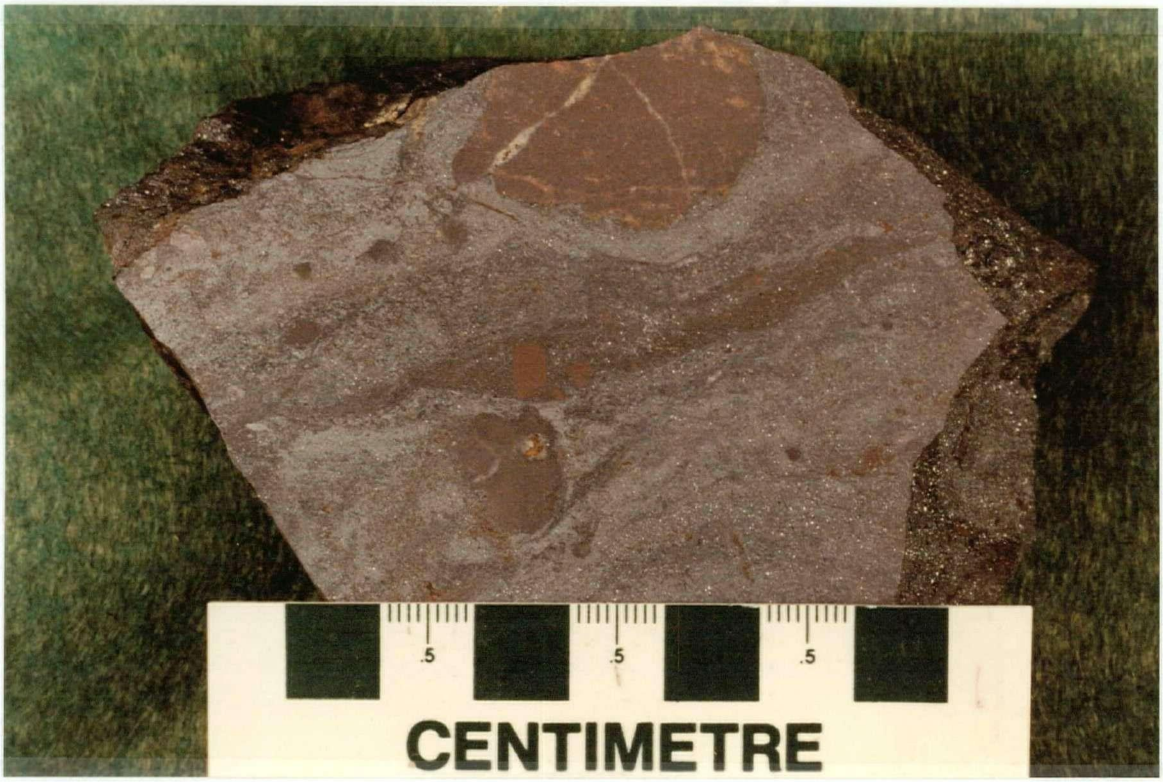

Plate 3.27 Hematite-rich matrix breccia (unit BHh; sample BL24-12) from southeast facing flank of ridge about 2 km southwest of *LALA* mineral showing (Map 1), Northern Breccia Belt. Note delicate laminations of specularite.

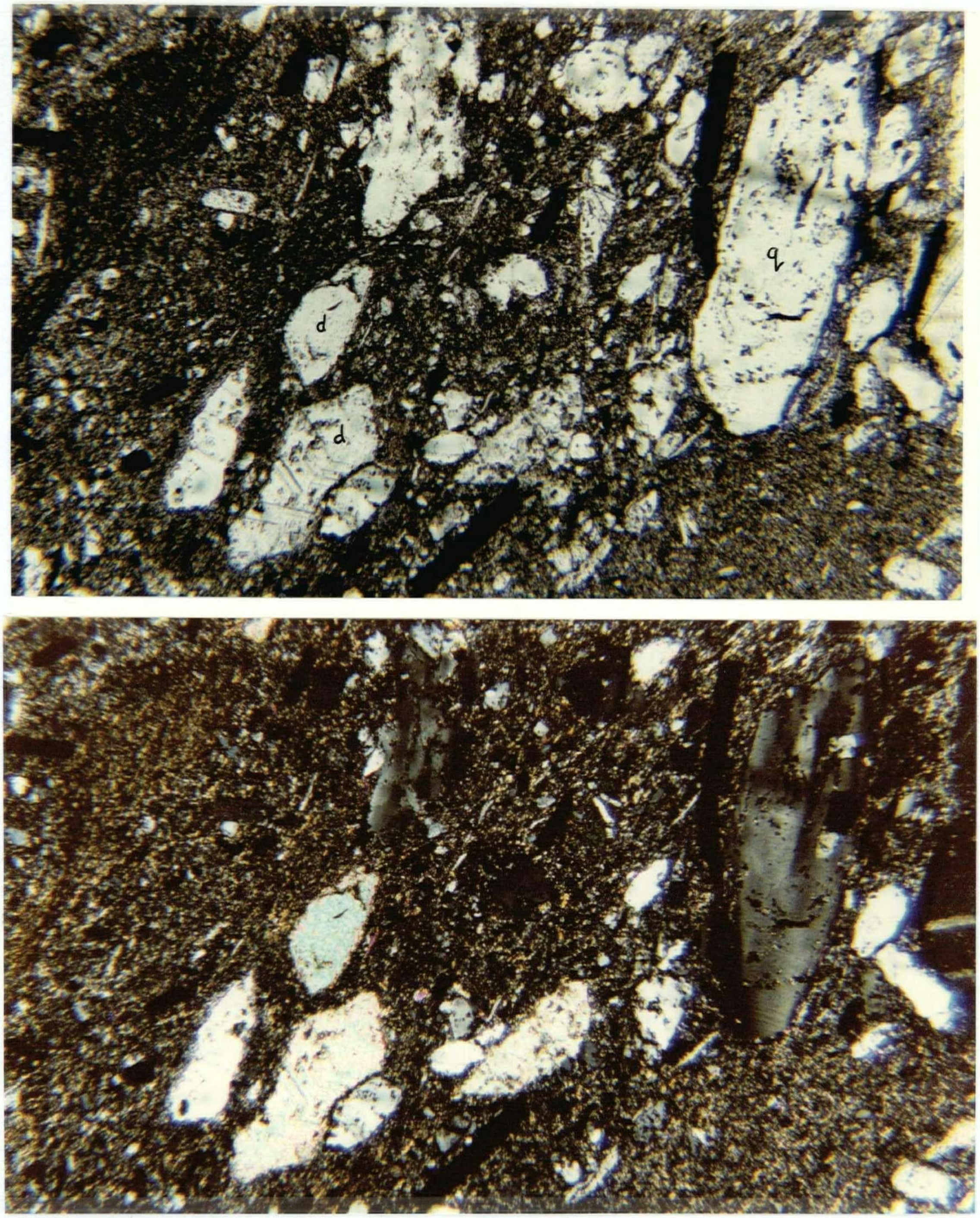

Plate 3.28 Photomicrograph of heterolithic hematite-rich matrix breccia (unit BHh; sample BL43-7) of broken crystals of quartz (q), dolomite (d), and hematite (opaque blades) in fine grained matrix. Note deformation lamellae and ghost zoning, outlined by hematite dust and fluid inclusions, in largest quartz grain. The broken end of this crystal and scalloped edges of other crystals attest to comminution during emplacement of this rock via a gaseous fluid. Fine grained matrix consists of muscovite, carbonate, hematite and quartz.

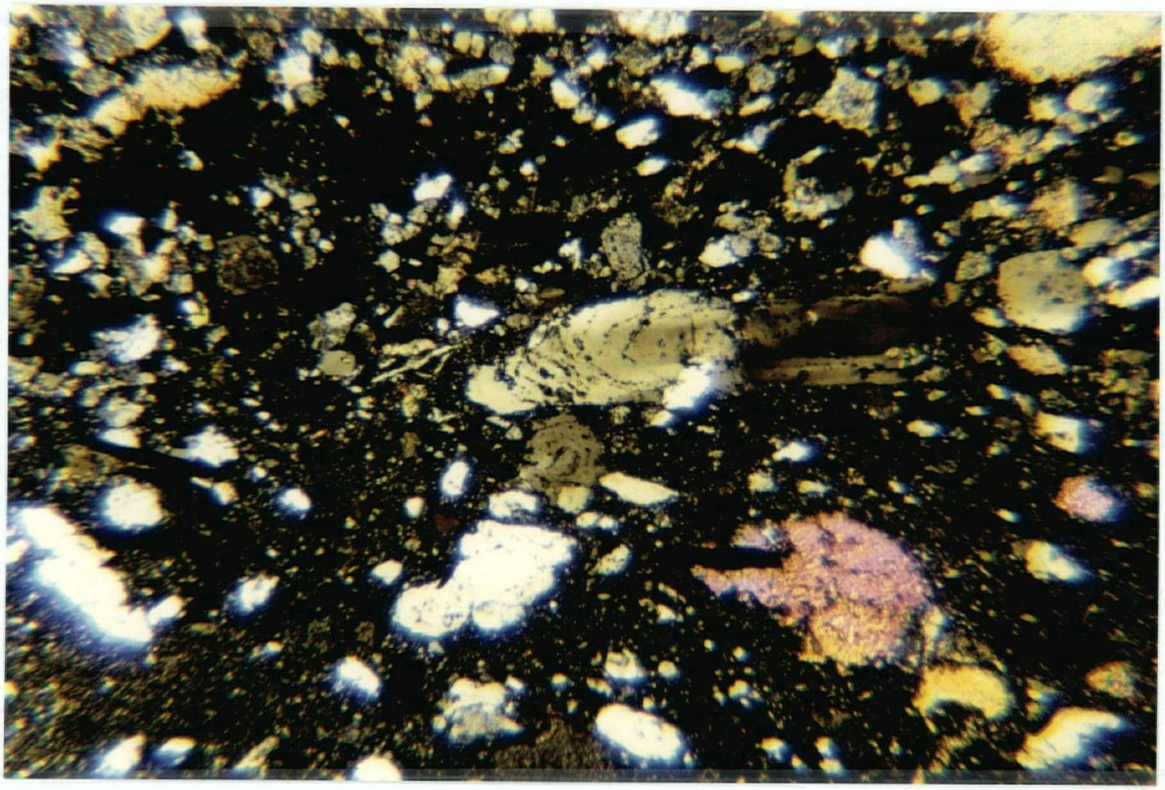

Plate 3.29 Photomicrograph of heterolithic hematite-rich matrix breccia (sample BL24-12) from area north of *LALA* locality. Note growth zones, defined by fluid inclusions, and undulose extinction in large quartz crystal (centre of photograph). Opaques grains are hematite; high birefringent minerals are carbonate. Fine grained matrix is hematite, chlorite and clay.

fine to medium grained specularite also form rare subrounded clasts. All fragments are of sedimentary rocks that are often strongly hematized.

3.2.2.3 Heterolithic chlorite-rich matrix Ogilvie Mountains Breccia (unit B_{Hcl})

Heterolithic chlorite-rich matrix **OMB** (B_{Hcl}; Plate 3.30) are common locally, but exposures are generally small. Several exposures of this breccia occur in a band that trends across two ridges to the south and east of the *LALA* prospect (Figure 3.1 and Map 1). The strike length of this elongate zone is more than 4 km, and it varies in width from 50 to 300 metres. It occurs at the contact between Fairchild Lake Group rocks to the north and Quartet Group rocks to the south. The southern contact of the breccia body is exposed where it crosses two prominent ridges. Here the contacts appear to be steep and sharp.

Fragments, generally subrounded, vary in lithology, but consist mostly of pink quartzite and silty dolostone from the Fairchild Lake Group. Other fragment types include dark grey to purple siliceous argillite (Quartet Group), banded pink chert, and quartz-carbonate vein material. Mafic igneous fragments are rare and Gillespie Lake Group fragments are absent.

Fragments, in thin section, commonly consists of recrystallized quartz and carbonate of various grain sizes; quartz overgrowths are abundant. Carbonate, clay and fine grained anhedral hematite is disseminated throughout the pink fragments.

Chlorite, minor carbonate and rare specularite cements the fragments. Micro fractures in fragments are healed with chlorite and lesser white to pink quartz and carbonate. Hematite, a common accessory mineral in the matrix component of the breccia, occurs in amounts from trace up to 3%. Specular hematite is commonly disseminated throughout the fragments.

Chlorite, as seen in thin section (Plate 3.31), occurs as fine to medium grained radiating masses and less commonly as coarse grained (2-3 mm) laths. It makes up between 35 and 70% of the matrix. Carbonate, iron carbonate and hematite, silica, and locally as much as 2% sericite comprise the remainder of the matrix. Sericite-bearing breccias are cross-cut by post-breccia sulphide-bearing quartz-carbonate veins.

Chlorite-rich matrix breccias are also present in the Southern Breccia Belt. Sample BL50-2 (see Plate 3.3) is a finely layered, matrix supported example that contains rare rounded fragments of pink spotted rock. These fragments

Plate 3.30 Two examples of heterolithic chlorite-rich-matrix breccia (unit BHcl; sample BL35-5, above, from ridge top about 1.5 km southeast of the *LALA* locality, and sample BL3-25, below, about 2.5 km east-southeast of *LALA* locality). Fragments are: quartzite (q), silty dolostone (o), mudstone (m) and mafic dyke (d). Fine grained matrix is chlorite and subordinate dolomite.

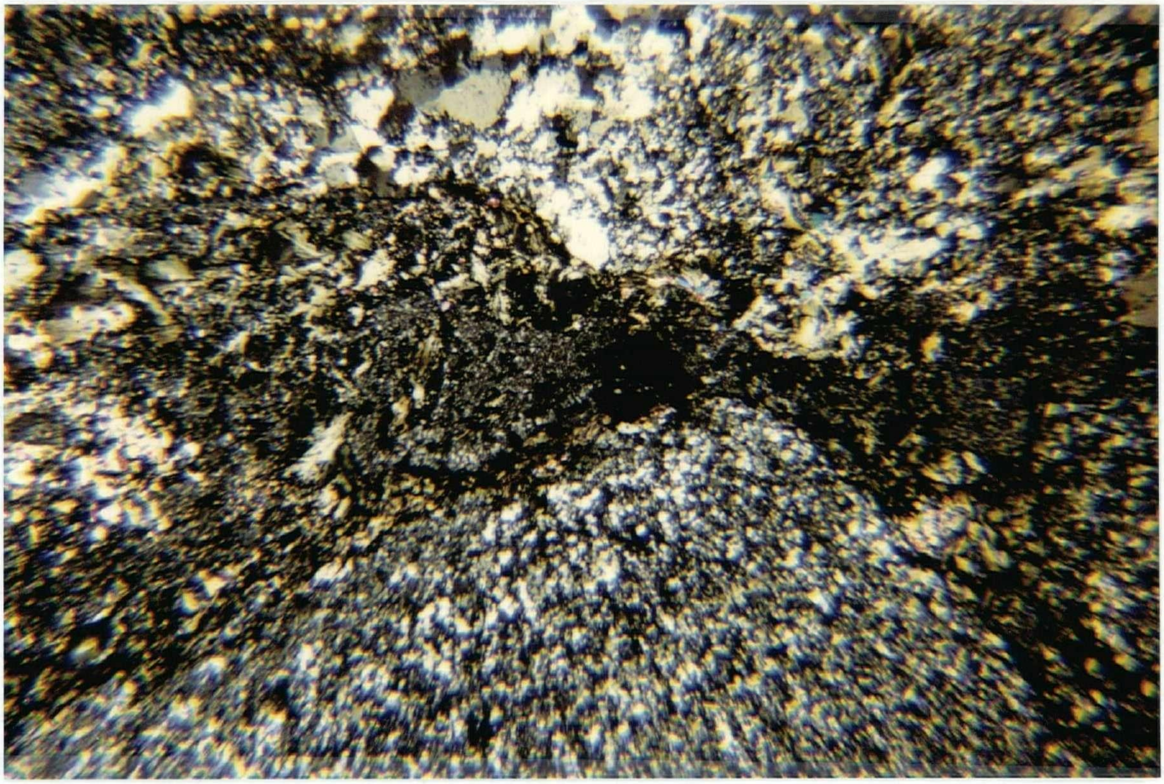

Plate 3.31 Photomicrograph of heterolithic chlorite-rich matrix breccia (unit BHcl; thin section of sample BL30-6 from elongate breccia body south of *LALA* mineral showing). Subrounded fragments of quartzite are cemented by chlorite, carbonate and rock flour.

consist of a mosaic of intergrown microcline, with euhedral tourmaline as inclusions, and quartz with subordinate carbonate and chlorite (Plate 3.32). The matrix contains abundant laths of chlorite that commonly replace quartz and fine grained portions of the matrix. The subparallel alignment of whispy, curvilinear chlorite, hematite laths, and the long axes of elongate fragments in other samples give the rock a planer fabric (Plate 3.33). This fabric appears to result from flow.

3.3 OTHER BRECCIA BODIES IN THE COAL CREEK INLIER

Fault breccia (?) made up of Quartet Group material is situated along a contact between brecciated Fairchild Lake Group and Quartet Group strata on the ridge about 1.5 km due west of the *BEEHIVE* (Figure 3.1 and Map 1). This occurrence is approximately 30 m wide and 300 or more metres in length. At this locality there has been no apparent introduction of siliceous or carbonate-rich material. The breccia is green-grey or rusty brown weathering but has a grey surface when fresh. Larger fragments are tabular and platy and generally less than 5 cm in length. Fragments smaller than 0.5 cm in diameter are subrounded to well rounded indicating that some fragment milling occurred. The matrix consists entirely of comminuted argillite. The rock is not well indurated and therefore dissaggregates easily. This breccia body is elongate and occurs on the contact between Quartet Group and

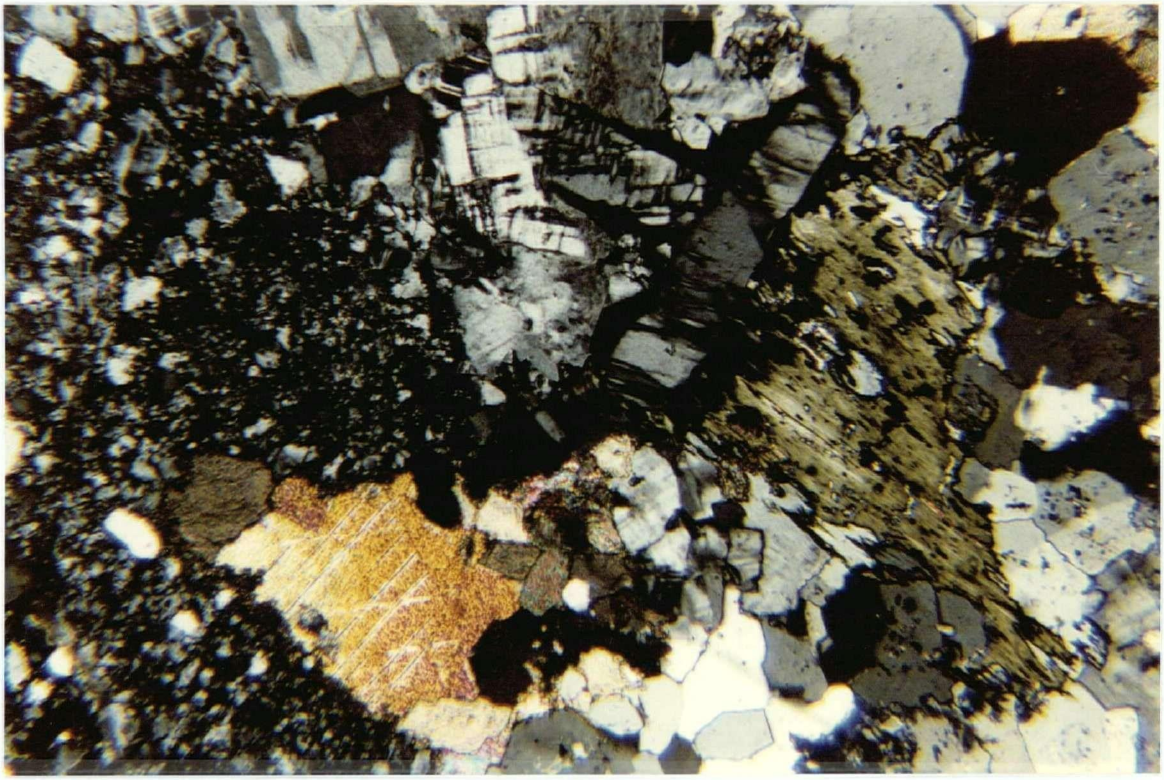

Plate 3.32 Photomicrograph of coarse crystalline (metasomatic) microcline and quartz fragment from a heterolithic chlorite-rich-matrix breccia (unit BHcl; thin section of sample BL50-2 from middle of Southern Breccia Belt). Large ragged, poikilitic chlorite lath and subhedral high birefringent dolomite are later forming minerals. A dashed line separates the fine grained matrix (left) from the clast.

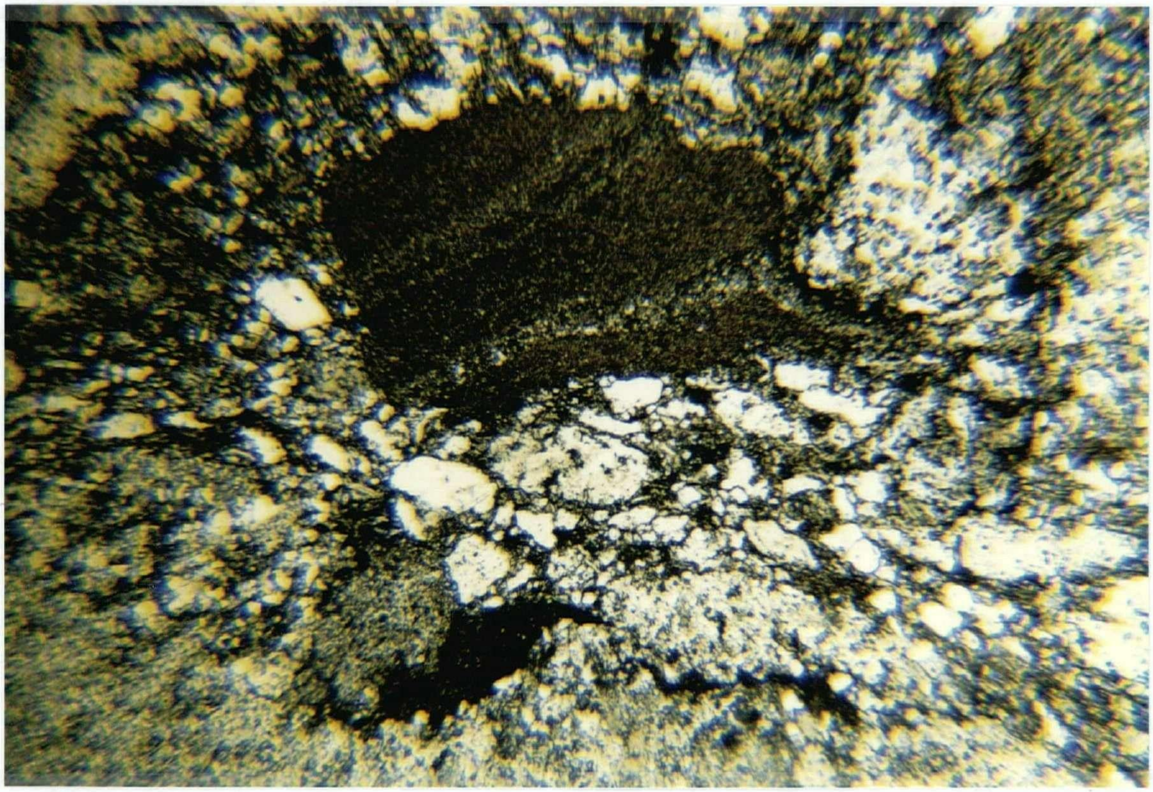

Plate 3.33 Photomicrograph of heterolithic chlorite-rich-matrix breccia (unit BHcl; sample BL3-25). Subrounded silty dolostone fragment is hosted in a bimodal matrix comprised of larger quartz and carbonate grains set in a fine grained mosaic of chlorite and hematite.

Fairchild Lake Group about 2.5 km west-northwest of the *BEEHIVE*. It likely formed in a fault zone.

Quartz-specularite breccia outcrops about 800 m southeast of the *BEEHIVE* (Figure 3.1 and Map 1). It occurs as a low relief sub-circular zone. Intensely hematized Quartet Group sandstones host this breccia occurrence. Coarse grained translucent, crystalline quartz and medium to coarse grained specular hematite comprise the irregularly-shaped fragments (Plate 3.34). The matrix consists of hematite. Pyrite and chalcopyrite, associated with hematite occur rarely. Quartz-sulphide veins (Pettet mineral showing; sample location BL34-17, Map 2), about 20 m south of this breccia, may be genetically related.

Intraformational breccia of the Gillespie Lake Group crops out in several exposures along one particular stratigraphic horizon in the northeastern part of the map area. It occurs at the base of unit 3a near the Quartet Group - Gillespie Lake Group contact. The best exposures are situated on the north bank of "Beehive" creek about 100 m northeast of the creek exposure of monolithic Quartet Group breccia mentioned above. This exposure is 150 m long and 4 m high and parallels the creek. To the northeast, along the trend of the outcrop, breccia gives way to fractured, wavy bedded flaggy dolostone over a distance of 12 m. Weathering of the exposed joint faces has highlighted the "jigsaw" or mosaic breccia texture of the outcrop (Plate 3.35).

Pale grey, thinly bedded, buff weathering dolostone with <0.5 cm interbeds of silty dolostone comprise the breccia fragments. They are cemented by an orangey-brown matrix consisting of siderite and fine dolostone bits. In hand sample it is clear that fragments have not moved far with respect to surrounding fragments. Larger fragments can be reconnected with little jockeying of individual pieces. The presence of the small bits that are less than 2 mm in diameter indicate that minor milling has occurred. Addition of material can not be determined: the carbonate matrix most likely was derived locally and is stained by iron originally present in the host rock.

The textures displayed at this locality are similar to those seen at the TART lead zinc prospect, (see Appendix A) visited during July of 1986. It occurs east of the field area and is also hosted in Gillespie Lake Group dolostone. These breccia deposits could be the result of insitu brecciation formed by solution-collapse. However no specific evidence of karsting has been documented.

<u>Pebble dykes</u> are rare; two such breccias were discovered in the field area. One pebble dyke outcrops at the *DONUT* (Figure 3.1 and Map 1; specifically at sample

Plate 3.34 Quartz-hematite breccia from Pettet mineral showing, located about 1 km southwest of the BEEHIVE locality.

Plate 3.35 Intraformational Gillespie Lake Group breccia (unit 3A) from outcrop on north bank of Beehive creek due north of *LALA* locality. This breccia forms a discontinuous zone near the base of unit 3A.

location BL87-21 on Map 2) where it crosscuts the folded Quartet Group core of the breccia complex. The other pebble dyke occurs cutting hematite stained Quartet Group rocks that outcrop on the north facing flank of the ridge north of the *LALA* mineral showing (Figure 3.1 and Map 1). Both dykes are limited in extent. The larger one is about 1.5 m in width.

Weathered outcrops are tan coloured and fresh surfaces are cream coloured. Fragments form resistant knobs against the recessive weathering matrix. Rounded fragments of white quartzite or laminated quartz sandstone are between 2 mm and 6 cm in diameter and comprise the only fragment types. The matrix consists of almost 100% coarse grained, likely recrystallized, dolomite with rare fine grained flecks of white mica and anhedral opaques.

Sandstone dykelets, several cm wide but more than 10 m in length crosscut Quartet Group sediments at the *DONUT* locality (Figure 3.1 and Map 1). They occur close to the pebble dyke and may be related genetically. However, the sandstone dykes are truncated by one section of heterolithic **OMB**. They therefore predate **OMB** formation at this point.

4.0 PETROCHEMISTRY

4.1 INTRODUCTION

Whole rock chemistry of the major stratigraphic units was measured and compared to published rock chemistry of the Wernecke Supergroup. Trace element concentrations and Rare earth element (REE) contents for stratified host rocks provide average "background" analyses. Total REE concentrations, normalized REE ratios and normalized REE patterns of the major lithostratigraphic units provide a range of upper crustal values for the Coal Creek Inlier.

The bulk chemical compositions of the breccias are dictated by fragment type and abundance. Consequently, quantitative interpretation of the major and trace element chemistry is not possible. Rare earth element (REE) chemistry of the Ogilvie Mountains breccia including rare earth element totals, normalized REE ratios and normalized REE patterns, provide a means to compare and contrast breccia units. Consequently REE patterns can be used to ascertain the origins of the breccias. For example, breccias related to carbonatite emplacement normally would have distinct REE patterns compared to those from breccias formed by sedimentary processes.

4.2 SAMPLING AND ANALYTICAL METHODS

Representative samples of the main lithologies in the map area (Map 1) were chemically analyzed. All were collected from surface outcrops. Specimens were cleaned of weathered or fracture surface material. Several analytical techniques (Appendix E) were used to measure major, minor, trace and REE concentrations. Three sample suites consist of: the main lithologies, all varieties of OMB and particular breccia matrix concentrates. The suites are representative of all regions of the area mapped. Sample locations are shown on Map 2 (in pocket), brief hand sample descriptions and chemical results are presented in Appendix E (Tables E.1 through E.6).

Suite 1 consists of samples of breccias (15 samples), stratified host rocks (6 samples) and dykes (2 samples). The Ottawa Branch of the Geological Survey of Canada measured major and minor oxide and trace element contents by X-ray fluorescence analysis (XRF), and trace and rare earth element concentrations by induced coupled plasma (ICP) techniques.

Suite 2 comprises 20 samples including breccias (13 samples) and stratified host rocks (7 samples). This suite was analyzed for over 50 trace and rare earth elements by ACME Analytical Laboratories in Vancouver using ICP techniques. Additionally, seven of the twenty samples were analyzed by ICP for major and minor oxides (Table E.4A). Suite 2 represents a reconnaissance geochemical survey, done in conjunction with Newmont Exploration of Canada Ltd. They were interested in identifying breccia bodies that were markedly anomalous in copper, gold, uranium and REE. The trace element analyses (Table E.4B) by ICP are not strictly quantitative; therefore they are not discussed further. However, several anomalous samples were discovered; these were incorporated into Suite 3 for qualitative analyses.

Suite 3 comprises 22 samples (18 breccias, four duplicates, three stratified host rocks, and one standard). This suite was analyzed for rare earth and trace elements by instrumental neutron activation analysis (INAA) by Bondar-Clegg & Company Ltd., North Vancouver.

4.3 MAJOR AND MINOR ELEMENT OXIDE AND TRACE ELEMENT CHEMISTRY

4.3.1 Major Element Oxides

Twenty-eight samples were analyzed for major element oxides (Tables E.2 and E.4A). There are no published analyses for Wernecke Supergroup rocks or OMB from the Ogilvie Mountains. Furthermore, there are few detailed studies of the geochemistry of stratified Wernecke Supergroup rocks from elsewhere. Delaney (1985) and Goodfellow (1979) have published some analyses of Wernecke Supergroup rocks from the Wernecke Mountains; these are used below.

Fairchild Lake Group and Quartet Group sediments from the Wernecke Mountains generally are similar chemically (Goodfellow, 1979; Delaney, 1985). There are two notable exceptions: specifically, Fairchild Lake Group rocks are higher in Ca+Mg, and lower in Na than Quartet Group rocks. Limited analyses of Fairchild Lake Group and Quartet Group rocks from the present study support this conclusion. A typical Quartet Group sandstone (sample BL54-3) plots in the potassic sandstone field of the Fe_2O_3+MgO, Na_2O, K_2O ternary diagram.

Fairchild Lake Group and Gillespie Lake Group are dolomite-rich rocks although megascopically and microscopically, Fairchild Lake Group rocks contain more silty to gritty clastic material. Chemical analyses of rocks from the two groups are reported in Table E.4A. Gillespie Lake Group dolostone (sample BL25-5) contains less SiO_2 (8% <u>vs.</u> 33%), more MgO and CaO (45% combined <u>vs.</u> 28% combined) and less Fe_2O_3 and K_2O (2.3% and 0.5% <u>vs.</u> 2.6% and

3.4%) than silty or sandy dolostones represented by sample BL3-7). Chemical analyses of two dolomitic siltstones of the Fairchild Lake Group (Table E.2; samples BL9-2 and BL9-22) are also chemically distinct from Gillespie Lake Group dolostone. In general, the whole rock chemical compositions reflect the different depositional settings of the lithologic units that comprise the Wernecke Supergroup.

4.3.2 Minor and Trace Elements

Forty-five samples were evaluated for their minor and trace element content (Tables E.2 and E.6). Trace elements can provide information about the petrogenesis of lithologic units. For example, Th, Hf, Co, La and Sc are not dispersed by interactions with sea water (Taylor and McLennan, 1985). Analyses of Fairchild Lake Group, Quartet Group and Gillespie Lake Group rocks are plotted in the ternary diagram La - Sc - Th (suite 3 data). Average upper crust (NASC; Haskin et al., 1968) is plotted for reference (Figure 4.1). The majority of data plot within, or close to, the dashed outline representing the compositional spectrum of post-Archean shales (Taylor and McLennan, 1985). Anomalous samples, relative to upper crust, occur as: (i) a cluster just below the La apex, and (ii) an isolated point offset toward the Sc apex. In the case of (i) the four analyses consist of two hematite-rich breccias (samples BL24-12 and BL34-15), a carbonate-rich matrix breccia (sample BL35-4), and an intrusive, coarsely crystalline carbonate dyke (sample MS-1I). The location of these samples reflects the relative enrichment of La in the rocks over both Th and Sc. This is particularly apparent for sample BL35-4, which is comprised of abundant clastic material. However, the remaining three samples are relatively depleted in Th (two are below detection limit of 0.5 ppm: these were assigned values of 0.3 ppm for plotting purposes) and Sc. Sedimentary rock fragments are rare to absent in the latter.

4.4 RARE EARTH ELEMENT GEOCHEMISTRY OF OGILVIE MOUNTAIN BRECCIAS

Sixteen breccias, three separates of breccia matrix and three sedimentary rock samples, briefly described in Table E.5, were analyzed by instrumental neutron activation analysis (INAA). Concentrations of the following REEs were determined: La, Ce, Pr, Nd, Sm, Eu, Gd, Tb, Dy, Ho, Er, Tm, Yb and Lu. The results are presented in Table E.6; analytical techniques are described in Gibson and Jagam (1980). Detection limits for the individual REE varied from 0.1 ppm for samarium to 200 ppm for gadolinium (see Table E.8). Rare earth element concentrations below detection limits are reported as less than ("<") the detection limit for that particular REE.

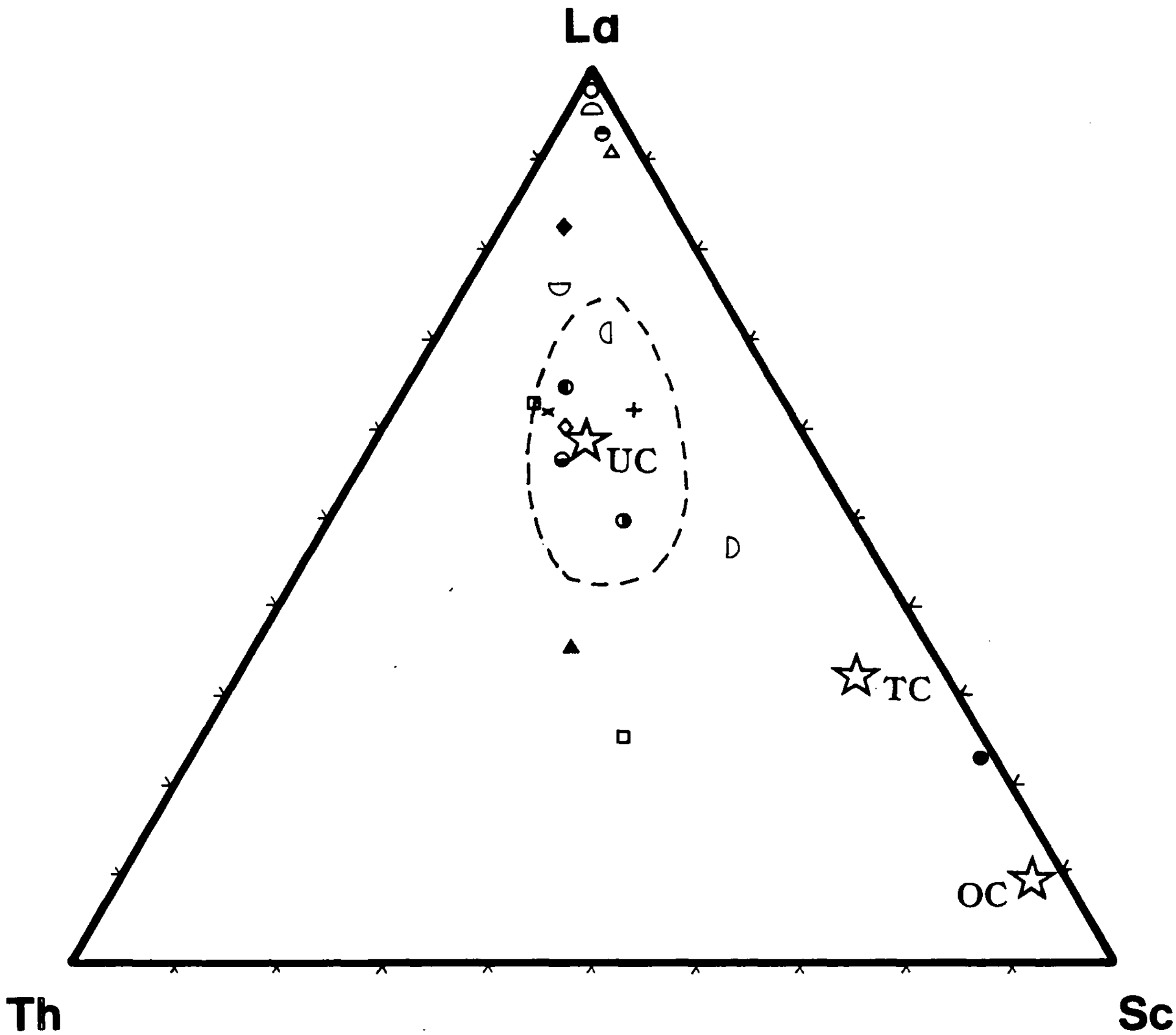

Figure 4.1a Ternary plot of La-Th-Sc. Data from sample suite 3 are plotted; symbol codes are listed on the following page. UC = upper crust; TC = bulk continental crust; OC = oceanic crust (from Taylor and McLennan, 1985). Dashed line represents field of 40 shale analyses (from Taylor and McLennan, 1985).

×	BL1-1	Quartet Group; sandstone
+	BL33-1	Fairchild Lake Group; iron formation
○	MS-1I	carbonate dyke
●	BL18-10	hematitic carbonate breccia matrix
□	TW-208A	BM1; chlorite-rich matrix and Monolithic breccia chloritic fragments
□	BL26-2	BM1; carbonate-rich matrix
△	BL34-15	hematite-vein quartz breccia
▲	BL54-1	BM1; carbonate-rich matrix
◇	BL50-6	BM4; matrix poor
◆	BL33-3	BM1; carbonate matrix and trace sulphides
◓	BL46-10	BHcl; abundant dolostone and mudstone fragments
◒	BL35-4	BHcb; abundant silty dolostone and quartzite fragments
◐	BL50-2	BHcl; abundant argillite and dolostone fragments
◑	BL87-70	BHcb; abundant dolostone, sandstone and mudstone fragments
◡	BL43-7	BHh; dolostone and mudstone fragments common
◠	BL24-12	BHh; clast poor
◖	BL27-6	Slats Creek group conglomerate
D	P-1	Coast Mountains granodiortite

Figure 4.1b List of symbols and their corresponding sample numbers and lithologic name for the La-Th-Sc diagram on Figure 4.1a.

4.4.1 Data Presentation

Numerical analysis and graphical methods are used to present and evaluate the rare earth element (REE) data. Numerical analysis of REE data consists mainly of: (i) comparing the sum of the 14 REEs analyzed with established ranges for different rock types from the literature, and (ii) evaluating the relative fractionation between REEs using chondrite normalized ratios. Graphical methods utilize plots of REE, normalized to chondrite, to produce spider diagrams or **REE patterns**.

Rare earth element totals reflect the degree of fractionation, relative to primordial mantle, that has taken place during the formation of a rock (Henderson, 1984). REE totals, listed in Table E.6 and discussed below, can be compared with typical REE totals for a number of reference materials such as chondritic meteorites (undifferentiated estimates of primordial earth), shale (average upper crust), mid-ocean ridge basalt (MORB), carbonatites (strongly fractionated, REE-rich carbonate rock). This comparison is limited because REE totals for many rock types have ranges that overlap significantly.

Chondrite normalized REE ratios are used to express the relative degree of fractionation of the REE (Henderson, 1984). The ratio La/Lu (Table E.5) provides one measure of the overall slope of the normalized REE pattern as long as the plot approximates a straight line (the higher the ratio the higher the degree of fractionation and the steeper the negative slope). It also provides the degree of relative fractionation between light (La to Sm), and heavy (Tb to Lu) REEs. Similarly the ratio La/Sm and Tb/Lu (Table E.5) give relative degrees of fractionation within the light REE and heavy REE portions of the REE pattern, respectively. These ratios are useful for general comparison of rocks, but in summing the data some critical information, such as anomalous values for single elements, is lost. Graphical representation has the attribute that all the data is illustrated and anomalous values are apparent.

The normalized REE abundances are plotted vs. the REE in order of increasing atomic number. The curve connecting the normalized rare earth element abundances is called a rare earth element pattern. Raw REE data is normalized relative to a composite of 12 chondrites from Wakita et al. (1971; in Boynton, 1984) (Table 4.1). The North American shales composite (NASC; Haskin et al., 1968), an estimate of the REE composition of the upper crust, is shown in Table 4.1. Calculated chondrite normalized values are shown in Table 4.2.

Normalization against chondritic meteorites is the commonly accepted procedure because chondritic meteorites are thought to approximate primordial earth REE abundances (Henderson, 1984). The REE pattern for the primordial mantle is assumed to be flat because REEs have not fractionated. Chondrite normalized REE patterns for all 18 samples are catalogued in Figures 4.2 to 4.4.

The REE content of shales are representative of the earth's upper crust because erosion of the continents and the sedimentary processes which deposit material in ocean basins have an homogenizing effect. Shales are reasonably invariable in REE concentration between different source areas, and are enriched in total and light REE relative to chondrite. Their constant nature with respect to REE concentrations provides a useful standard for comparison of the crustal rocks from this study.

Several rare earth element concentrations are below detection limit (e.g. Pr, Gd and Er), and for these REE the detection limits themselves were normalized. These ratios, however, could be used only in a limiting sense. Thus, gaps are created in the REE patterns making their interpretation more difficult. For example, in the case of sample BL33-1 (banded iron formation) only 3 of 9 elements are reported so that the REE pattern consists of three isolated points.

Table 4.1 Rare earth element abundances in chondritic meteorites (Wakita et al., 1971), used to normalize the raw sample data (Table E.6), and the North American shales composite (NASC; Haskin et al., 1968). NASC, an estimate of the REE compostion of the upper crust, is plotted in Figures 4.2, 4.3 and 4.4 for reference. Normalized abundances are in Table 4.2.

Element	Name	Atomic Number	Chondrites (composite of 12)	Shale (NASC) North America
La	lanthanum	57	0.34	32
Ce	cerium	58	0.91	73
Pr	praeseodymium	59	0.121	7.9
Nd	neodymium	60	0.64	33
Pm[1]	promethium	61		
Sm	samarium	62	0.195	5.7
Eu	europium	63	0.073	1.24
Gd	gadolinium	64	0.26	5.2
Tb	terbium	65	0.047	0.85
Dy	dysprosium	66	0.30	-
Ho	holmium	67	0.078	1.04
Er	erbium	68	0.20	3.4
Tm	thulium	69	0.032	0.50
Yb	ytterbium	70	0.22	3.1
Lu	lutetium	71	0.034	0.48

1: promethium, virtually absent in terrestrial matter because of it's short half life, is not reported.

Table 4.2 Chondrite normalized REE data for 17 rocks from the Coal Creek Inlier, southern Ogilvie Mountains, west-central Yukon Territory. The duplcate analyses for four samples, presented in Table E.6, were averaged prior to normalizing. Normalizing standards are in Table 4.1.

	BL33-1	BL1-1	BL27-6	BL26-2	BL33-3	BL54-1	TW-208A	BL50-6	BL18-10	BL35-4	BL87-70	BL24-12	BL34-15	BL43-7	BL46-10	BL50-2	MS-1I
La	9.4	167	177	81.9	300	51.5	30.9	151	12.6	1100	57.1	270	37.2	254	94.7	152	353
Ce	7.7	117	117	57.7	185	38.5	24.2	109	12.1	239	41.8	117	41.8	150	64.3	103	223
Pr	<413	<413	<413	<413	<413	<413	<413	<413	<413	<413	<413	<413	<413	<413	<413	<413	<413
Nd	<15.6	68.8	70.3	40.6	98.4	28.1	<15.6	65.6	<15.6	203	34.4	40.6	36.7	78.1	41.4	64.1	144
Sm	7.7	40.0	36.9	19.5	54.4	14.4	8.2	33.8	12.8	106	21.0	15.9	52.1	40.5	21.5	32.3	106
Eu	<13.7	13.7	27.4	<13.7	27.4	<13.7	<13.7	13.7	<13.7	82.2	13.7	54.8	68.5	41.4	<13.7	27.4	41.1
Gd	<770	<770	<770	<770	<770	<770	<770	<770	<770	<770	<770	<770	<770	<770	<770	<770	<770
Tb	<21.3	<21.3	<21.3	<21.3	21.3	<21.3	<21.3	<21.3	<21.3	42.6	<21.3	<21.3	138	<21.3	<21.3	<21.3	63.8
Dy	3.3	16.7	13.3	8.3	20.0	6.7	3.3	16.7	6.7	25.0	16.7	<3.3	115	13.3	8.3	13.3	56.7
Ho	<12.8	<12.8	<12.8	<12.8	<12.8	<12.8	<12.8	<12.8	<12.8	<12.8	<12.8	<12.8	89.7	<12.8	<12.8	<12.8	25.6
Er	<500	<500	<500	<500	<500	<500	<500	<500	<500	<500	<500	<500	<500	<500	<500	<500	<500
Tm	<15.6	<15.6	<15.6	<15.6	<15.6	<15.6	<15.6	<15.6	<15.6	<15.6	<15.6	<15.6	34.4	<15.6	<15.6	<15.6	<15.6
Yb	<2.3	10.9	6.8	6.7	8.2	5.9	5.0	11.4	5.9	16.1	8.6	<2.3	32.7	8.6	6.8	9.5	10.9
Lu	<2.9	11.8	5.9	5.9	8.2	5.9	5.9	11.8	5.9	11.8	8.8	<2.9	19.1	5.9	5.9	8.8	5.9

1 The "less than" sign (<) denotes that the normalized abundance is below the normalized detection limit (see also Appendix E).

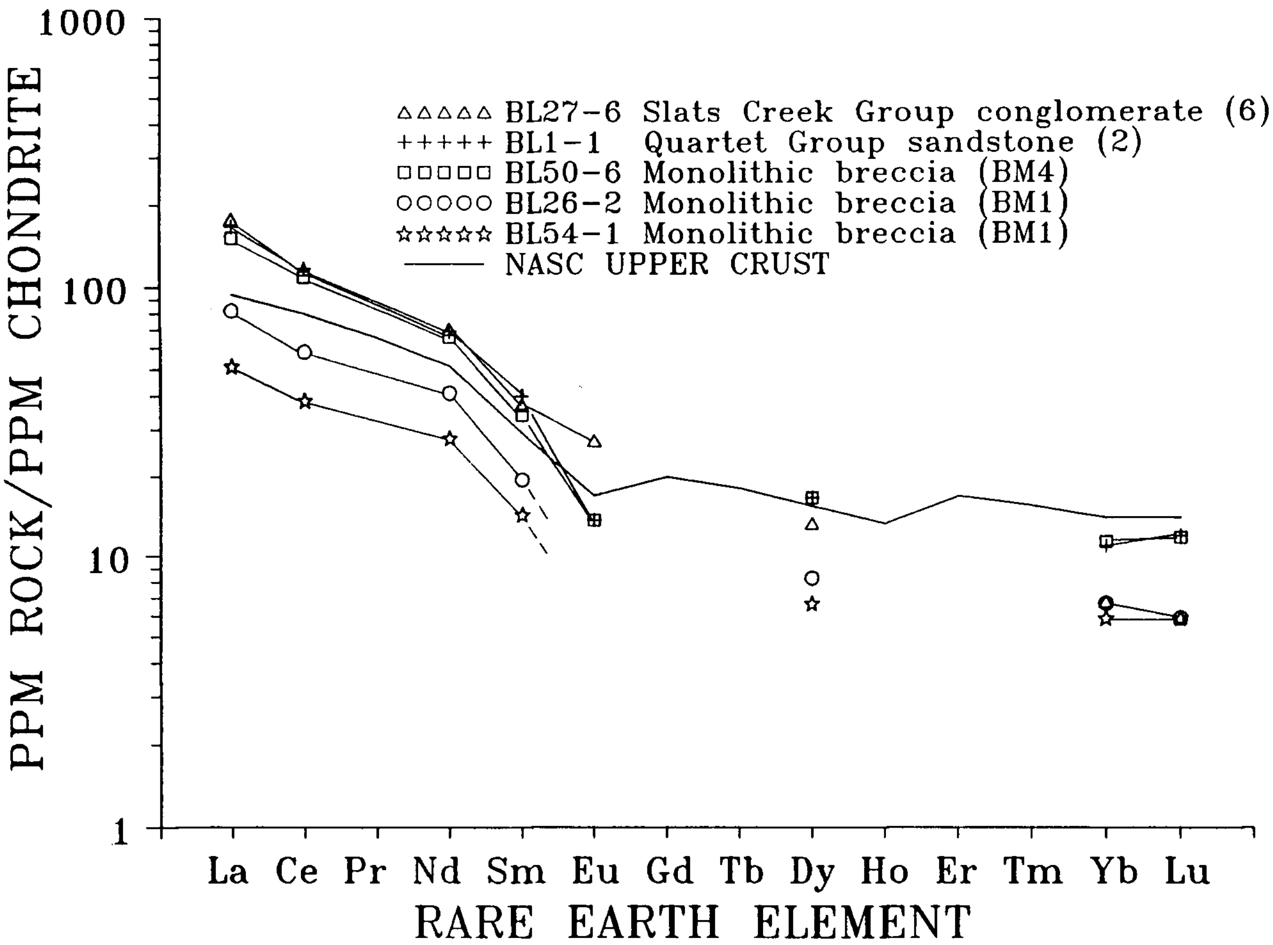

Figure 4.2 Chondrite normalized REE plot of some host sedimentary rocks and monolithic breccias from the Coal Creek Inlier, southern Ogilvie Mountains, west-central Yukon Territory. NASC (solid line) is plotted for reference as a typical REE pattern of the upper crust.

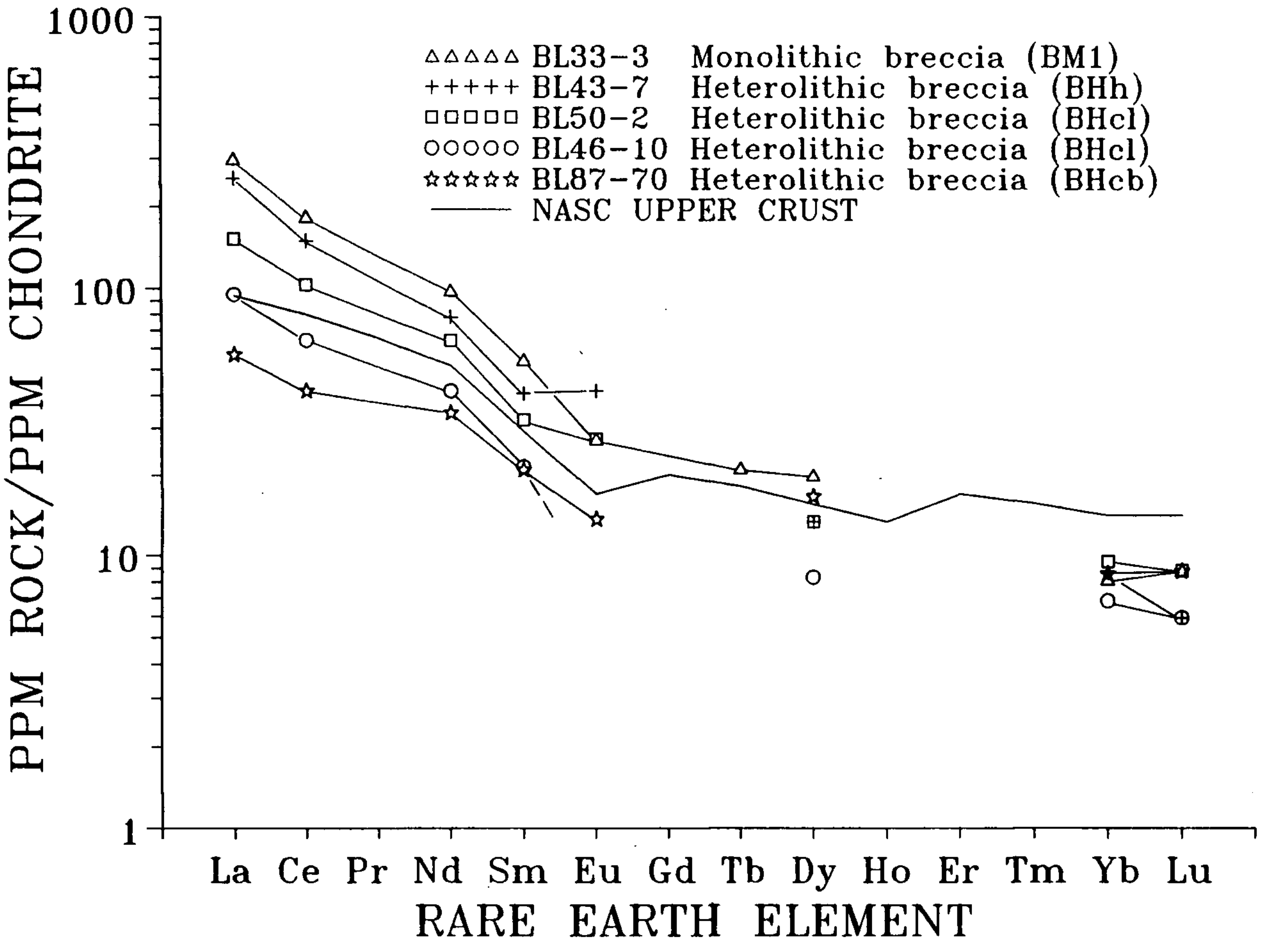

Figure 4.3 Chondrite normalized REE plot of some monolithic breccias and heterolithic breccias from the Coal Creek Inlier, southern Ogilvie Mountains, west-central Yukon Territory. NASC (solid line) is plotted for reference as a typical REE pattern of the upper crust.

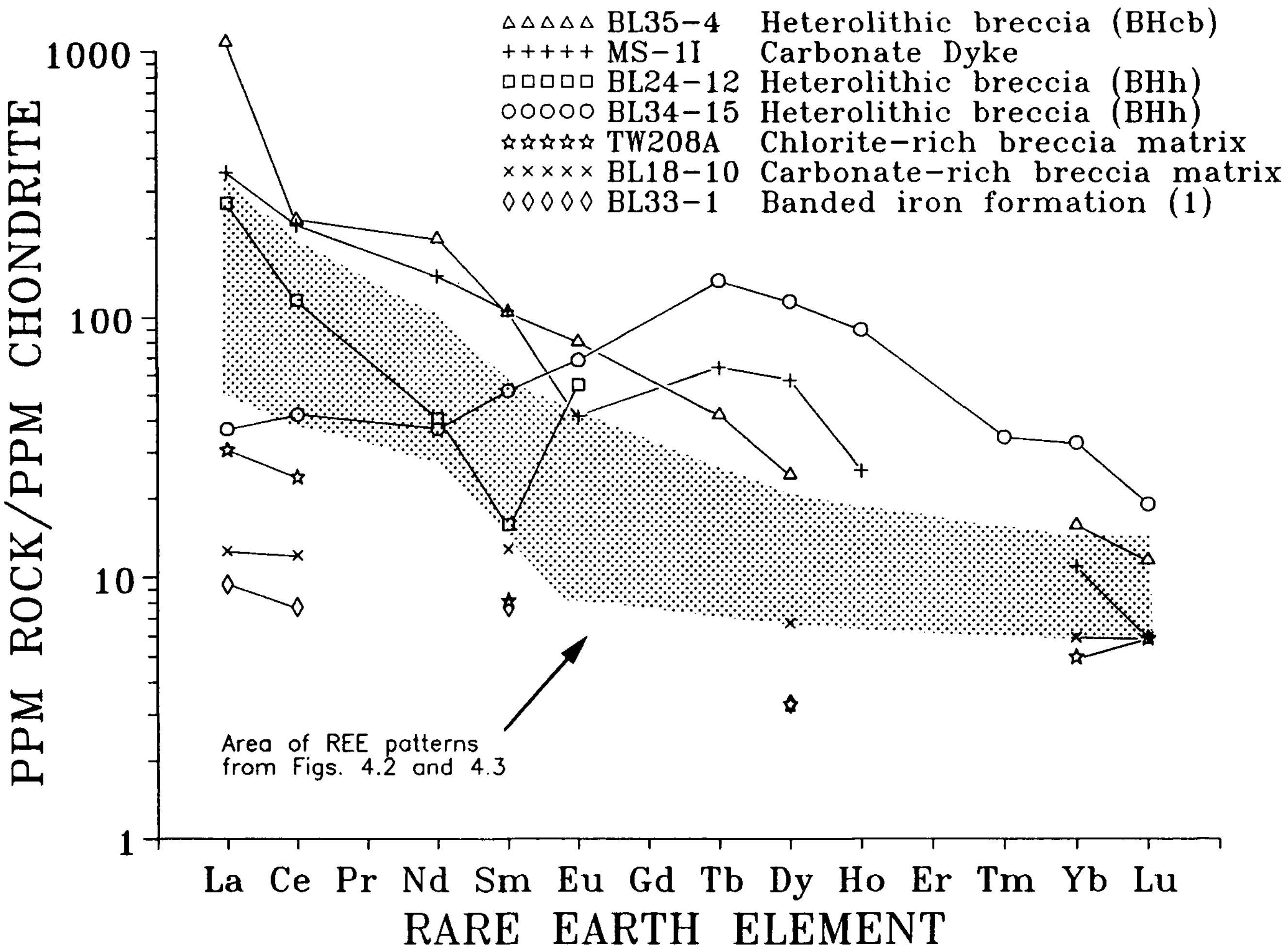

Figure 4.4 Chondrite normalized REE plot of heterolithic breccias, breccia matrix concentrates, a carbonatite(?) dyke, and a banded iron formation from the Coal Creek Inlier, southern Ogilvie Mountains, west-central Yukon Territory. These "anomalous" REE patterns are compared to the field of REE patterns from Figures 4.2 and 4.3 (patterned area) that closely resemble NASC.

4.4.2 Data Analysis

Total REE contents are tabulated in Table E.6. All samples are enriched in REEs relative to chondrite. Some samples are geochemically anomalous. Total REE content for breccia samples ranges from 77 ppm to 769 ppm. Representative samples of regional sedimentary units range from 13 ppm to 226 ppm.

The samples can be divided, based on total REE content, into one of the following three categories: (i) very low REE total (chemical precipitates), (ii) moderate REE total consistent with upper crustal rocks, and (iii) high REE total (anomalous rocks).

REE Ratios for La/Lu range from 2.1 and 93.2. The highest degree of fractionation has occurred in a heterolithic breccia (sample BL35-4) and is a result of the rock being relatively enriched in La. The lowest La/Lu value corresponds to hematite-stained carbonate matrix material (sample BL18-10). This material is apparently not fractionated.

Eu/Sm values range from 0.34 to 3.45. The three hematite-rich breccia samples have an Eu/Sm ratio of greater than one, whereas the sediments range from 0.34 to 0.74. Monolithic breccias range between 0.41 and 0.50, and other heterolithic breccias (including the breccia matrix separates) range from 0.39 to 0.85.

<u>Chondrite-normalized REE patterns</u> (Figures 4.2 to 4.4) fall into two distinct groups: (i) patterns similar to an upper crustal signature (Figures 4.2 and 4.3) and (ii) anomalous REE patterns (Figure 4.4). Anomalous REE patterns were observed for the following sample rock types:

(1) intrusive coarse crystalline carbonate dyke [carbonatite (?)] (sample MS-1I): REE pattern displays a somewhat irregular, but approximately linear negative slope (high lanthanum and low lutetium). The irregularities define a negative europium anomaly, and relatively enriched terbium and dysprosium.

(2) chlorite-rich heterolithic breccia (sample BL35-4): REE pattern has a more regularly negative slope and a negative Ce anomaly.

(3) massive hematite-quartz breccia (sample BL34-15): REE pattern approximates a wave with moderately concentrated light REE (enriched in Sm) and a positive Eu anomaly; it also is relatively enriched in heavy REE that are highly fractionated (steep negative slope). (Two hematite-rich heterolithic breccias, samples BL12-24 and BL43-7, also display positive Eu anomalies, however that is the only similarity between the REE patterns for the two rock types.

(4) hematite-stained carbonate matrix (sample BL18-10): REE pattern is relatively flat.

(5) chlorite matrix (sample 85-208A): REE pattern is concave upwards and is enriched in Yb and Lu relative to other heavy REEs.

4.4.3 Interpretation of Data

The REE patterns for most samples (Figure 4.2 and 4.3 reflect upper crustal rock chemistry and are marked by relatively steep light REE fractionation compared to the heavy REE tail. Dips in Eu abundances are characteristic of upper crustal affinities (Henderson, 1984).

The following samples display markedly anomalous features in their REE patterns (Figure 4.4). These patterns are summarized in Table 4.3. Anomalous samples are: BL33-1 (part of unit 1a, banded iron formation), BL18-10 (unit BHh, iron carbonate matrix to hematite- and carbonate-rich-matrix heterolithic breccia), BL35-4 (unit BHcb, chlorite-rich-matrix heterolithic breccia), BL24-12 (unit BHh, hematite-rich-matrix heterolithic breccia), BL34-15 (BM1, hematite-quartz-chalcopyrite breccia), and MS-1I (a uniform coarsely crystalline carbonate dyke that cross-cuts Fairchild Lake Group Monolithic breccia).

The generally weak, or lack of REE enrichment in OMB relative to unaltered wallrock and similarity of REE patterns and slopes to NASC, with a few exceptions, suggest

Table 4.3 Description of anomalous REE patterns in samples of breccias from the Coal Creek Inlier, Ogilvie Mountains, west-central Yukon.

Sample No.	Features of Anomalous REE Patterns
BL33-1	uniformly depleted, flat REE pattern
BL18-10	relatively flat REE pattern
BL35-4	steep negative slope; enriched in La and depleted in Ce
BL24-12	steep negative slope; likely positive Eu anomaly
BL34-15	depleted light REE end resulting in a "hump" in the middle of the pattern
MS-1I	enriched light REE; steep negative slope

a lack of deep-seated (mantle) involvement. However breccias are generally fragment supported and the abundance of sedimentary material would likely dilute material that was added by a different (and otherwise chemically recognizable) process.

A few samples are enriched in total REE, have variable La/Lu ratios, and anomalous REE patterns relative to upper crust. These samples are either fragment-poor breccias or samples of matrix material from breccias. The anomalous samples might indicate restricted zones of concentrated transport and hydrothermal deposition of REE.

5.0 ORIGIN OF THE OGILVIE MOUNTAINS BRECCIA OF THE COAL CREEK INLIER

5.1 WORLD EXAMPLES OF BRECCIAS SIMILAR TO OGILVIE MOUNTAINS BRECCIA (OMB)

Ogilvie Mountains breccia (**OMB**), and Wernecke Mountain or Wernecke-type breccia, are hosted in Wernecke Supergroup rocks. Both breccias are similar in age and structural style (Bell, 1982), matrix and fragment composition, and alteration (Abbott, 1986; Delaney, 1981). However, significant mineralization is known only in the Wernecke-type breccias (Eaton, pers. comm., 1988).

Wernecke-type breccias are similar in general geometry, approximate age and minor element signature to breccias of the Adeladian Province, Australia (Bell, 1982, 1986). Breccias in the Adeladian Province host deposits in the Flinders Ranges, Australia (Dalgarno and Johnson, 1965; Thomson, 1965) and the world class Olympic Dam Cu-U-Au-Ag deposit (Orestes and Einuadi, 1988; Orestes et al., 1989). Bell and Jefferson (1987) and Jefferson (1978) speculated that similarities in regional stratigraphic sequence, age and possibly paleomagnetic indicators suggest that Proterozoic rocks in central Yukon and the Adeladian Province were once adjacent. This hypothesized supercontinent may have broken up either around 1300 or 750-600 Ma. Both shelf edges were later deformed by accretion of island arc and continental fragments--namely the Cordilleran margin in North America and the Great Divide Range in Eastern Australia.

Ogilvie Mountains breccia features are similar to those from Middle Proterozoic breccia deposits on the East Arm of Great Slave Lake (Reinhardt, 1972) and near Bathurst Inlet (Cecile and Campbell, 1977), both in the District of Mackenzie, Northwest Territories. The continental margin setting of these are similar to **OMB**. East Arm breccias do, however, involve basement rocks and **OMB** do not. However, both breccias are emplaced along faults and along bedding. Textural varieties of breccia are also similar. Locally Bathurst Inlet and **OMB** breccias display contorted fragments and disrupted zones that possibly represent semiplastic brecciation and dewatering, respectively. Bathurst Inlet and **OMB** breccias both host unusually zoned quartz and carbonate crystals that are identical in thin section. These crystals are considered by Cecile and Campbell (1977) to be evidence for the presence of interstitial solutions among the breccia fragments. Table 5.1 summarizes physical features of these breccias upon which genetic interpretations have been based.

Mud volcanoes and diapirs of the Barbados, Caribbean (Brown and Westbrook, 1988) and Timor, eastern Indonesian (Barber et al., 1986) areas, share many features with **OMB** of the Coal Creek Inlier. Most significantly, they formed in continental shelf settings and are similar in size and extent. Emplacement of the diapirs are tectonically triggered and structurally controlled. A pressurized source bed for brine, and brittle and plastic fragments, is fundamental to the generation of a mud diapir. An appropriate source unit appears to be involved in the **OMB**. Hydrothermal alteration and the variety of breccia textures observed in **OMB** could have been generated during the formation of mud diapirs. Because mud diapirs breach the surface as mud volcanoes, related sea-floor sedimentary processes may have been important. Specifically, some of the iron formation associated with **OMB** might be related to hydrothermal exhalations from mud diapirs in this way.

5.2 ORIGINS PROPOSED BY OTHERS FOR OGILVIE MOUNTAINS BRECCIA (OMB)

Several theories for the origin of the Ogilvie Mountains breccia (**OMB**) have evolved. In the Coal Creek Inlier, Southern Ogilvie Mountains, Mercier (1987), observed concordant contacts in a few locations, and proposed that

Table 5.1 A comparison of the characteristics of Proterozoic breccia deposits from the Ogilvie and Wernecke Mountains to Olympic Dam and Mt. Painter, Australia, and to East Arm of Great Slave Lake and Bathurst Inlet.

	Coal Creek[1] Inlier	Wernecke[2] Mtns.	Olympic Dam[3]	Flinders Ranges[4]	East Arm of Great Slave Lake[5]	Bathurst Inlet[6]
Regional Setting	Continental margin	Continental margin	Adelaide Geosyncline	Adelaide Geosyncline	Continental margin	Continental margin
Tectonic Setting	Compressional regime	Extensional regime	Extensional regime	Orogeny (mild)	Extensional regime	Transtensional
Structural Control	Major Proterozoic faults	Faults	Deep-seated fractures	Fold axes, Deep faults	Deep-seated fractures	Sinistral strike-slip faults
Host Rock and period of deposition	Wernecke SG and Lower Fifteenmile group >0.9-1.6? Ga	Wernecke SG 1.2-1.6? Ga	Alkalic granite 1.6 Ga	Adelaide Series Heysen SG Warrina SG 1.4-0.55 Ga	Hornby Channel FM Proterozoic Archean granitic gneiss >2.1 Ga	Goulburn Group Early Proterozoic 1.7-2.5 Ga
Approx. age of Deposit	Middle to Late Proterozoic	Late Proterozoic	1.4-1.5 Ga	Late Proterozoic to Early Cambrian	Early Proterozoic	Early Proterozoic
Mineralogy	Cu, U ?	Cu, Co, U	U-Cu-Au-Ag (REE and P)	Cu	U, Cu	U ?
Alteration	carbonate hematite quartz chlorite tourmaline sericite clay k-spar	carbonate hematite quartz chlorite k-spar sericite albite clay	hematite quartz sericite chlorite kaolinite carbonate	refer to Coats (1965)	carbonate quartz sericite chlorite white mica	carbonate quartz chlorite tourmaline
Morphology	Discontinuous linear zones; irregularly-shaped bodies	Discontinuous linear zones; irregularly-shaped bodies	Breccia pipes, stockworks, irregular replacements, and exhalative seds	Irregular and domal	Pipe-like Fault bounded linear zones	Dykes and large cylindrical bodies

1 = this study; 2 = Laznicka and Gaboury (1988), Bell (1986, 1982), Laznicka and Edwards (1979); 3 = Oreskes and Einaudi (1988), Oreskes et al. (1989); 4 = Coats (1965), Dalgarno and Johnson (1968), Lemon (1985), Bell (1987); 5 = Reinhardt (1972); 6 = Cecile and Campbell (1977).

the breccias were sedimentary--a product of weathering and erosion. However, his proposed sedimentary processes do not effectively address cross-cutting relationships and the concentration of breccias along regional structural breaks. The latter probably represents faults that were active before and during emplacement of breccia. Although layered breccias and breccias with preferred alignment of elongate fragments occur in the Coal Creek Inlier, they are subordinate in volume to cross-cutting breccia bodies. Dyke- and pipe-like exposures are not consistent with a normal sedimentary origin. The interpretation of Mercier (1987), furthermore, provides neither an explanation for the pervasive alteration displayed by and surrounding the breccias, nor the occurrence of breccias at four stratigraphic levels in the Wernecke Supergroup.

Support for either a glacial or alluvial origin of OMB is meager (cf. Yeo, 1981). Glacial action leaves a blanket of sand, gravel and clay with at least some clasts that were not locally derived (exotic); rounded matrix supported clasts are common. Isolated breccia-like bodies with either gradational contacts or sub-vertical contacts are not likely to be glacial in origin. Furthermore, since glacial deposits represent a time-horizon, the requirement of four advances of lithologically similar breccias to explain their occurrence at four levels in the stratigraphy of the Ogilvie Mountains seems unlikely. Alluvial processes are similarly inappropriate. In addition, such deposits are stratified, commonly display graded beds, and thicken toward their source.

Widespread exposure of **OMB** crosscut Wernecke Supergroup stratigraphy at a high angle (Thompson and Roots, 1982; Abbott, 1986). The association of mafic dykes with breccias has also been recognized in these studies. An epigenetic origin followed by lithification and deformation, including extensional faulting of the Wernecke Supergroup, was proposed by Thompson and Roots (1982). No mechanism for breccia generation was discussed.

Numerous genetic theories have been developed for the Wernecke-type breccias. Most of these origins have been assumed to apply to **OMB**. These include: steam brecciation from dykes (Laznicka and Edwards, 1979), diatremes from deep-seated igneous activity (Bell, 1978; Bell and Delaney, 1977; Archer et al., 1977; Archer and Schmidt, 1978), and diapirism of evaporitic material (Bell, 1986).

5.3 GEOLOGICAL CONSTRAINTS ON GENESIS OF THE OGILVIE MOUNTAINS BRECCIA (OMB)

The genesis of the **OMB** is constrained by the geology reported in this thesis. Field observations, which relate directly to the genesis of the **OMB**, and interpretive comments follow:

(1) Breccia bodies follow regional east-trending faults (> 20 km long) that are deep-seated and are appropriate conduits for the intrusion of breccia and associated fluids.

(2) Bodies of crackle breccia, that show dilation between (and rotation of) angular fragments, appear to have been formed by hydrofracturing.

(3) Bodies of crackle breccia are common in the hangingwall of breccia bodies.

(4) Breccia bodies are both conformable (sill-like) and cross-cutting (pipe- or dyke-like).

(5) Breccia fragments in heterolithic **OMB** are dominantly Fairchild Lake Group (the proposed source unit).

(6) Rare breccia fragments of igneous rock are from chloritized diabase dykes.

(7) Breccia fragments of crystalline basement do not occur and therefore, basement was probably not involved in the development of **OMB**.

(8) Breccia fragments show undeformed bedding and sedimentary textures which implies that they generally resulted from brittle fracturing of sedimentary units.

(9) Rare breccia fragments show conspicuous plastic deformation as though formed from partially lithified sediments.

(10) Breccia matrix consists of mineral grains of dolomite, quartz and clay that was most likely derived from comminution of host sedimentary rock.

(11) Breccia matrix generally contains significant clay of primary or secondary origin: chlorite, quartz, calcite, hematite, muscovite, tourmaline, potassium feldspar (microcline) and albite are likely secondary products derived from metasomatic alteration during formation of the breccias.

(12) Breccia matrix that is chlorite- and hematite-rich commonly displays trains of quartz and carbonate crystals and small rounded wall rock fragments that indicate fluid flow or streaming; hydrothermal fluids accompanying the breccia could have caused the hematization and chloritization.

(13) Breccia matrix has REE patterns that are generally consistent with average crustal sedimentary rocks; there is no evidence of a deep-seated mantle source (such as a carbonatitic source).

(14) Sedimentary iron formations appear to be spatially associated with the OMB at several localities; it may have formed on the sea floor from Fe-rich exhalations associated with intrusions of the breccia.

(15) The Fairchild Lake Group unit is an probable source unit for much of the breccia because:

- (a) it makes up large volumes of crackle breccia and block breccia that comprise the majority of OMB,
- (b) it is carbonate- and iron-rich and therefore could contribute these components to fluids resulting in carbonate- and hematite-rich matrix breccias and

associated replacement and exhalitive iron formation deposits,

(c) it is overlain by a turbiditic unit that could have been deposited relatively quickly so that high pore fluid pressure could have formed, and

(d) although lithified, parts of the Fairchild Lake Group could have been partly lithified resulting in the noted plastically deformed fragments.

5.4 GENETIC MODEL PROPOSED FOR THE OGILVIE MOUNTAINS BRECCCIA

Figure 5.1 is a genetic model for the **OMB**. This genetic model is based on field and laboratory observations (summarized in section 5.3). It has been molded from interpretations of Proterozoic breccia deposits (summarized in sections 5.1 and 5.2). The relationships among classic examples from the literature support the conclusions presented here.

Ogilvie Mountains breccia are most readily likened to mud diapirs active in the shelf setting (described in Appendix G.5). Major controls on brecciation are: stratigraphic level, structural weakness, availability of fluids and a driving mechanism. Applying this model to the Ogilvie Mountains breccia (**OMB**) the carbonate-rich rocks of the Fairchild Lake Group are the source beds for diapirs and the generated carbonate- and chloride-rich brines. The overlying sequence of Quartet Group turbidites represents a rapidly deposited load that sealed off the Fairchild Lake Group. The Northern and Southern Breccia Belts would correlate to frontal imbricate faults that extended to a basal detachment zone or decollement that lay within the Fairchild Lake Group.

The process of evaporite diapirism (Bell, 1986) is not invoked here for the generation of **OMB** because, apart from rare gypsum-anhydrite casts in Fairchild Lake Group silty dolostone, no evidence exists for significant evaporite deposition in the Coal Creek Inlier. In fact nowhere in the Fairchild Lake Group have evaporite-rich strata been reported. Textures are dissimilar also. Most evaporite diapirs are highly matrix-dominated bodies that gradually make their way toward the surface passively by gently deflecting overlying strata and flowing around detached blocks of wall rock. The chaotic textures observed in **OMB** indicate that a more violent process than evaporite diapirism was responsible for creating abundant angular fragments. In addition, a process is required to move large volumes of heated brine that could be responsible for causing the metasomatic alteration associated with many of the breccia occurrences in the Coal Creek Inlier.

The mud (sediment) diapir model for formation of the Ogilvie Mountains breccia in the Coal Creek Inlier is supported by:

(1) an appropriate regional tectonic setting (i.e. continental margin with a rapid buildup of deposited turbidite layers that could by sealing and loading create high pore fluid pressures in the overlain Faichild Lake Group).

(2) the likely presence of imbricate reverse faults (see cross-sections on Map 1: in pocket).

(3) a plausible source horizon in the Fairchild Lake Group (limey, algal laminated silty mud) that could have been mobilized by high pore fluid pressure (1, above) along a release route (2, above).

(4) an appropriate scale of brecciation (the area of OMB occurrence is similar in size to that of actively produced mud volcanoes of the Barbados Ridge Accretionary Complex (cf. Map 1 to figure 2 in Brown and Westbrook, 1988; Figure 5.1).

(5) the distribution of elongate and isolated breccia bodies is typical of mud diapirs (cf. figure 2 in Brown and Westbrook, 1988; Figure 5.1).

(6) geometric relationships that indicate relatively low temperature, forceful intrusion that caused breccia to crosscut the sedimentary pile and deflect bedding upwards.

(7) disruption of the country rock that decreases away from

the breccia bodies.

(8) upward transport of fragments from lower strata.

Fairchild Lake Group fine grained limey siltstones and mudstones were deposited on the passive margin of North America during Early to Middle Proterozoic time. Relatively rapid deposition of the Quartet Group turbidite succession followed. The Quartet Group turbidites and overlying Gillespie Lake Group carbonates created the load necessary to create very high pore fluid pressure in the Fairchild Lake Group sediments--assuming they had not completely lithified. The high fluid pressure resulted from interstitial water that could not escape, leaving the sediments undercompacted. The high fluid pressure zone became a plane of detachment or basal decollement (cf. Brown and Westbrook, 1988) in part because it had a low shear strength due to high fluid pressure. Fluid-rich phases were guided along this decollement. The limey (and algal or stromatolitic) fine grained Fairchild Lake Group sediments were thus an appropriate source for the fluid-rich muds which were driven upwards. Pore fluid pressure could have been increased further by the formation of CO_2, due to decarbonation of limey sediments, and by the addition of methane gas produced by the decomposition of organic matter (cf. Hedberg, 1974).

The development of reverse faults, whose distribution

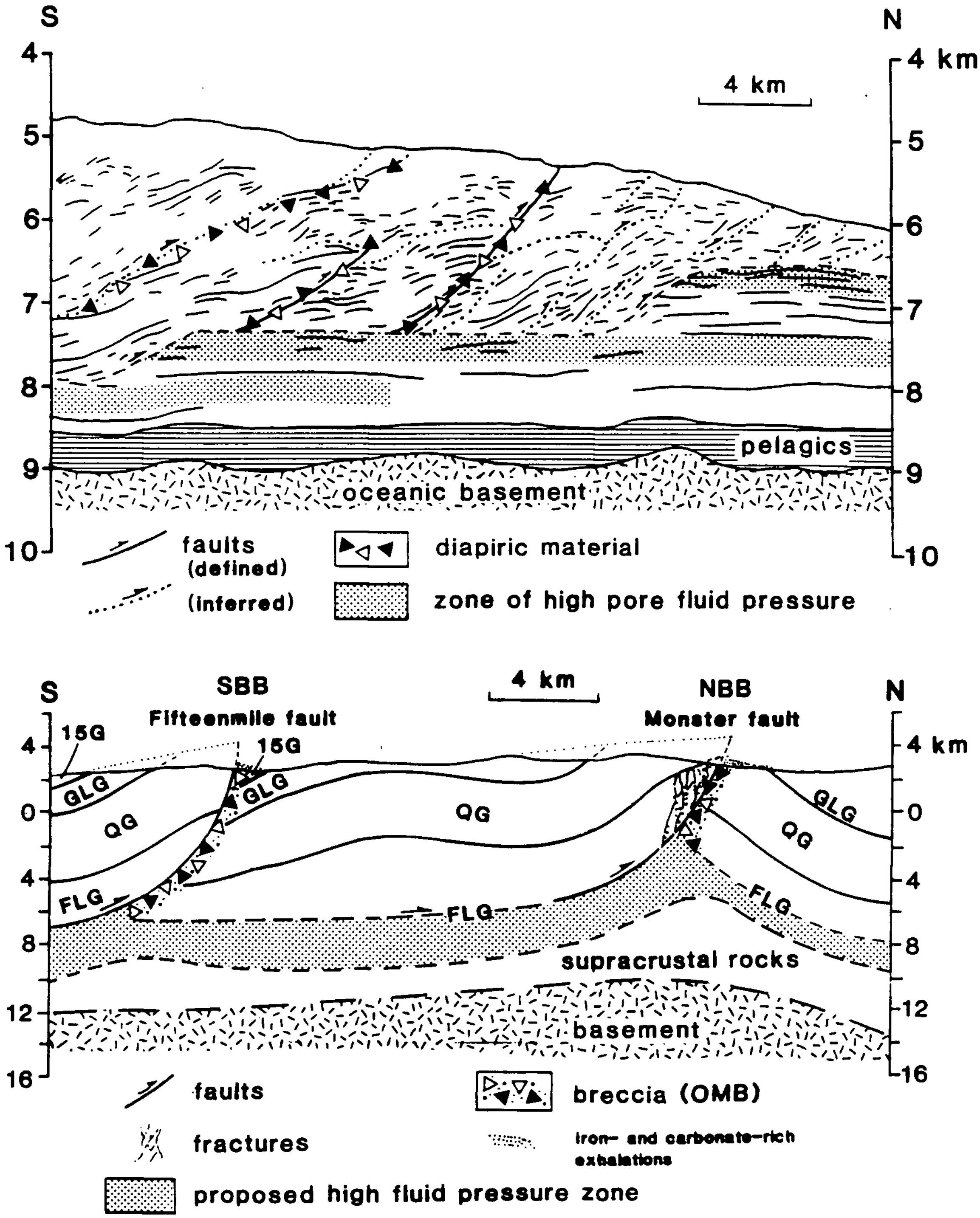

Figure 5.1 Comparison of (top) seismic reflection section across a mud diapir field from Barbados (after Brown and Westbrook, 1988) and (bottom) proposed model for formation of Ogilvie Mountain breccia (OMB). Note particularly the comparable scales, the imbricate faulting and the associated gentle folding. In the OMB model the zone of high fluid pressure would have been the FLG silty carbonate and muddy sediment. These pressures were induced by deposition of Quartet Group turbidites. The Monster and Fifteenmile faults localized emplacement and formation of OMB. FLG = Fairchild Lake Group; QG = Quartet Group; GLG = Gillespie Lake Group; and 15G = lower Fifteenmile group. SBB = Southern Breccia Belt and NBB = Northern Breccia Belt.

and geometry indicate an association with a basal decollement, were developed during deposition of lower Fifteenmile group. This activity appears to have triggered formation of olistoliths in the lower Fifteenmile group and may have triggered diapirism. Subsequent extension or dilation or relaxation along major faults (coinciding with the end of the compressional event that resulted in the development of the Monster and Fifteenmile reverse faults) could have aided the movement of pressurized muds. These faults acted as guides to the ascending, fluid-charged diapirs.

Features observed in the field that support and embellish this theory include:

(1) a disconformity to angular unconformity between the Fairchild Lake and Quartet groups that marks a change in depositional setting from relatively shallow to deeper water,

(2) structural breaks, interpreted as reverse faults, that are spatially associated with the occurrence of OMB along the NBB and SBB; these faults mirror seismic profiles of some modern continental margins (i.e. Barbados: Figure 5.1),

(3) hydrothermal alteration that implies high fluid pressures leading to:

   (a) hangingwall monolithic breccia,

   (b) forceful emplacement of breccia,

(c) heterolithic breccia where multiple units are cut by intruding breccia, and

(d) replacement of matrix--and fragments to a lessor extent--by carbonate, hematite and chlorite.

(4) temperature of the altering fluids, if derived at depth from within the sedimentary basin, would be in the 50 to 200^{o}C range (Hanor, 1979).

One potential problem with this model is the time lag between deposition of the source beds and the subsequent development of mud diapirs. Modern mud diapirs of West Timor (Barber et al., 1986) have ejected blocks of Triassic and Permian sedimentary rock. Thus strata involved in diapirism spans about 250 Ma. The age of the OMB is not known accurately, but evidence presented above and in Appendix A suggests that they are syn- or post-lower Fifteenmile group in age (younger than 1200 Ma). If the Fairchild Lake Group is the source region then at least 250 Ma, and possibly as much as 500 Ma, passed prior to the formation of the breccias.

A modified mud diapir model, in which a fluid (gas and liquid) is driven by high fluid pressures, caused by rapid burial and sealing of underlying sediments, is favoured here. The sediment with entrained fluid had the consistency of a thick slurry able to transport blocks of strata. Less viscous fluid phases generated additional fragments by hydrofracturing.

Possible physical evidence for venting of hydrothermal fluids on the sea floor are layered hematite-rich breccias and iron formation that outcrop near the *BEEHIVE* locality. Hematite-rich breccias (e.g. near the *LALA* showing) indicate a highly oxidizing carbonate- and iron-rich hydrothermal fluid was associated with the breccia.

REFERENCES

Abbott, J.G., 1987: Field activities, 1986; in 1986 Yukon mining and exploration overview. Mineral Resources Directorate Northern Affairs Program, Yukon. D.I.A.N.D.

Aitken, J.D., 1981: Stratigraphy and sedimentology of the upper Proterozoic Little Dal Group, Mackenzie Mountains, Northwest Territories; in Proterozoic Basins in Canada, ed. F.H.A. Campbell; Geological Survey of Canada, Paper 81-10, p. 47-72.

Aitken, J.D. and McMechan, M.E., in press: Middle Proterozoic Assemblages; in DNAG.

Andrew, A., Godwin, C.I. and Sinclair, A.J., 1984: Mixing Line Isochrons: A New Interpretation of Galena Lead from Southeastern British Columbia; Economic Geology, v. 79, p. 919-932.

Armstrong, R.L., Eisbacher, G.H. and Evans, P.D., 1982: Age and stratigraphic-tectonic significance of Proterozoic diabase sheets, Mackenzie Mountains, northwestern Canada; Canadian Journal of Earth Sciences, v. 19, p. 316-323.

Archer, Cathro and Associates (1981) Limited, 1983: Northern Cordillera Mineral Inventory; private file.

Archer, A.R. and Schmidt, U., 1978: Mineralized breccias of early Proterozoic age, Bonnet Plume River district, Yukon Territory; Canadian Institute of Mining and Metallurgy, Bulletin, v. 71, no. 796, p.53-58.

Archer, A.R., Bell, R.T., Delaney, G.D., and Godwin, C.I., 1977: Mineralized Breccias of the Wernecke Mountains, Yukon; Paper presented at the GAC joint session with the Society of Economic Geologists, Vancouver, B.C.

Barber, A.J., Tjokrosapoetro, S. and Charlton, T.R., 1986: Mud volcanoes, shale diapirs, wrench faults and melanges in accretionary complexes, eastern Indonesia; A.A.P.G. Bulletin 70, no. 11, p. 1729-1741.

Bell, R.T., 1978: Breccias and uranium mineralizatoin in the Wernecke Mountains - a progress report; Geological Survey of Canada, Paper 78-1A, p. 317-322.

Bell, R.T., 1982: Comments on the geology and uraniferous mineral occurances of the Wernecke Mountains, Yukon and District of Mackenzie; Geological Survey of Canada, Paper 82-1B, p. 279-284.

Bell, R.T., 1986: Megabreccias in northaeastern Wernecke Mountains, Yukon Territory; Geological Survey of Canada, Paper 86-1A, p. 375-384.

Bell, R.T., 1987: A conceptual model for development of megabreccias in Wernecke Mountains, Canada, Copperbelt, Zaire and Flinders Range, Australia; in Proceedings of Tecnical Communications: Uranium Deposits and Geology of North America; IAEA, p. .

Bell, R.T. and Delaney, G.D., 1977: Geology of some uranium occurances in Yukon Territory; Geological Survey of Canada, Paper 77-1A, p. 33-37.

Bell, R.T. and Jefferson, C.W., 1987: An hypothesis for an Australian - Canadian connection in the Late Proterozoic and the birth of the Pacific Ocean: in International Congress of the Geology , Structure, Mineralization and Economics of the Pacific Rim, proceedings of the Pacific Rim Congress 87, The Australian Institute of Mining and Metallurgy, Parkville, Victoria, p. 39-50.

Best, M.G., 1982, Igneous and metamorphic petrology: San Francisco, W.H. Freeman and Company, 630 p.

Biju-Duval, B., Le Quellec, P., Mascle, A., Renard, V. and Valery, P., 1982: Multibeam bathymetric survey and high resolution seismic investigation on the Barbados Ridge Complex (Eastern Caribbean): A key to the knowledge and interpretation of an accretionary wedge; Tectonophysics, v. 86, p. 275-304.

Boynton, W.V., 1984: Cosmochemistry of the rare earth elements: meteorite studies; in Rare Earth Element Geochemistry (P. Henderson, editor), Developments in Geochemistry 2, Elsevier, Amsterdam, p. 63-114.

Brown, K. and Westbrook, G.K., 1988: Mud diapirism and subcretion in the Barbados Ridge Accretionary Complex: The Role of Fluids in Accretionary Processes; Tectonics, v. 7, no. 3, p. 613-640.

Bryant, D.G., 1968, Intrusive breccias associated with ore, Warren (Bisbee) mining district, Arizona. Econ. Geol., v. 63, p. 1-12.

Bryner, L., 1961, Breccia and pebble columns associated with epigenetic ore deposits. Economic Geology, v.56, p. 488-508.

Burnham, C.W.,1985, Energy release in subvolcanic environments: Implications for breccia formation. Econ. Geol., v. 80, p. 1515-1522.

Burwash, R.A., Baagsgaard, H., and Peterman, Z.E., 1962: Precambrian K/Ar dates from the western Canada sedimentary basin; Journal of Geophysical research, v. 67, p. 1617-1625.

Cairnes, D.D., 1914: The Yukon-Alaska international boundary between Porcupine and Yukon Rivers; Geological Survey of Canada, Memoir 67.

Cecile, M.P., 1982: The lower Paleozoic Misty creek embayment, Selwyn Basin, Yukon and N.W.T., Geological Survey of Canada, Bulletin 335.

Cecile, M.P. and Campbbell, F.H.A., 1977: Large-scale stratiform and intrusive sedimentary breccias of the lower Proterozoic Goulburn Group, Bathurst Inlet, N.W.T.; Canadian Journal of Earth Sciences, v. 14, p. 2364-2387.

Delaney, G.D., 1981: The mid-Proterozoic Wernecke Supergroup, Wernecke Mountains, Yukon Territory; in Proterozoic Basins of Canada; ed. F.H.A. Campbell, Geological Survey of Canada, Paper 81-10, p.1-23.

Delaney, G.D., 1985: The middle Proterozoic Wernecke Supergroup, Wernecke Mountains, Yukon Territory, unpublished PhD. Thesis, University of Western Ontario, London, 372 p.

Delaney, G.D., Jefferson, C.W., Yeo, G.M., McLennan, S.M., Bell, R.T. and Aitken, J.D., 1982: Some Proterozoic sediment-hosted metal occurances of the northeastern Canadian Cordillera; in Society of Economic Geologists, Coeur d'Alene Field Conference, Idaho (R.R. Reid and G.A. Williams, editors), Idaho Bureau of Mines Bulletin, v. 24, p. 97-116.

Delgarno, C.R. and Johnson, J.E., Diapiric structures and late Precambrian - Early Cambrian sedimentation in Flinders Range, South Australia, in Diapirism and Diapirs (J. Braunstein and G.D. O'Brien, editors) A.A.P.G. Memoir 8, p. 301-314.

Devlin, 1988:

Donaldson, J.A., 1976: Paleoecology of Conophyton and associated stromatolites in the Dismal Lakes and Rae groups, Canada; in Stromatolites (M.R. Walter, editor), Elsevier, Amsterdam, p. 523-534.

Eisbacher, G.H., 1976: Proterozoic Rapitan and related rocks, Redstone River area, District of Mackenzie: in Report of Activities, Part A, Geological Survey of Canada, Paper 76-1A, p. 117-125.

Eisbacher, G.H., 1978: Re-definition and subdivision of the Rapitan Group, Mackenzie Mountains; Geological Survey of Canada, Paper 77-35, 21 p.

Eisbacher, G.H., 1981: Sedimentary tectonics and the glacial record in the Windermere Supergroup, Mackenzie Mountains, north-western Canada; Geological Survey of Canada, Paper 80-27, 40 p.

Fritz, W.H., 1980: International Precambrian-Cambrian boundary working group's 1979 field study to Mackenzie Mountains, NWT, Canada; in Current Research, Part A, Geological Survey of Canada, Paper 80-1A, p.41-45.

Gabrielse, H., 1967: Tectonic Evolution of the northern Canadian Cordillera; Canadian Journal of Earth Sciences, v. 4, p. 271-298.

Gabrielse, H., 1972: Younger Precambrian of the Canadian Cordillera; American Journal of Science, v. 272, p. 521-536.

Gabrielse, H., Blusson, S.L. and Roddick, J.A., 1973: Geology of the Flat River, Glacier Lake and Wrigley Lake map-areas, District of Mackenzie and Yukon Territory; Geological Survey of Canada, Memoir 366, 153 p.

Gabrielse, H. and Campbell, R.B., in press: Upper Proterozoic Assemblages; in DNAG.

Gibson, I.L. and Jagam, P., 1980: Instrumental Neutron Activation Analysis of Rocks and Minerals; in Neutron Activation Analysis in the Geosciences, MAC Short Course Handbook v.5, G.K. Muecke, editor, Halifax.

Godwin, C.I. and Sinclair, A.J., 1982: Average Lead Isotope Growth Curves for Shale-Hosted Zinc-Lead Deposits, Canadian Cordillera; Economic Geology, v. 77, p. 675-690.

Godwin, C.I. and Sinclair, A.J., 1981: Preliminary interpretations of lead isotopes in galena lead from shale-hosted deposits in British Columbia and the Yukon Territory; in Geological Fieldwork 1980, BCMEMPR, Geology Division, Paper 1981-1, p. 179-194.

Godwin, C.I., Sinclair, A.J. and Ryan, B.D., 1982: Lead Isotope Models for the Genesis of Carbonate-Hosted Zn-Pb, Shale-Hosted Ba-Zn-Pb, and Silver-Rich Deposits in the Northern Canadian Cordillera; Economic Geology, v. 77, p. 82-94.

Godwin, C.I., Gabites, J. and Andrew, A., 1988: LEADTABLE: A Galena Lead Isotope Data Base For the Canadian Cordillera, With a Guide to its Use by Explorationists, British Columbia Ministry of Energy, Mines and Petroleum Resources, Paper 1988-4.

Goodfellow, W.D., 1979: Geochemistry of copper, lead and zinc mineralization in Proterozoic rocks near Gillespie Lake, Yukon; in Current Research, Part A, Geological Survey of Canada, Paper 79-1A, p. 333-348.

Gordy, S.P., in press: Evolution of the cordilleran miogeocline, Nahanni map-area (105I), Yukon Territory and District of Mackenzie; Geological Survey of Canada, Memoir

Goutier, F.M., 1986: Galena lead isotope study of mineral deposits in the eagle bay formation, Southeastern British Columbia, Unpublished M.Sc. Thesis, University of British Columbia, Vancouver, 153 p.

Graf, J.L. Jr., 1977: Rare earth elements as hydrothermal tracers during the formation of massive sulphide deposits in volcanic rocks; Economic Geology, v. 72, no. 4, p. 527-548.

Green, L.H., 1972: Geology of Nash Creek, Larsen Creek and Dawson map-areas, Yukon Territory; Geological Survey of Canada, Memoir 156, 157 p.

Green, L.H. and Roddick, J.A., 1962: Dawson, Larsen Creek and Nash Creek map-areas, Yukon Territory; Geological Survey of Canada, Paper 62-7.

Grommet, L.P., Dymek, R.F., Haskin, L.A. and Korotev, R.L., 1984: The "North American shale composite": Its compilation, major and trace element characteristics; Geochimica et Cosmochimica Acta, v. 48, p. 2469-2482.

Gussow, W.C., 1968: Salt Diapirism: importance of temperature, and energy source of emplacement, in Diapirism and Diapirs (eds. Braunstein, J. and O'Brien, G.D.) A.A.P.G. Memoir 8, p. 16-52.

Hanor, J.S., The Sedimentary Genesis of Hydrothermal Fluids; in Geochemistry of Hydrothermal Ore Deposits (editor Barnes, H.L.), p. 137-172.

Hearn, B.C., 1968, Diatremes with Kimberlitic Affinities in North-Central Montana. Science, v. 159, p. 622-625.

Hedberg, H.D., 1974: Relation of Methane Generation to Undercompacted Shales, Shale Diapirs, and Mud Volcanoes; A.A.P.G. Bulletin v.58, no. 4, p. 661-673.

Henderson, P., 1984: General geochemical properties and abundances of the rare earth elements; in Rare Earth Element Geochemistry (P. Henderson, editor), Developments in Geochemistry 2, Elsevier, Amsterdam, p. 1-32.

Jefferson, C.W., 1978: Correlation of middle and upper Proterozoic strata between western Canada and south and central Australia; Geological Society of America Abstracts with Programs, v. 10, p. 429.

Jefferson, C.W. and Parrish, R.R., 1989: Late Proterozoic stratigraphy, U-Pb zircon ages and rift tectonics, Mackenzie Mountains, northwestern Canada; Canadian Journal of Earth Sciences, v. 26, no. 9, p. 1784-1801.

Jefferson, C.W. and Ruelle, J.C.L., 1986: The Redstone Copper belt, Mackenzie Mountains, N.W.T.; Geological Survey of Canada, Bulletin

Johnson, W.P., and Lowell, J.D., 1961, Geology and origin of mineralized breccia pipes in Copper Basin, Arizona. Econ. Geol., v. 56, p. 916-940.

Laznicka, P., 1977: Geology and mineralization in the Delores Creek area, Bonnet Plume Range, Yukon; Geological Survey of Canada, Paper 77-1A, p. 435-439.

Laznicka, P., 1987: Breccias and Coarse Fragmentites: Petrology, Environments, Associations, Ores; Developments in Economic Geology, Elsevier, Amsterdam, 832 p.

Laznicka, P., 1989: Breccias and Ores. Part 1: History, Organization and Petrography of Breccias; Ore Geology Reviews, v. 4, p. 315-344.

Laznicka, P and Edwards, R.J., 1979: Delores Creek, Yukon - a disseminated copper mineralization in sodic metasomatites, Econ. Geol., v. 74, p. 1352-1370.

Laznicka, P and Gaboury, D., 1988: Wernecke breccias and Fe, Cu, U mineralization: Quartet Mountain-Igor area (NTS 106E); in Yukon Geology, v. 2; Exploration and Geological Services Division, Yukon, Indian and Northern Affairs Canada, p. 42-50.

Lemon, N.M., 1985: Physical modeling of sedimentation adjacent to diapirs and comparison with Late Precambrian Oratunga breccia body in Central Flinders Ranges, South Australia; American Association of Petroleum Geologists Bulletin, v. 69, no. 9, p. 1327-1338.

McMechan, M.E., 1981: The Middle Proterozoic Purcell Supergroup in the southwestern Rocky and southeastern Purcell Mountains, B.C. and the initiation of the Cordilleran miogeocline, southern Canada and adjacent United States; Canadian Society of Petroleum Geologists, Bulletin, v. 29, p. 583-621.

McMechan, M.E. and Price, R.A., 1982: Superimposed low-grade metamorphism in the Mount Fisher area, southeastern British Columbia - implications for the East Kootenay orogeny; Canadian Journal of Earth Sciences, v. 19, p. 476-489.

Mercier, E., 1985: Precambrien de "Coal Creek Dome" (Montagnes Ogilvie, Yukon, Canada); Unpublished these de 3ieme cycle (Ph.D. thesis), Universite des Sciences et Technologie de Lille, France.

Mercier, E., 1987: Nouvelle interpretation d'une breche proterozoique des montagnes Ogilvie (Cordilliere canadienne - Yukon); Extrait des Annales de la Societe Geologique du Nord, T. CVI, p. 65-72.

Mercier, E., 1989: Evenements tectoniques d'origine compressive dans le proterozoique du nord de la Cordillere canadienne (montagnes Ogilvie - Yukon); Canadian Journal of Earth Sciences, v. 26, no. 1, p. 199-205.

Mertie, J.E., 1933: The Tatonduk-Nation District, Alaska; in U.S.G.S. Bulletin 836, 347 p.

Monger, J.W.H. Souther, J.G., and Gabrielse, H., 1972: Evolution of the Canadian Cordillera: a plate tectonic model; American Journal of Science, v. 272, p. 577-602.

Morin, J.A., 1977: Uranium-copper mineralization and associated breccia bodies in the Wind-Bonnet Plume River area; in Yukon Mineral Industry Report for Yukon Territory 1976, Indian and Northern Affairs Canada, p.1352-1370.

Morin, J.A., 1979: A preliminary report on Hart River (116A/10)-a Proterozoic massive sulphide deposit: Yukon Territory; Mineral Industry Report, 1977, Economic Geology Survey, 1979-9, p.22-24.

Motyka, R.J., Poreda, R.J. and Jeffrey, A.W.A., 1989: Geochemistry, isotopic composition, and origin of fluids emanating from mud volcanoes in the Copper River basin, Alaska; Geochimica et Cosmochimica Acta, v. 53, p. 29-41.

Muecke, G.K. and Moller, P., 1988: The Not-So-Rare Earths; Scientific American, January, p. 72-77.

Mustard, P., 1990: Upper Proterozoic - Lower Cambrian Sedimentary Rocks of the Mount Harper Group, Ogilvie Mountains, Yukon; Unpublished PhD Thesis, Carleton University, 328 p.

Mustard, P.S., Roots, C.F. and Donaldson, J.A., 1990: Stratigraphy of the middle Proterozoic Gillespie Lake Group in the southern Wernecke Mountains, Yukon; Geological Survey of Canada, Paper 90-1E, p. 43-53.

Nance, W.B. and Taylor, S.R., 1976: Rare earth element patterns and crustal evolution - I. Australian-post Archean sedimentary rocks; Geochimica et Cosmochimica Acta 40, p. 1539-1551.

Norris, D.K., 1976: Structural and stratigraphic studies in the northern Cordillera; Geological Survey of Canada, Paper 76-1A, p. 457-466.

Norten, D.L., and Cathles, L.M., 1973, Breccia pipes - Products of Exsolved Vapour from Magmas. Economic Geology, v. 68, p. 540-546.

Olson, J.C., Shawe, D.R., Pray, L.C. and Sharp, W.N., 1954: Rare earth mineral deposits of the Mountain Pass District, San Bernardino County, California; U.S.G.S. Professional Paper 261, 75 p.

Oreskes, N., Hitzman, M.W. and Einaudi, M.T., 1989: Tectonic setting of Olynpic Dam and relation to other Proterozoic Fe-REE deposits (abst.); International Geological Congress, Washington D.C., p. .

Oreskes, N. and Einaudi, M.T., 1988: Origin of LREE-enriched hematite breccias at Olynpic Dam, Roxby Downs, South Australia; G.S.A. Abstracts with Programs, v. 20, p. A143.

Phillips, W.J., 1972, Hydraulic fracturing and mineralization. Jl geol. Soc. Lond., v.128, p. 337-359.

Piper, D.Z.,1974: Rare earth elemants in the sedimentary cycle; Chemical Geology, v. 14, p. 285-304.

Price, R.A., 1964: The Precambrian Purcell System in the Rocky Mountains of southern Alberta and British Columbia: Canadian Petroleum Geologists Bulletin, v. 12, p. 399-426.

Reesor, J.E., 1957: The Proterozoic of the Cordillera in southeastern British Columbia and southwestern Alberta: Royal Society of Canada Special Publication 2, p. 150-177.

Reinhardt, E.W., 1972: Occurances of exotic breccias in the Petitot Islands (85H/10) and Wilson Island (85H/15) map areas, East Arm of Great Slave Lake, District of Mackenzie; Geological Survey of Canada, Paper 72-25, 43 p.

Reynolds, D.L., 1954: Fluidization as a geologic process and its bearing on the problem of intrusive granites. American Journal of Science, v. 252, p. 577-614.

Roots, C.F., 1982: Ogilvie Mountains project, Yukon; Part B: Volcanic rocks in north-central Dawson map-area; Geological Survey of Canada, Paper 82-1A, p. 411-414.

Roots, C.F., 1987: The Regional tectonic setting and evolution of the Late Proteozoic Mount Harper Volcanic Complex, Ogilvie Mountains, Yukon; Unpublished PhD. Thesis, University of Carlton, Ottawa, Canada.

Taylor, S.R. and McLennan, S.M., 1985: The Continantal Crust: its composition and evolution, Oxford, Blackwell Scientific Publications, 312 p.

Tempelman-Kluit, D., 1979: Transported cataclasite, ophiolite and granodiorite in Yukon: evidence of arc-continent collision; Geological Survey of Canada, Paper 79-14, 27 p.

Thompson, R.I., 1986: Repeated extension on the proto-Pacific margin, west-central Yukon (abst.): Current Activities Forum 1986, Geological Survey of Canada, Paper 86-8, p. 11.

Thompson, R.I. and Roots, C.F., 1982: Ogilvie Mountains project, Yukon: Part A: a new regional mapping program; Geological Survey of Canada, Paper 82-1A, p. 405-411.

Thomson, B.P., 1965: Geology and mineralization of South Australia; in Geology of Australia ore deposits, 2nd edition, v. 1 (J. McAndrews, editor): 8th Com. Min. Metall. Cong. Australia and New Zealand, p.

Wakita, H., Rey, P. and Schmidt, R.A., 1971: Abundances of the 14 rare earth elements and 12 other trace elements in Apollo 12 samples: five igneous and one breccia rocks and four soils; Proc. 2nd Lunar Science Conf., p. 1319-1329.

Wanless and Loveridge, 1972:

Yeo, G.M., 1981: The Late Proterozoic Rapitan glaciation in the northern Cordillera; in Proterozoic Basins of Canada; ed. F.H.A. Campbell, Geological Survey of Canada, Paper 81-10, p. 25-46.

Yeo, G.M., Delaney, G.D., and Jefferson, C.W., 1978: Two major Proterozoic unconformities, northern Cordillera: Discussion; Geological Survey of Canada, Paper 78-1B, p. 225-230.

Young, G.M., Campbell, R.B. and Poulton, T.P., 1973: The Windermere Supergroup of the southeastern Canadian Cordillera; in Belt Symposium, v. 1, Department of Geology, University of Idaho and Idaho Bureau of Mines and Geology, p. 181-203.

Young, G.M.,1977: Stratigraphic correlation of Upper Proterozoic rocks of northwestern Canada; Canadian Journal of Earth Sciences, v. 14, p. 1771-1787.

Young, G.M., 1982: The Late Proterozoic Tindir Group, east-central Alaska: Evolution of a continental margin; Geological Society of America, Bulletin, v. 93, p. 759-783.

Young, G.M.,Jefferson, C.W.,Delaney, G.D. and Yeo, G.M., 1979: Middle and Late Proterozoic evolution of the northern Canadian Cordillera and Shield; Geology, v. 7, p. 125-128.

Young, G.M.,Jefferson, C.W.,Delaney, G.D. and Yeo, G.M., 1978: Upper Proterozoic stratigraphy of northwestern Canada and Precambrian history of the North American Cordillera; Idaho Bureau of Mines, 76.p.

APPENDIX A

METALLOGENY OF THE COAL CREEK INLIER

A.1 GALENA-LEAD ISOTOPE INTERPRETATIONS OF MINERAL PROSPECTS HOSTED IN THE COAL CREEK INLIER, NORTHERN CANADIAN CORDILLERA

Galena from nine prospects in Proterozoic rocks of the Southern Ogilvie Mountains of the Northern Cordillera (Figure A.1 and Table A.1) were analyzed for lead isotope ratios. These data have been compiled (Table A.2) to evaluate the age of mineralization and how they might relate to the formation of the Ogilvie Mountain breccias (**OMB**) and related tectonic events. The Coal Creek Inlier is within the pericratonic tectono-stratigraphic environment of the Canadian Cordillera. Since this is upper crustal, all data are evaluated relative to the Pericratonic model (Gautier, 1986; Godwin et al., 1988; cf. Godwin and Sinclair, 1981, 1982) and the Bluebell growth curve (Andrew et al., 1984). In general, the lead isotope values fall on or close to the pericratonic growth curve. These data probably are dated to within 50 Ma by the pericratonic growth curve. Those data that plot below this curve are probably evaluated more accurately using mixing lines between the pericratonic and Bluebell growth curves (Andrew et al., 1984).

Galena lead isotope classification of showings in the Northern Cordillera, including some from the Coal Creek

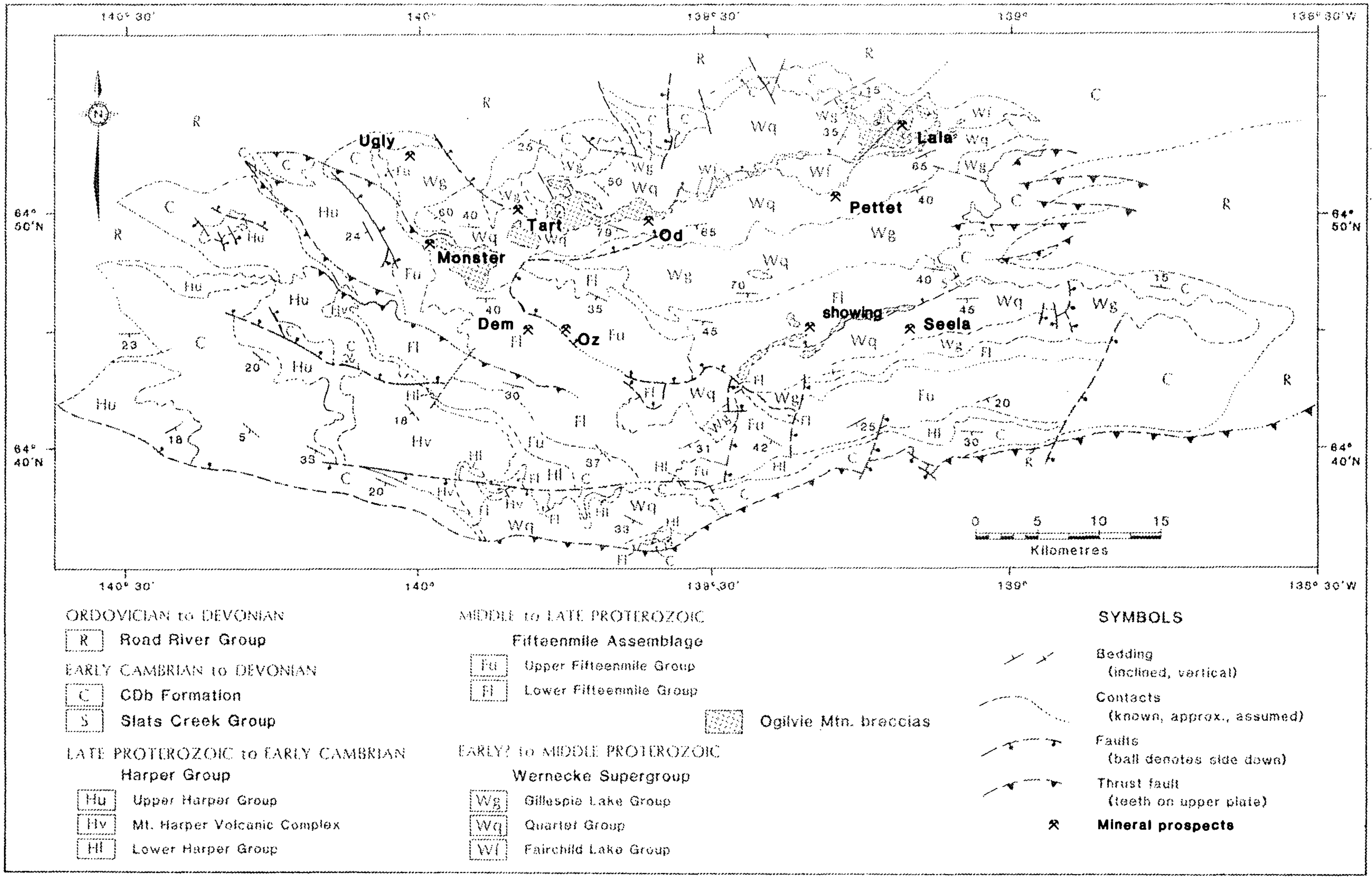

Figure A.1 Map of the Coal Creek Inlier, southern Ogilvie Mountains, west-central Yukon Territory, showing the location of Proterozoic hosted galena bearing mineral occurrences. These occurrences are discussed with respect to their galena lead isotope signatures and there implications on host rock age and age of the Ogilvie Mountain breccia.

Table A.1 Brief descriptions of deposits and showings, evaluated using galena lead isotope analyses, hosted by Proterozoic rocks in the Coal Creek Inlier, southern Ogilvie Mountains, west-central Yukon Territory.

Deposit name	Sample number[1]	NTS: Lat(N), Long(W)	Host unit[2,3]	Deposit type; mineralization[4]
GROUP A (stars)				
OZ	037-AVG7	116B/12W 64.75, 139.75	Gillespie Lake Group (grey dolostone)	Vein, breccia Pb-Zn
MONSTER	038-AVG3	116B/13W: 64.82, 139.97	Fairchild Lake Group	Breccia Zn-Pb
OD	188-201	116B/13E: 64.84, 139.60	Quartet Group	Breccia Pb-?
HART RIVER[5] (cross)				
	082-AVG2	116A/10W: 64.63, 136.87	Gillespie Lake Group (argillite)	Stratiform massive sulphide
TART (triangle)				
	020-AVG8	116B/12: 64.83, 139.83	Gillespie Lake Group (grey dolostone)	Breccia Zn-Cu-Pb
GROUP B (boxes)				
UGLY	013-AVG2	116C/16E: 64.87, 140.03	Gillespie Lake Group	Fault breccia Pb-Zn
SEELA	187-AVG2	116B/14E: 64.78, 139.10	Lower Fifteenmile group	Breecia Pb-?
showing (circle)				
	190-AVG2	116B/11W: 64.45, 139.19	dyke cutting breccia and Lower Fifteenmile group	Veins Pb
DEM (diamond)				
	023-001	116B/13W: 64.75, 139.80	Gillespie Lake Group	Breecia Pb-?

1 Sample numbers are prefixed by the number "10".
2 Host lithologies of deposits not visited are from R.I. Thompson (unpublished open file maps).
3 Refer to Table of Formations (Table 2.1) for host lithologies of those deposits visited.
4 Information regarding deposit type and mineralization is from C.I. Godwin (unpublished galena lead isotope data base).
5 Hart River deposit is in the Wernecke Mountains.

Inlier, was attempted by Godwin et al. (1982). Their interpretation outlined three metallogenic events (Cambrian, Devono-Mississippian, and Cretaceous), none of which can be related to the time of breccia emplacement. Consequently, the five prospects reported for the Coal Creek Inlier in Godwin et al. (1982) were resampled and reanalyzed together with four additional samples from galena-bearing mineral occurrences in the Coal Creek Inlier. A brief summary of each prospect appears in Table A.1. Results from the present study suite, together with adjusted values from an earlier study by Godwin et al. (1982), are shown in Table A.2.

A.1.1 REGIONAL GEOLOGY AND PROSPECT DESCRIPTIONS

Regional geology of the Coal Creek Inlier is described in Chapter 2 (see especially Table 2.1). All samples collected were hosted in Proterozoic rocks of the Coal Creek Inlier. Although none of the samples are from within the breccia complexes that are the focus of this thesis work, it is speculated that metallogenic events might be synchronous with major crustal disturbances reflected by the formation of the breccias.

Detailed information does not exist for the mineral prospects sampled here (Table A.1). The most informative source is the private Yukon Mineral Inventory that was compiled by Archer, Cathro and Associates (Eaton, pers. comm., 1988). Data from their inventory is incorporated in Table A.1

and in the galena lead data base at The University of British Columbia. Data from D.I.A.N.D. publications has also been used. Major categories of deposits are carbonate hosted (4 deposits), vein (2 deposits) and volcanogenic or sedimentary exhalitive (1 deposit), and fault related (2 deposits). Unfortunately, host unit designations in Table A.1 for the Oz mineral occurrence (Gillespie Lake Group) does not match the interpretation in Figure A.1 from recent mapping (Upper Fifteenmile group). This discrepancy cannot be resolved with available information.

A.1.2 GALENA LEAD ISOTOPE ANALYSES

Galena lead isotope analyses were performed at the Geochronology Laboratory, Department of Geological Sciences, The University of British Columbia, by the author, J.E. Gabites or B.D. Ryan (Table A.2). Laboratory procedures used follow those described in Godwin et al. (1988).

Galena lead isotope ratio plots are shown in Figures A.2 through A.4. Fractionation error and ^{204}Pb error trends are included on the lead-lead diagrams to facilitate evaluation of data trends. The Pericratonic and Bluebell model curves are included as references of the upper crust and lower crust, respectively. The Pericratonic model is applicable to the area studied. Estimates of ages using this model are within 50 Ma (cf. Godwin and Sinclair, 1986).

Table A.2 Galena lead isotope data for mineral occurrences in the Coal Creek Inlier, southern Ogilvie Mountains, west-central Yukon Territory. Data from the Hart River massive sulphide deposit (Godwin <u>et</u> <u>al.</u>, 1988), Wernecke Mountains, described in the text, is also shown. Deposits are located in Figure A.1 and Table A.1.

Deposit Name Sample Number[1]	Anal[2]	Normalized Lead Ratios 206/204	207/204	208/204	207/206	208/206
<u>OZ</u>						
037-016	RL	16.190	15.404	35.821	0.95145	2.21261
037-048	BR	16.275	15.412	35.901	0.94696	2.20690
037-048	RL	16.259	15.414	35.868	0.94802	2.20601
037-070	RL	16.215	15.360	35.731	0.94727	2.20360
037-070D	RL	16.265	15.420	35.888	0.94808	2.20646
037-071	RL	16.277	15.417	35.893	0.94717	2.20522
037-201	RL	16.260	15.414	35.865	0.94797	2.20572
037-AVG7		16.249	15.405	35.852	0.94813	2.20665
		[0.033][3]	[0.020]	[0.060]	[0.00148]	[0.00284]
<u>MONSTER</u>						
038-006	RL	16.247	15.426	35.911	0.94949	2.21025
038-015*	BR	16.265	15.417	35.024	0.94785	2.15434
038-015	RL	16.224	15.426	35.893	0.95080	2.21229
038-201	RL	16.188	15.406	35.818	0.95167	2.21263
038-AVG3		16.219	15.419	35.874	0.95065	2.21172
		[0.030]	[0.011]	[0.050]	[0.00112]	[0.00141]
<u>OD</u>						
188-201	RL	16.263	15.418	35.904	0.94809	2.20771
<u>HART RIVER</u>						
082-001	BR	16.520	15.452	36.464	0.93535	2.20726
082-100	BR	16.516	15.457	36.296	0.93588	2.19763
082-AVG2	BR	16.518	15.455	36.380	0.93562	2.20245
		[0.002]	[0.003]	[0.084]	[0.00027]	[0.00482]
<u>TART</u>						
020-001	RL	17.022	15.491	36.758	0.91007	2.15949
020-001R	RL	17.016	15.488	36.732	0.91022	2.15865
020-001D	RL	16.950	15.500	36.681	0.91442	2.16403
020-002	JG	16.703	15.481	36.435	0.92687	2.18139
020-002R	RL	16.696	15.480	36.394	0.92719	2.17981
020-003	RL	16.763	15.689	36.710	0.93595	2.18995
020-003R	RL	16.498	15.445	36.139	0.93616	2.19051
020-100	BR	16.806	15.447	36.403	0.91914	2.16607
020-AVG8		16.807	15.511	36.550	0.92298	2.17483
		[0.181]	[0.078]	[0.222]	[0.01061]	[0.01323]

Table A.2 (continued)

Deposit Name Sample Number[1]	Anal[2]	Normalized Lead Ratios 206/204	207/204	208/204	207/206	208/206
UGLY						
013-002	BR	17.097	15.543	36.723	0.90909	2.14889
013-002	RL	17.032	15.510	36.667	0.91066	2.15280
013-002R*	RL	17.288	15.616	36.905	0.90330	2.13475
013-201*	JG	16.544	15.044	35.523	0.90937	2.14719
013-201D*	JG	16.975	15.468	35.532	0.91122	2.15214
013-AVG2		17.065	15.527	36.695	0.90988	2.15085
		[0.047]	[0.023]	[0.040]	[0.00109]	[0.00275]
SEELA						
187-201*	RL	16.805	15.287	36.246	0.90967	2.15686
187-201R	RL	17.081	15.536	36.896	0.90955	2.16003
187-201D	RL	17.072	15.514	36.985	0.90873	2.16634
187-AVG2		17.077	15.525	36.941	0.90914	2.16319
		[0.067]	[0.017]	[0.065]	[0.00069]	[0.00438]
showing-10190						
190-001	RL	17.615	15.579	37.523	0.88446	2.13020
190-001D	RL	17.598	15.574	37.491	0.88500	2.13042
190-AVG2		17.607	15.577	37.507	0.88473	2.13031
		[0.014]	[0.000]	[0.021]	[0.00000]	[0.00000]
DEM						
023-001	BR	18.824	15.671	38.811	0.83248	2.06273

1 Sample numbers are prefixed by the number "10". Suffixes are as follows: "D" = duplicate analysis, "R" = repeat analysis, and "AVG" followed by a number defines the arithmetic average and the number of analyses used.

2 "Anal" refers to the analyst who produced the data for each sample or sample analyzed: BR = Barry Ryan, JG = Janet Gabites, and RL = Robert Lane

3 Standard deviation is in square brackets.

* The asterisk marks data excluded from cluster averages on basis of probable poor analysis.

A.1.3 RESULTS

Galena lead isotope data from prospects hosted in Proterozoic stratigraphy of the Coal Creek Inlier plot in six separate groups or points (Figures A.2 to A.4). Averaged values, for those prospects with more than one analysis, are plotted. "Groups" are made up of two or more values and "points" consist of one value.

GROUP A (Oz, Monster and Od)

Group A plots as a tight cluster (Figures A.2 to A.4) on the Pericratonic curve and is defined by the isotopic signatures of the **Oz**, **Monster**, and **Od** prospects. These mineral prospects are early Middle Proterozoic (about 1.6 Ga). They appear to represent the oldest deposits in the Coal Creek Inlier. The host rock, therefore, is at least this old. All three prospects are breccia and/or vein deposits and are in different host rocks (see Table A.1) The $^{206}Pb/^{204}Pb$ ratios taken overall are statistically indistinct from each other. If the Od occurrence, in Quartet Group, and the Oz occurrence, in Gillespie Lake Group are syngenetic, then the boundary between Gillespie Lake Group and Quartet Group would be at about 1.6 Ga. This is a reasonable location for this boundary. If, on the other hand, the Monster mineral occurrence is syngenetic, then the Fairchild Lake Group would be earliest Middle Proterozoic. However, since the Fairchild

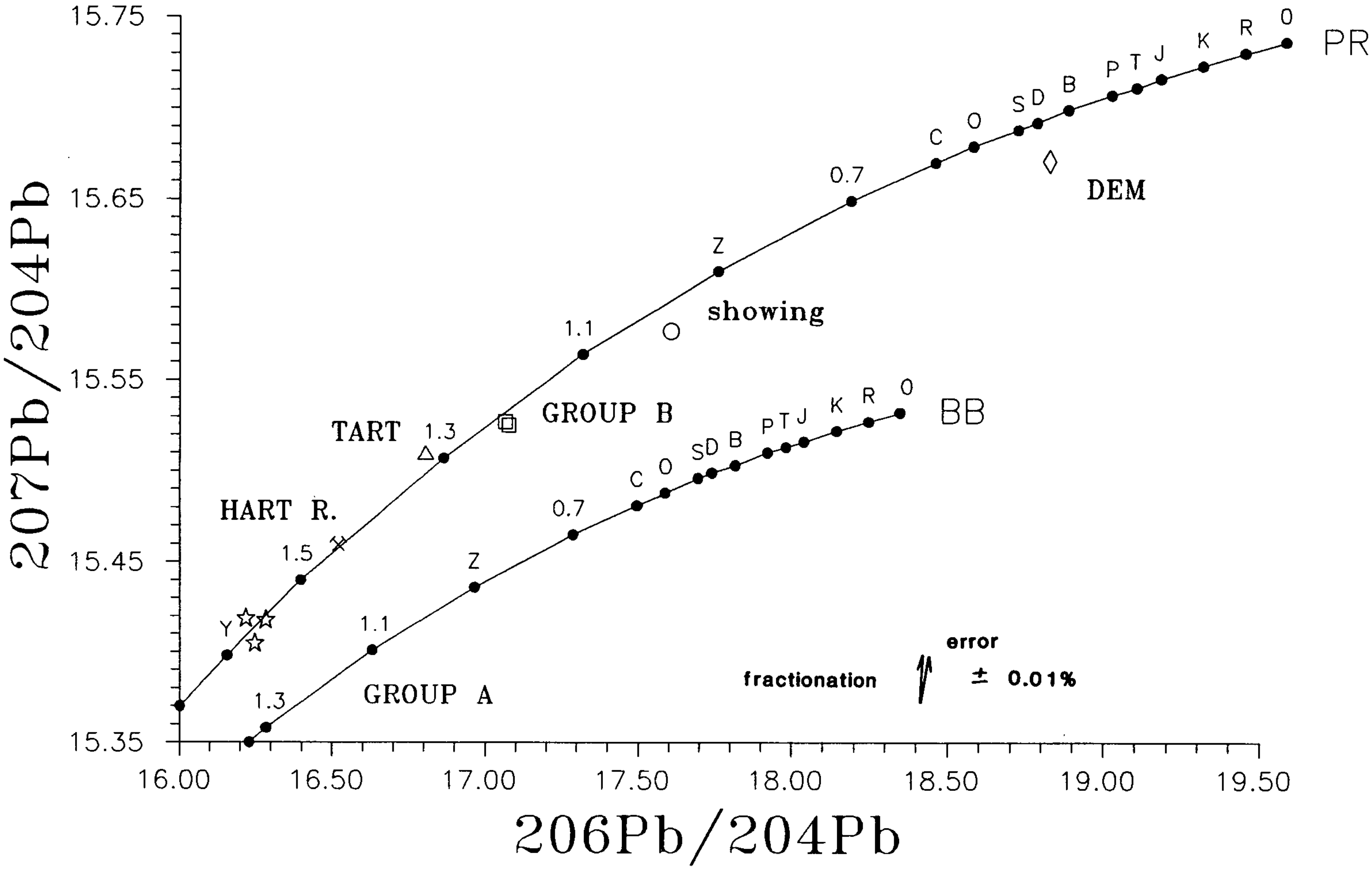

Figure A.2 Galena lead isotope plot of $^{207}Pb/^{204}Pb$ vs. $^{206}Pb/^{204}Pb$ showing the distribution of data from Proterozoic hosted mineral occurrences in the Coal Creek Inlier, southern Ogilvie Mountains, west-central Yukon Territory. Tables A.1 and A.2 present brief descriptions and galena lead isotope data for the mineral occurrences, respectively. Figure A.1 shows their locations.

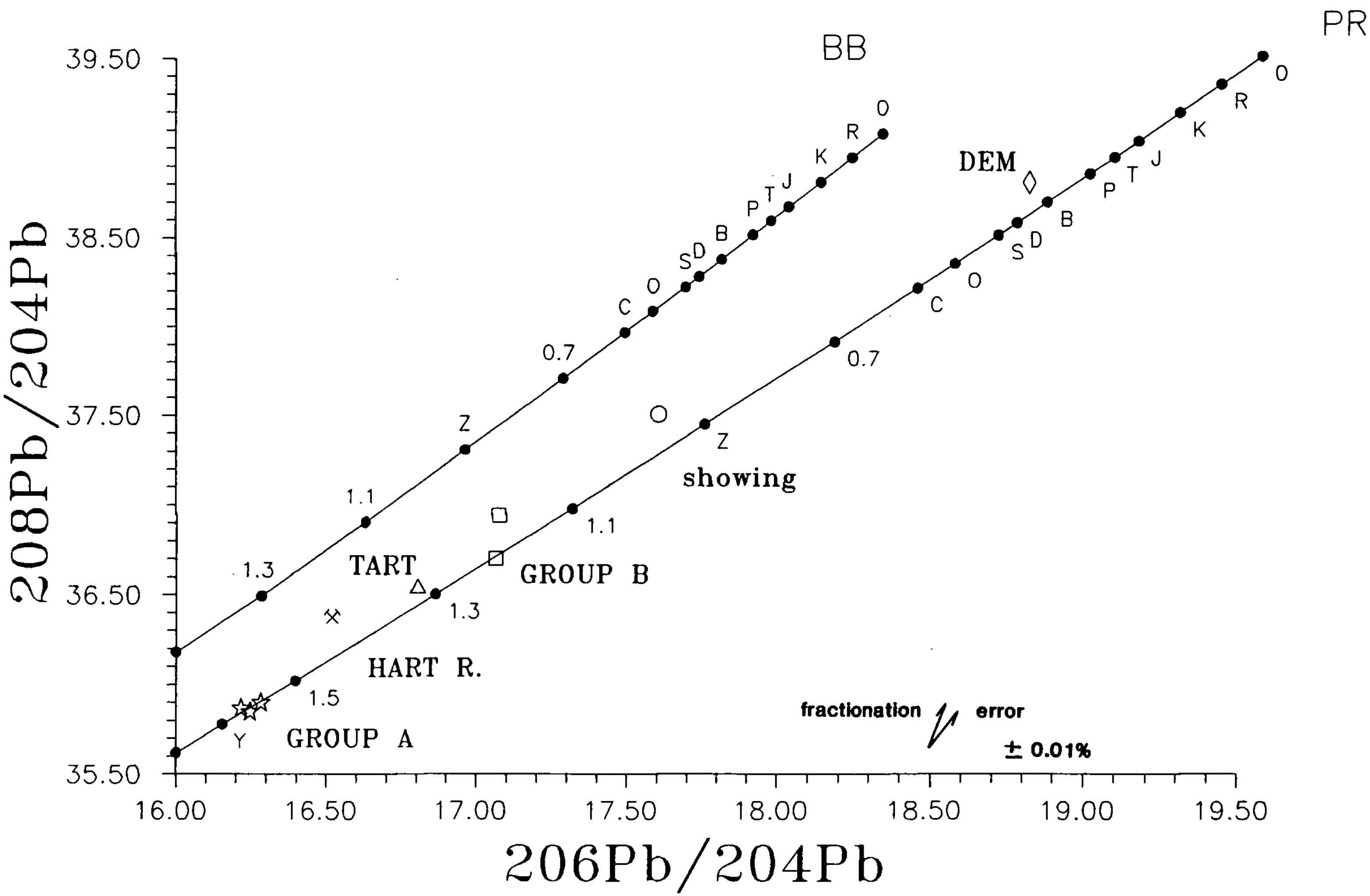

Figure A.3 Galena lead isotope plot of $^{208}Pb/^{204}Pb$ vs. $^{206}Pb/^{204}Pb$ showing the distribution of data from Proterozoic hosted mineral occurrences in the Coal Creek Inlier, southern Ogilvie Mountains, west-central Yukon Territory. Tables A.1 and A.2 present brief descriptions and galena lead isotope data for the mineral occurrences, respectively. Figure A.1 shows their locations.

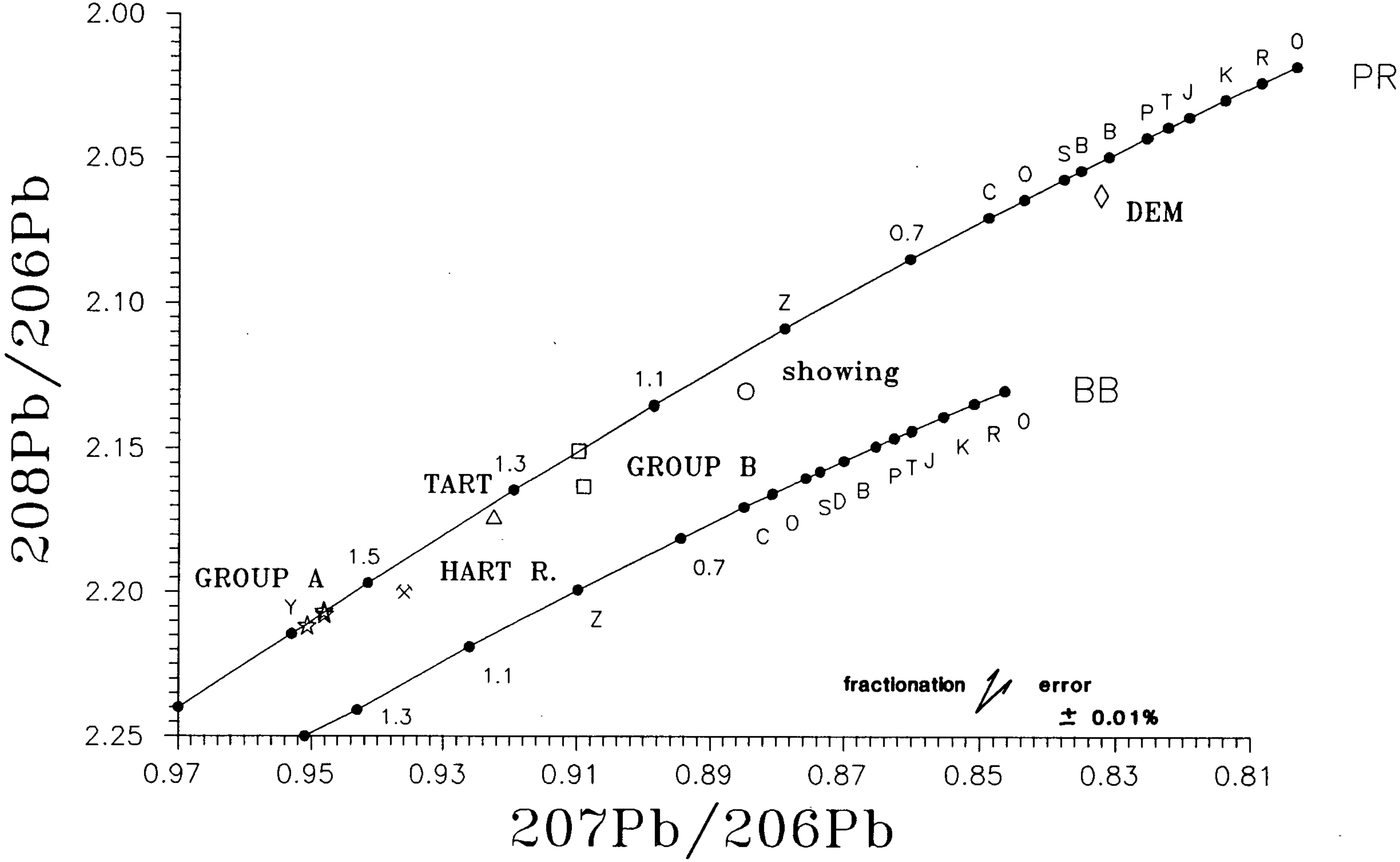

Figure A.4 Galena lead isotope plot of $^{208}Pb/^{206}Pb$ vs. $^{207}Pb/^{206}Pb$ showing the distribution of data from Proterozoic hosted mineral occurrences in the Coal Creek Inlier, southern Ogilvie Mountains, west-central Yukon Territory. Tables A.1 and A.2 present brief descriptions and galena lead isotope data for the mineral occurrences, respectively. Figure A.1 shows their locations.

Lake Group is considered to be Early Proterozoic, then the Monster mineral prospect is more likely epigenetic and probably formed during the same metallogenic event that made the Od and Oz mineral occurrences.

Hart River

Hart River stratiform massive sulfide deposit (Morin, 1977) occurs about 150 km east of the Coal Creek Inlier. It occurs in an argillaceous facies of the Gillespie Lake Group, the youngest member of the Wernecke Supergroup. This syngenetic deposit (Morin, 1977) has a galena lead model age of about 1.35 to 1.45 (cf. Godwin et al., 1988). This date is approximately equivalent to the age of the Sullivan deposit (Godwin, 1986), southeast B.C. It also defines the approximate age of the youngest member of the Wernecke Supergroup.

Tart

The Tart deposit has an interpreted age of about 1.3 Ga. It is hosted in dolostone of the Gillespie Lake Group. If the Tart is co-genetic with its host rock this date might give an upper age for the Gillespie Lake Group. Such an age is compatible with presently known geology.

GROUP B (Ugly and Seela)

Group B is made up of two showings, the **Ugly** and **Seela.** These prospects occur in breccias spatially associated with faults. The former occurs in Gillespie Lake Group rocks and the latter occurs in the Lower Fifteenmile group. The interpreted isotopic age is 1.2 Ga. (The $^{208}Pb/^{204}Pb$ ratio for the Seela prospect appears to be erratic; this ratio displaces it from the Ugly mineral occurrence on Figures A.3 and A.4.) This date coincides with the age of the Racklan Tectonic Event (Gabrielse, 1967; Eisbacher, 1978). It might also represent the time of movement along the Fifteenmile fault with which the Seela prospect is spatially associated. If the Seela showing is syngenetic, then the 1.2 Ga date may also approximate the age of the lower Fifteenmile group. The 1.2 Ga date is probably younger than the Gillespie Lake Group. Therefore the Ugly prospect is likely epigenetic.

Showing-10190

Showing-10190 plots just below the Pericratonic growth curve but can be modeled at about 0.9 Ga by using the mixing line between the pericratonic and Bluebell growth curves. This date coincides with the boundary between Middle Proterozoic and Late Proterozoic (point Z in Figures A.2 to A.4). Galena for this point came from veinlets in an altered mafic dyke that cuts **OMB** hosted in lower Fifteenmile group rocks. The date therefore probably approximates the age of the mafic dyke and establishes a minimum age for **OMB**. Clearly the mafic dyke fragments in **OMB** are older.

Dem

The **Dem** prospect plots just below the Pericratonic growth curve in Figure A.2. It can be modeled at about 0.3 Ga (Carboniferous). This deposit is hosted in lower Fifteenmile group and is therefore epigenetic. It is unrelated to the **OMB**.

A.1.4 CONCLUSION

The interpretation of data from the present study has yielded significantly different results from that of Godwin et al. (1982). In this study data can be divided into 2 groups and 4 points (Figures A.2 to A.4). All data are distributed along or close to the Pericratonic growth curve from about 1.6 Ga to Carboniferous time. The clusters and points allow the dating of mineralizing events and constrain the age of the rock units that host the mineralization. Wernecke Supergroup rocks are at least as old as 1.56 Ga (Group A), are as young as about 1.35 to 1.45 Ga (Hart River) and might even be 1.30 to 1.35 Ga (Tart).

The age of the OMB, if related to the age of the dykes, has an upper limit of about 0.90 Ga (Showing-10190). The age of Group B, 1.2 Ga, may define a lower limit to the age of the breccia, especially since the breccias are in lower Fifteenmile group. In fact, one implication of the galena lead isotope data is that the Racklan Tectonic Event, which affects the lower Fifteenmile group, may be related to movement along the Fifteenmile fault. OMB occupies this fault; the genetic model (of section 5.4) implies that the fault and breccia are genetically related. Therefore Ogilvie Mountains breccia, the lower Fifteenmile group, major faulting and the Racklan Tectonic Event might all be approximately equivalent in age.

Carboniferous (Dem) metallogenic events are recorded in the Coal Creek Inlier. These are prominent in the northern Canadian Cordillera.

APPENDIX B

POTASSIUM-ARGON PREPARATION AND ANALYTICAL PROCEDURES

B.1 SAMPLE PREPARATION

Five samples were prepared for potassium-argon dating methods. The initial stages are listed below and specific treatments follow under respective sub-headings.

(1) weathered material removed,

(2) crushed to less than 0.5 cm in a jaw crusher,

(3) grind sample in disc mill, and

(4) sieve sample to -40 mesh and retain the -40 mesh fraction. Steps 3 and 4 are repeated with +40 mesh fraction until entire sample passes -40 mesh.

B.1.1 POTASSIUM-ARGON ANALYSIS

Five potassium-argon analyses were made from three chlorite-rich separate samples and two amphibole separate samples. Amphibole mineral separates were made from two visually "least altered" coarse-grained diabase dykes. The three chlorite-rich separates were from three isolated occurances of chlorite-rich-matrix breccias. The various sample preparations are described as follows.

Chlorite-rich separates

(1) The -40 mesh is hand picked for chlorite and the and the chlorite-rich fraction is retained (The chlorite-poor fraction is saved as a back-up).

(2) Sieve each sample in a set of "mini" nested sieves (-60 mesh on top, -80 mesh in the middle, and -100 mesh on the botom) by hand for approximately 10 minutes. Retain the -80 +100 for further analysis and save the -40 +60 mesh and -100 mesh as back-ups.

(3) The fraction is passed through a magnetic column to remove any magnetic grains.

(4) A slightly inclined vibrating plane table is used to further concentrate the platy chlorite grains.

Amphibole separates

(1) Sieve each sample in a set of "mini" nested sieves (-60 mesh on top of -80 mesh) by hand for about 10 minutes. Retain the -60 +80 mesh for further analysis and save the -40 +60 mesh and -80 mesh as back-ups.

(2) The fraction is passed through a magnetic column to remove any magnetite grains.

(3) The fraction is passed through a magnetic separator several times to remove both the most magnetic and least magnetic grains. This material constitutes about 20% of the -60 +80 mesh separate; it is discarded.

(3) Heavy liquids (bromoform and methylene iodide) are used to further concentrate the amphibole grains.

Potassium and analysis

(1) The chemical techniques used for potassium analysis are those described in detail in the unpublished

laboratory instructions manual in the Geochronology Laboratory at UBC. Potassium concentration is determined on duplicate samples by atomic absorption using a Techtron AA4 spectrophotometer on dilute sulphate solutions bufered by Na and Li nitrates.

(2) Five samples (plus five duplicates) were analyzed for their potassium content.

Argon analysis

(1) The laboratory techniques used for argon analysis are those described by White *et al.* (1967). Argon is determined by isotope dilution using an AEI MS-10 mass spectrometer with Carey Model 10 vibrating reel electrometer, high purity ^{38}Ar spike and conventional gas extraction and purification methods.

(2) Two of the initial five samples were analyzed for argon.

The precision and accuracy of the age dates are the estimated analytical uncertainties at one standard deviation. The decay constants used are those recommended by the IUGS Subcommision on Geochronology ($_{40}$K decay to $_{40}$Ar = $0.58x10_{-10}$ yr_{-1} and 40K decay to $_{40}$Ca = $4.962x10_{-10}$ yr_{-1}, Steiger and Jager, 1977).

B.2 RESULTS

Results are shown in Table B.1.

TABLE B.1 Analytical data for K-Ar dates from the Coal Creek Inlier, southern Ogilvie Mountains, west-central Yukon Territory. All analyses were performed at the Geochronology Laboratory, Department of Geological Sciences, The University of British Columbia: potassium analyses was by D. Runkle and argon analyses were by J. Harakal.

Sample No. Material	Location Unit	K (wt%)	^{40}Ar (radiogenic) ^{40}Ar (total)	^{40}Ar (radiogenic) (10^{-6} $cm^3 g^{-1}$)	Date (Ma)[1] Time[2]
TW208 Whole rock chlorite-rich matrix concentrate	Lat. 64°53.68N Long. 139°09.12W Unit BM1: monoclastic breccia	3.48 ±0.01	0.862	29.307	205±6 lowest Jurassic
BL30-6 Whole rock chlorite-rich matrix concentrate	Lat. 64°50.23N Long. 139°38.28W Unit BM1: monoclastic breccia	3.31 ±0.04	0.981	51.239	360±10 Devonian- Carboniferous

1 Decay constants are from Steiger and Jager (1977): $\lambda_e = 0.581 \times 10^{-10}$ yr^{-1}; $\lambda_b = 4.962 \times 10^{-10}$ $year^{-1}$; $^{40}K/K = 1.167 \times 10^{-4}$. Errors are one standard deviation.

2 Time intervals are from Decade of North American Geology (Palmer, 1983).

APPENDIX C

SPECIFIC REFERENCES USED TO CONSTRUCT FIGURE 2.1

The superscripted numbers on Table 2.1 match the column of numbers on the left. Full listings are in "REFERENCES".

1. Brabb, E.E., 1967.
2. Churkin, M. Jr., 1973.
3. Norris, D.K. and Hopkins, W.S., 1977
4. Fritz, W.H., 1980
5. Roots, C.F., 1982; 1987.
6. Thompson, R.I. and Roots, C.F., 1982
7. Thompson, R.I., pers. comm., 1987
8. Mercier, E., 1985
9. Mercier, E., 1987
10. Cecile, M.P., 1982
11. Gordy, S.P., in press.
12. Young, G.M. et al., 1978; Young, G.M. et al., 1979; Eisbacher, G.H., 1978.
13. Eisbacher, G.H., 1981.
14. Delaney, G.D., 1981; 1985.
15. Eisbacher, G.H., 1976; Yeo, G.M., 1981.
16. Jefferson, C.W., 1978; DNAG in press
17. Gabrielse, H. et al., 1973.
18. Aitken, J.D., 1981
19. Jefferson, C.W., and Ruelle, J.C.L., 1986.
20. McMechan, M.E. and Price, R.A., 1982.
21. Price, R.A., 1964.
22. Gabrielse, H., 1972

APPENDIX D

SUMMARY OF OGILVIE MOUNTAIN BRECCIAS IN THIN SECTION

Table D.1 Lithology and mineral abbreviations for Table D.2

Abbreviation	Mineral	Abbreviation	Rock Name
ab	albite	arg	argillite
ba	barite	cht	chert
cb	carbonate	dol	dolostone
cl	chlorite	fef	iron formation
cy	clay	int	mafic dyke
dl	dolomite	mds	mudstone
ep	epidote	qzt	quartzite
he	hematite	sds	sandstone
ks	potassium feldspar	sld	silty dolostone or dolomitic siltstone
lm	limonite		
ms	muscovite	met	metasomatized sedimentary rock
pl	plagioclase		
py	pyrite		
qz	quartz		
se	sericite		
tr	tourmaline		

TABLE D. 2 Thin section summary of Ogilvie Mountain breccias and some other breccias from the Coal Creek Inlier, southern Ogilvie Mountains, west-central Yukon Territory.

UNIT	CLAST LITHOLOGY									PRIMARY GRAINS						SECONDARY MINERALS														COMMENTS
(thin section #)	qzt	sds	dol	sld	mds	chr	fef	int	met	he	cb	qz	ks	pl	cy	ks	al	tr	ms	cl	se	ep	dl	qz	cb	py	cy	lm	he	
MONOLITHIC BRECCIAS																														
FAIRCHILD LAKE GROUP																														
BM1 (BL3-25)			X							X				X	X					X								X		flow texture
(BL6-2)				X																			X	X				X		cockade texture
(BL30-2)	X		X	X	X			?		X					X	X				X				X						aligned he
(BL30-6)	X									X						X			X	X										clast supported
(BL54-1)	X		X	X		X				X		X						X	X					X						clastic texture
(TW85-206A,B)	X													X		X				X	?	X	X				X	X		poikilitic ks
QUARTET GROUP																														
BM2 No sections																														
GILLESPIE LAKE GROUP																														
BM3 (BL87-7B,C)			X																	X			X		X		X			recrystalized strained qz
FIFTEENMILE GROUP																														
BM4 No sections																														
HETEROLITHIC BRECCIAS																														
CARBONATE-RICH-MATRIX																														
BHcb (BL10-14A)			X		X	X		X		X					X			X	X					X		X				vein cb,he,qz
(BL45-5)	X		X		X					X	X	X	X	X	X			X	X	X		X		X	X		X			bleached
(BL87-70)	X		X		X	X														X				X						strained qz
(BL87-7A)			X	X	X						X	X	X		X	X				X	?		X	X	X			X	X	
HEMATITE-RICH-MATRIX																														
BHh (BL24-12)				X	X					X	X	X			X	X		X	X	X				X	X			X	X	he-vein qz brx
(BL37-18)	X		X	X		X						X											X	X	X	X		X	X	martite ?
(BL43-7)				X	X					X	X	X						X	X				X	X	X					aligned clasts
(BL48-3)	X			X		X				X		X			X				X	X	?		X	X	X					felsic igneous
(BL67-57)	X		X		X			X		X	X	X			X		X			X		X	X		X		X	X	X	poikilitic cb
CHLORITE-RICH-MATRIX																														
BHcl (BL35-4)	X			X	X			X		X	X	X			X					X					X	X		X		igneous frags.
(BL50-2)	X								X	X	X				X	X	X	X	X	X	?			X	X			X	X	flow texture
HYDROTHERMAL BRECCIAS																														
(BL18-12)	X																						X	X		X		X		recrystalized
(BL40-27)			X		X																		X	X					X	qz overgrowths
PEBBLE DYKE																														
(BL87-21)	X			X							X	X																		dolomite matrix

1 Lithology and mineral abbreviations are listed in Table D.1.

APPENDIX E

GEOCHEMICAL TECHNIQUES AND RESULTS

E.1 GEOCHEMICAL TECHNIQUES

Each major unit was sampled for analyses of the major, trace and rare earth elements. Prior to shipment to the various laboratories the samples were cleaned of all weathered material.

E.1.1 Suite 1: XRF and ICP analyses

Twenty-four samples were submitted to the Geological Survey of Canada, Mineral Resources Division, Analytical Chemistry Section, X-ray Flourescence and ICP-Emmision Spectrometry laboratories in Ottawa. Sample descriptions are in Table E.1 and results are shown in Table E.2. Major element oxides and trace elements (see Table E.2) were analyzed by XRF wavelength dispersive analysis on fused disks. FeO, H_2OT, CO_2T, C and S were analyzed by rapid chemical methods. Fe_2O_3 was calculated using $Fe_2O_3 = Fe_2O_3T - 1.11134 * FeO(volumetric)$. Detection limits for major and trace elements, given by the laboratory, were:

0.50% for Na_2O;
0.40% for SiO_2 and Al_2O_3;
0.2% for TiO_2, Cr_2O_3, P_2O_5, S and CO_2;
0.1% for Fe_2O_3, MgO and CaO;
0.05% for K_2O and H_2O;
0.03% for FeO and 0.01% for MnO.

Detection limits for trace elements, provided by the laboratory, were:

30 ppm for Nb and Y;
20 ppm for Ba, Rb, Sr and Zr

Results of tests for precision are presented in Table E.7. Standards were not run therefore the accuracy of the data is not known.

ICP data for 7 trace and 2 rare earth elements were obtained 1.0 gram of sample (acid + fusion of residue) dissolved in 10% HCL and diluted to 100 ml. Detection limits for this set of ICP data, given by the laboratory, were:

10 ppm for Cr, Cu, La and Ni;
5 ppm for Co, V and Zn;
0.5 ppm for Be and Yb.

These samples were also analyzed for selected trace (Nb, Ba and Th) and rare earth (La and Ce) elements using ICPMS methods by X-ray Assay Laboratories Limited (XRAL), Don Mills, Ontario. Detection limits are listed below, are:

1.0 ppm for Nb, Ba and La
0.5 ppm for Ce and 0.1 ppm for Th

E.1.2 Suite 2: Whole rock and 30 element ICP analyses

Twenty samples were submitted to ACME Analytical Laboratories in Vancouver. These analyses were provided by Newmont Exploration of Canada Ltd. All samples were analyzed by ICP techniques for 30 elements and by ICP-MS for 26 trace and rare earth elements. Seven of these samples were also anlayzed for oxides plus LOI and Ba. Sample descriptions are shown in Table E.3 and results are tabulated in Table E.4. The data is not quantitative and was meant to be used as an exploration guide to anomalously mineralized breccia bodies. Some samples anomalous in their rare earth element content were re-analyzed quantitatively for REE in Suite 3 (see section E.3).

For ICP analysis the samples were crushed to -5 mm using a jaw crusher and then pulverized to -100 mesh and split. A one-half gram sample was digested with 3 ml of 3-1-2 HCL-HNO3-H2O at 90oC for one hour and diluted to 10 ml with water. The leach is near total for base metals, partial for rock forming elements and poor for refractory elements. Detection limits are as follows:

5 ppm for U,
2 ppm for As, Au, B, Ba, Bi, La, Pb, Sb, Th, V and W,
1 ppm for Cd, Co, Cu, Mn, Mo, Ni, Sr and Zn,
0.1 ppm for Ag, and
0.01% for Al, Ca, Fe, K, Mg, Na, P and Ti.

For whole rock ICP-MS analyses 0.200 gram samples were fused with 0.60 grams of $LiBO_2$, are dissolved and diluted in 50 ml of 5% HNO_3. Detection limits are 1 ppm for all elements except for Be which is 10 ppm and Rb, Y, Zr, Nb, Cs and W.

For whole rock ICP analyses 0.1000 gram samples were fused with 0.60 grams of $LiBO_2$ and are dissolved in 50 ml of 5% HNO_3. Detection limits were not provided by the laboratory.

E.1.3 Suite 3: Instrumental neutron activation analyses (INAA) for rare earth elements (REE)

Twenty-two samples were submitted to Bondar-Clegg and Company Ltd. in North Vancouver. Four of the samples were duplicates and 1 was a standard. Fourteen rare earth elements plus Sc, Th and U were evaluated using INAA techniques that are described in detail in Gibson and Jagam (1980). Sample descriptions in Table E.5 and results are shown in Table E.6. Atomic absorption was used to determine Co and Cu contents and XRF was used to determine Ba concentration. Precision and accuracy of the data is shown in Tables E.7 and E.8. Relative precision is variable and ranges from less than 5% for Lu and Sc to 31% for Dy. Relative precision is found to be eratic for elements with concentrations only slightly higher than their detection limits (compare Lu with Dy; Table E.7). Detection limits are shown in Table E.9.

E.2 SAMPLE DESCRIPTIONS AND RESULTS

Table E.1 Brief hand sample descriptions for Sample Suite 1 consisting of 24 samples (including duplicates) from the southern Ogilvie Mountains, west-central Yukon Territory. These are evaluated for major and minor oxides, trace and rare earth elements. Sample locations are shown on Map 2 (in pocket). Results are tabulated in Table E.2.

Unit	Sample No. (Lat.N, Long.W)	Sample Description
1	BL6-4A (139°09.12'N, 64°53.10'W)	Iron formation: thinly bedded white quartz, jasper, hematite and brown calcareous sandstone; trace chalcopyrite
1	BL6-4B (139°09.12'N, 64°53.10'W)	Iron formation: laminated hematite and fine-grained black siliceous sediment; trace chalcopyrite and pyrite
1	BL9-2 (139°16.13'N, 64°52.46'W)	Fairchild Lake Group: grey weathering, brownish grey limestone; thinly bedded; chlorite partings
1	BL9-22 (139°15.13'N, 64°52.54'W)	Fairchild Lake Group: grey weathering, pale grey limestone; thinly bedded; chlorite partings
1	BL43-10 (139°24.94'N, 64°44.01'W)	Fairchild Lake Group: maroon mudstone; crowded with rhombs (1 mm in diameter) of dolomite
2	BL2-5 (139°08.18'N, 64°53.38'W)	Monolithic breccia/conglomerate: pale brown weathering, grey and brown mottled calcareous sandstone and mudstone fragments; mud matrix
2	BL54-3 (139°37.42'N, 64°50.13'W)	Quartet Group: grey weathering, dark grey fine-grained sandstone
Dyke	BL10-6 (139°16.32'N, 64°51.58'W)	Diabase: medium green, chloritized and carbonatized intermediate to mafic dyke; amygdules have iron carbonate rims and quartz cores; common pyrite euhedra

Table E.1 (continued)

Unit	Sample No. (Lat.N, Long.W)	Sample Description
Dyke	BL47-5 (139°19.21'N, 64°44.73'W)	Diabase: pale grey-green carbonatized and sericitized intermediate to mafic dyke; glomerocrysts of relict plagioclase; abundant calcite veinlets; trace galena
BM1	BL3-25 (139°09.12'N, 64°53.64'W)	Monolithic breccia: subrounded fragments of pale grey quartzite; chlorite matrix
BM1	BL30-6 (139°38.23'N, 64°50.21'W)	Monolithic breccia: maroon dolomitic sandstone fragments; medium-grained chlorite matrix with minor iron carbonate
BM1	85-208A (139°09.12'N, 64°53.68'W)	Monolithic breccia: chloritic fragments in a coarse grained chlorite matrix
BM1	85-208B (139°09.12'N, 64°53.68'W)	Monolithic breccia: pink siliceous clasts in a coarse grained chlorite matrix
BM2	BL33-7 (139°09.37'N, 64°54.93'W)	Monolithic breccia: angular fragments of grey sandstone; iron carbonate matrix; 1-2% pyrite and trace chalcopyrite
BM4	BL50-6 (139°12.98'N, 64°46.02'W)	Monolithic breccia: dark grey angular clasts of laminated mudstone
BHcb	BL3-5 (139°08.55'N, 64°53.18'W)	Heterolithic breccia: grey weathering, grey and pink mottled; clasts are pink silty dolostone, grey sandstone, grey mudstone; carbonate matrix; accessory chlorite; trace hematite
BHcb	BL3-16 (139°08.84'N, 64°53.13'W)	Heterolithic breccia: mottled grey and pink; pink and maroon mudstone, black argillite, grey sandstone and dolostone fragments; carbonate and chlorite matrix
BHcb	BL8-8 (139°10.89'N, 64°53.42'W)	Heterolithic breccia: subrounded fragments of pink sandy dolostone, pink oolitic limestone, white quartzite and jasper; carbonate matrix

Table E.1 (continued)

Unit	Sample No. (Lat.N, Long.W)	Sample Description
BHcb	BL18-10 (139°23.13'N, 64°52.46'W)	Breccia matrix: red, coarse grained carbonate
BHcb	BL43-7 (139°25.25'N, 64°44.14'W)	Heterolithic breccia: layered; clasts of pink silty dolostone, black argillite, grey mudstone and specular hematite masses; carbonate and hematite matrix with minor chlorite
BHh	BL47-11 (139°19.25'N, 64°44.39'W)	Heterolithic breccia: subangular fragments of pink to maroon dolomitic mudstone and sandy dolostone; hematite, chlorite and carbonate matrix
BHcl	BL45-4 (139°22.61'N, 64°44.64'W)	Heterolithic breccia: mottled pale pink and green; silicified pink dolostone, white quartzite and green mudstone fragments; fine-grained chlorite-quartz matrix
BHcl	BL47-6 (139°19.21'N, 64°44.73'W)	Heterolithic breccia: white quartzite, dark grey and green mudstone and rare pink dolostone fragments; chlorite-carbonate matrix

Table E.2 Major and minor element oxides and trace elements for sample suite 1 from Proterozoic rocks, Coal Creek Inlier, southern Ogilvie Mountains, west-central Yukon Territory. Rocks are described in Table E.1. Sample locations are in Table E.1 and on Map 2 (in pocket). All analyses were by the Geological Survey of Canada, Ottawa.

Sample No.		BL6-4a	BL6-4b	BL9-2	BL9-22	BL43-10	BL2-5
XRF analyses							
SiO_2	(wt%)	25.4	53.0	39.5	42.6	47.0	34.4
TiO_2	(wt%)	0.22	0.20	0.45	0.51	0.46	0.20
Al_2O_3	(wt%)	7.8	5.7	9.5	8.8	10.3	4.7
Cr_2O_3	(wt%)	0.01	0.01	0.00	0.00	0.00	0.00
Fe_2O_3	(wt%)	46.4	29.8	1.9	2.5	7.9	0.9
FeO	(wt%)		2.0	1.0	1.4	1.9	5.4
MnO	(wt%)	0.03	0.08	0.58	0.53	0.13	0.89
MgO	(wt%)	1.82	1.28	2.27	2.64	7.94	4.41
CaO	(wt%)	0.38	2.05	21.14	18.32	7.28	21.49
Na_2O	(wt%)	0.0	1.7	0.00	0.3	0.0	0.0
K_2O	(wt%)	3.89	1.22	3.57	3.31	3.78	1.65
H_2OT	(wt%)		1.0	2.0	2.2	2.7	1.1
CO_2T	(wt%)	0.4	2.4	16.9	4.8	11.1	24.3
P_2O_5	(wt%)	0.29	0.27	0.20	0.20	0.13	0.08
S	(wt%)	3.82	0.02	0.00	0.03	0.00	0.32
Ba	(ppm)	595	293	375	1289	205	234
Nb	(ppm)	0	0	0	0	0	0
Rb	(ppm)	35	0	161	107	126	63
Sr	(ppm)	0	0	278	346	3	48
Y	(ppm)	0	0	0	0	0	0
Zr	(ppm)	29	60	106	149	101	72
Total	(wt%)	90.5	100.7	99.1	98.3	100.6	99.9
Fe_2O_3T	(wt%)	46.4	32.5	3.1	4.0	10.0	6.9
ICP analyses-set 1							
Nb	(ppm)	3	3	8	8	8	3
Ba	(ppm)	591	279	412	1422	188	203
La	(ppm)	1	3	19	6	62	15
Ce	(ppm)	2.6	5.4	37.1	11.2	107	31.0
Th	(ppm)	4.2	4.2	10.4	11.1	12.9	4.2
ICP analyses-set 2							
Be	(ppm)	0.4	0.4	1.8	1.5	1.5	1.1
Co	(ppm)	47	13	12	21	17	16
Cr	(ppm)	0	0	51	51	48	44
Cu	(ppm)	70000	400	15	36	17	40
La	(ppm)	5	4	16	6	58	17
Ni	(ppm)	9	14	32	5	33	26
V	(ppm)	240	140	59	56	57	35
Yb	(ppm)	0.6	0.0	1.6	1.5	1.6	0.9
Zn	(ppm)	170	31	79	59	69	42

Table E.2 (continued)

Sample No.		BL54-3	BL10-6	BL47-5	BL3-25	BL30-6	TW208a
XRF analyses							
SiO_2	(wt%)	67.6	39.2	41.2	61.3	62.1	54.0
TiO_2	(wt%)	0.68	1.25	1.00	0.52	0.51	0.66
Al_2O_3	(wt%)	17.1	11.9	14.8	12.6	11.9	14.5
Cr_2O_3	(wt%)	0.01	0.01	0.03	0.01	0.01	0.01
Fe_2O_3	(wt%)	2.1	22.2	1.4	3.3	5.8	1.7
FeO	(wt%)	0.9		13.5	3.3	4.3	9.9
MnO	(wt%)	0.02	0.22	0.23	0.05	0.10	0.10
MgO	(wt%)	0.79	7.69	6.33	3.04	5.14	8.35
CaO	(wt%)	0.28	4.81	5.49	2.79	0.77	0.33
Na_2O	(wt%)	1.3	0.0	0.3	0.1	0.1	0.0
K_2O	(wt%)	5.15	1.39	1.99	6.76	5.97	4.39
H_2OT	(wt%)	2.5		5.12	2.5	2.9	5.5
CO_2T	(wt%)	0.3	6.8	8.1	3.5	0.9	0.0
P_2O_5	(wt%)	0.06	0.09	0.08	0.12	0.12	0.19
S	(wt%)	0.00	1.39	0.15	0.00	0.00	0.00
Ba	(ppm)	573	161	190	602	593	396
Nb	(ppm)	0	0	0	0	0	0
Rb	(ppm)	236	45	48	151	84	78
Sr	(ppm)	31	0	0	38	3	0
Y	(ppm)	51	6	0	0	15	0
Zr	(ppm)	224	59	46	223	156	265
Total	(wt%)	98.9	97.0	99.8	99.1	100.7	99.1
Fe_2O_3T	(wt%)	3.1	22.2	16.4	6.9	10.5	12.7
ICP analyses-set 1							
Nb	(ppm)	143	4	3	5	7	9
Ba	(ppm)	628	102	143	597	598	342
La	(ppm)	19	33	3	34	4	8
Ce	(ppm)	39.8	60.6	10.2	63.	8.15	16.8
Th	(ppm)	23.0	1.7	0.9	12.	11.23	10.9
ICP analyses-set 2							
Be	(ppm)	2.8	1.1	1.2	1.	0.72	1.1
Co	(ppm)	7	97	39	11	24	32
Cr	(ppm)	63	50	200	56	57	58
Cu	(ppm)	23	29	25	10	23	26
La	(ppm)	16	50	1	32	6	8
Ni	(ppm)	25	100	130	30	53	70
V	(ppm)	65	300	300	70	83	120
Yb	(ppm)	5	1.9	1.2	1.	2.17	0.8
Zn	(ppm)	38	80	220	32	75	92

Table E.2 (continued)

Sample No.		TW208b	BL33-7	BL50-6	BL3-5	BL3-16	BL8-8
XRF analyses							
SiO_2	(wt%)	73.7	49.7	66.0	46.8	56.3	41.5
TiO_2	(wt%)	0.35	1.95	0.64	0.47	0.59	0.20
Al_2O_3	(wt%)	9.9	13.9	14.7	8.4	14.0	3.1
Cr_2O_3	(wt%)	0.00	0.01	0.01	0.00	0.01	0.00
Fe_2O_3	(wt%)	0.5	3.1	1.2	3.4	3.4	0.9
FeO	(wt%)	2.3	7.5	3.6	2.4	3.5	1.9
MnO	(wt%)	0.04	0.16	0.01	0.32	0.12	0.42
MgO	(wt%)	2.52	5.78	3.44	7.11	5.14	10.11
CaO	(wt%)	0.60	1.50	0.61	9.56	4.91	15.43
Na_2O	(wt%)	0.1	0.0	0.3	0.1	5.2	0.0
K_2O	(wt%)	6.66	7.43	5.59	4.80	0.88	1.51
H_2OT	(wt%)	1.5	4.2	3.7	1.5	2.8	0.7
CO_2T	(wt%)	0.8	2.1	0.8	14.5	3.7	23.5
P_2O_5	(wt%)	0.10	0.15	0.19	0.16	0.17	0.23
S	(wt%)	0.00	0.61	0.01	0.00	0.00	0.00
Ba	(ppm)	668	466	489	382	114	95
Nb	(ppm)	0	0	0	0	0	0
Rb	(ppm)	90	103	173	107	17	33
Sr	(ppm)	72	0	68	63	30	80
Y	(ppm)	0	13	37	0	0	0
Zr	(ppm)	203	119	183	222	127	98
Total	(wt%)	98.3	99.8	100.9	99.5	99.8	98.3
Fe_2O_3T	(wt%)	3.1	11.4	5.2	6.1	7.3	3.0
ICP analyses-set 1							
Nb	(ppm)	4	9	14	4	10	2
Ba	(ppm)	692	454	478	414	107	78
La	(ppm)	41	22	48	34	34	34
Ce	(ppm)	73.0	38.3	94.1	66.0	68	61.8
Th	(ppm)	13.3	3.7	18.1	9.6	15	4.8
ICP analyses-set 2							
Be	(ppm)	0.3	0.6	4.4	1.1	1	0.6
Co	(ppm)	12	42	15	12	20	11
Cr	(ppm)	35	33	73	42	63	31
Cu	(ppm)	21	300	26	15	26	19
La	(ppm)	35	16	47	32	32	32
Ni	(ppm)	28	53	33	29	42	22
V	(ppm)	42	420	85	49	86	35
Yb	(ppm)	0.9	3.1	2.7	1.8	2.1	3.1
Zn	(ppm)	58	55	68	67	95	59

Table E.2 (continued)

Sample No.		BL18-10	BL43-7	BL47-11	BL45-4	BL47-6	BL3-5d[1]
XRF analyses							
SiO_2	(wt%)	1.9	44.5	49.9	58.2	53.8	
TiO_2	(wt%)	0.02	0.45	0.52	0.32	0.57	
Al_2O_3	(wt%)	0.1	10.1	11.2	6.5	13.1	
Cr_2O_3	(wt%)	0.00	0.01	0.00	0.00	0.01	
Fe_2O_3	(wt%)	5.0	14.1	7.1	0.4	0.8	
FeO	(wt%)	0.7	3.1	2.3	1.9	4.8	
MnO	(wt%)	1.27	0.21	0.17	0.19	0.08	
MgO	(wt%)	18.27	5.55	6.75	5.82	6.93	
CaO	(wt%)	28.18	5.67	5.19	8.39	4.32	
Na_2O	(wt%)	0.0	0.0	1.5	0.0	2.9	
K_2O	(wt%)	0.00	5.08	5.30	3.62	1.92	
H_2OT	(wt%)	0.2	2.1	1.9	1.0	3.3	
CO_2T	(wt%)	44.2	7.6	7.4	12.8	6.2	
P_2O_5	(wt%)	0.00	0.28	0.16	0.15	0.18	
S	(wt%)	0.00	0.03	0.00	0.00	0.13	
Ba	(ppm)	69	1896	290	323	127	
Nb	(ppm)	0	3	0	0	0	
Rb	(ppm)	0	104	43	94	66	
Sr	(ppm)	51	0	41	37	96	
Y	(ppm)	0	0	15	0	0	
Zr	(ppm)	0	137	151	256	155	
Total	(wt%)	97.0	99.0	100.6	99.5	99.1	
Fe_2O_3T	(wt%)	5.8	17.6	9.7	2.5	6.1	
ICP analyses-set 1							
Nb	(ppm)	<1	8	6	2	7	4
Ba	(ppm)	38	2120	268	321	132	420
La	(ppm)	4	78	41	26	30	34
Ce	(ppm)	9.7	138.	73.3	52.2	55.4	67.9
Th	(ppm)	0.2	12.6	14.8	7.0	16.6	9.4
ICP analyses-set 2							
Be	(ppm)	0.5	1.5	1.2	0.7	2.3	1.0
Co	(ppm)	22	22	13	8	14	10
Cr	(ppm)	32	41	52	28	61	35
Cu	(ppm)	27	32	20	16	100	10
La	(ppm)	8	73	36	26	30	28
Ni	(ppm)	19	27	31	19	71	24
V	(ppm)	15	86	62	30	52	49
Yb	(ppm)	1.4	1.7	2.5	1.3	1.5	1.7
Zn	(ppm)	55	43	65	40	62	36

1: suffix "d" denotes duplicate sample; whole rock analysis not performed on sample BL3-5d.

Table E.3 Brief hand sample descriptions for Sample Suite 2, evaluated for major and minor oxides, trace and rare earth elements, consisting of 20 samples from the Coal Creek Inlier, southern Ogilvie Mountains, west-central Yukon Territory. Sample locations are shown on Map 2 (in pocket). Results are tabulated in Tables E.4A and E.4B.

Unit	Sample No. (Lat.N, Long.W)	Sample Description
1	BL3-7 (139°08.55'N, 64°53.16'W)	Fairchild Lake Group: brown weathering pink dolostone; calcite veinlets
1	BL4-7 (139°09.31'N, 64°53.92'W)	Fairchild Lake Group: interlayered brown weathering buff dolomite and fine-grained pale quartzite
1	BL11-10 (139°11.82'N, 64°53.74'W)	Fairchild Lake Group: densely fractured white quartzite; abundant carbonate veinlets; trace chalcopyrite and pyrite
1	BL53-4 (139°36.92'N, 64°50.40'W)	Banded iron formation: interbedded, thickly laminated hematite and red fine grained silica
2	BL1-1 (139°08.24'N, 64°53.09'W)	Quartet Group: dark grey fine grained sandstone; hematite veinlets
2	BL12-25 (139°14.09'N, 64°53.76'W)	Quartet Group: interbedded maroon mud-stone and fine grained calcareous sandstone
3	BL25-5 (139°08.87'N, 64°53.42'W)	Gillespie Lakes Group: tan weathering pale grey 'crackled' dolostone; iron carbonate cemented
BM1	BL33-3 (139°10.28'N, 64°54.41'W)	Monolithic "crackle breccia": pink dolostone; foliation defined by plates of chalcopyrite (1-2%); white carbonate cement; trace pyrite
BM1	BL40-11 (139°10.47'N, 64°54.14'W)	Monolithic breccia: pink to maroon dolostone fragments; carbonate matrix with accessory quartz; abundant sericite
BM1	BL40-27 (139°10.77'N, 64°54.18'W)	Monolithic breccia: weakly silicified pink dolostone; open space filling textures

Table E.3 (continued)

Unit	Sample No. (Lat.N, Long.W)	Sample Description
BM1	BL54-1 (139^{o}36.10'N, 64^{o}50.23'W)	Monolithic breccia: pale siliceous dolostone fragments; carbonate matrix with minor chlorite
BHcb	BL3-4 (139^{o}08.55'N, 64^{o}53.12'W)	Heterolithic breccia: white carbonate matrix; clasts are pink dolostone, grey and maroon mudstone and pale green quarzite; trace chalcopyrite
BHcb	BL10-7 (139^{o}16.04'N, 64^{o}51.60'W)	Heterolithic breccia: angular fragments of green and brown mudstone, grey sandstone, black argillite, pink dolostone, white quartzite and hematite stained intrusive; carbonate matrix with minor quartz; trace specularite and pyrite
BHcb	BL39-4 (139^{o}10.03'N, 64^{o}54.03'W)	Heterolithic breccia: angular pink and maroon mudstone, pink dolostone and red jaspillite fragments; fragment supported; minor white calcite matrix
BHcb	BL40-29 (139^{o}10.91'N, 64^{o}54.33'W)	Heterolithic breccia: silicified; pink dolostone and black argillite clasts; open space filling textures
BHcb	BL45-5 (139^{o}23.25'N, 64^{o}44.75'W)	Heterolithic breccia: pink dolostone and black argillite clasts; dark grey muddy matrix; trace specularite
BHcb	BL49-4 (139^{o}16.45'N, 64^{o}45.68'W)	Heterolithic breccia: pink dolostone and green mudstone clasts in a carbonate-rich matrix; trace chlorite and iron carbonate
BHh	BL48-3 (139^{o}18.97'N, 64^{o}44.37'W)	Heterolithic breccia: hematite matrix; subangular fragments of pink dolostone, grey dolostone, jasper and black argillite
BHcl	BL32-5 (139^{o}10.88'N, 64^{o}53.24'W)	Heterolithic breccia: chlorite with lessor hematite matrix; pink silty dolostone and mafic intrusive fragments

Table E.3 (continued)

Unit	Sample No. (Lat.N, Long.W)	Sample Description
BHcl	BL46-10 (139°21.12'N, 64°44.89'W)	Heterolithic breccia: chlorite-rich matrix; pink dolostone, green mudstone, jasper and minor black argillite fragments; trace specularite

Table E.4A Major and minor element oxides plus barium for seven selected Proterozoic rock specimens from sample suite 2 from the Coal Creek Inlier, southern Ogilvie Mountains, west-central Yukon Territory. Sample locations are on Map 2 (in pocket). Analyses, by whole rock ICP techniques, were by ACME Analytical Laboratories, Vancouver.

Sample No.		BL3-7	BL4-7	BL53-4	BL1-1	BL12-25	BL25-5	BL48-3
SiO_2	(wt%)	33.11	45.42	57.61	52.03	48.68	8.26	51.86
TiO_2	(wt%)	0.24	0.42	0.03	1.15	0.41	0.03	0.51
Al_2O_3	(wt%)	5.22	8.15	0.54	14.12	10.20	0.96	11.51
Cr_2O_3	(wt%)	0.01	0.01	0.01	0.01	0.01	0.01	0.01
Fe_2O_3T	(wt%)	2.62	7.32	29.24	9.84	8.91	2.32	10.73
MnO	(wt%)	0.29	0.26	0.15	0.26	0.43	0.55	0.17
MgO	(wt%)	10.96	8.49	2.30	4.71	5.30	18.82	5.73
CaO	(wt%)	16.75	9.91	4.00	6.68	7.84	6.07	4.75
Na_2O	(wt%)	0.05	0.05	0.05	2.25	0.05	0.05	3.10
K_2O	(wt%)	3.40	2.40	0.10	2.05	4.80	0.45	1.55
P_2O_5	(wt%)	0.18	0.16	0.07	0.11	0.16	0.04	0.15
Ba	(ppm)	392	251	23	666	1159	146	151
LOi	(wt%)	27.1	17.3	5.9	6.3	13.0	42.5	9.8
Total	(wt%)	100.01	99.94	100.00	99.64	100.01	100.09	99.90

Table E.4B Oxides, trace and rare earth elements for sample suite 2 from Proterozoic rocks, Coal Creek Inlier, southern Ogilvie Mountains, west-central Yukon Territory. Sample locations are on Map 2 (in pocket). All analyses, by ICP techniques, were by ACME Analytical Laboratories, Vancouver.

Element	Sample number							
	BL3-7	BL4-7	BL11-10	BL53-4	BL1-1	BL12-25	BL25-5	BL33-3
Mo (ppm)	1	2	1	31	1	2	1	2
Cu (ppm)	2	6	3508	37	81	1	14	9162
Pb (ppm)	2	2	34	5	69	4	2	2
Zn (ppm)	6	20	23	2	393	3	8	16
Ag (ppm)	0.3	0.3	0.5	0.1	0.4	0.3	0.1	0.7
Ni (ppm)	3	23	5	12	30	3	1	2
Co (ppm)	3	22	2	5	27	4	3	3
Mn (ppm)	2092	1829	1270	1128	1465	3174	3774	4808
Fe (wt%)	1.46	3.94	1.14	14.24	4.64	4.70	1.36	3.22
As (ppm)	3	4	9	3	12	5	3	2
U (ppm)	6	5	5	5	5	5	5	5
Th (ppm)	6	5	1	2	5	13	1	9
Sr (ppm)	26	16	3	5	50	30	45	18
Cd (ppm)	1	1	1	1	1	1	1	1
Sb (ppm)	2	2	2	3	4	5	5	2
Bi (ppm)	2	3	3	2	2	2	4	2
V (ppm)	4	41	3	22	194	18	3	7
Ca (wt%)	13.52	7.42	2.01	2.82	3.74	6.14	19.02	9.28
P (wt%)	.06	.05	.01	.02	.04	.06	.019	.05
La (ppm)	25	8	2	2	9	51	4	259
Cr (ppm)	7	15	5	3	63	15	3	5
Mg (wt%)	6.23	4.41	0.91	1.23	2.14	2.53	9.33	3.15
Ba (ppm)	56	54	17	6	263	476	51	103
Ti (wt%)	.01	.01	.01	.01	.15	.04	.01	.01
B (ppm)	2	2	2	2	6	7	11	2
Al (wt%)	0.16	1.41	0.04	0.14	1.96	0.54	0.08	0.22
Na (wt%)	0.05	0.05	0.01	0.02	0.14	0.04	0.03	0.05
K (wt%)	0.09	0.15	0.01	0.01	0.29	0.37	0.02	0.19
W (ppm)	1	1	1	2	1	2	1	1
Au (ppb)	7	2	4	3	2	2	2	3
Rare earth elements								
Be (ppm)	10	10	10	10	10	10	10	10
Rb (ppm)	88	96	4	2	77	173	11	115
Y (ppm)	20	37	2	6	19	21	18	38
Zr (ppm)	91	116	3	13	79	127	31	73
Nb (ppm)	12	8	5	7	10	5	5	6
Sn (ppm)	4	2	3	1	3	6	1	5
Cs (ppm)	2	2	2	2	4	6	2	2
La (ppm)	33	31	1	3	15	61	8	348
Ce (ppm)	59	55	3	5	29	86	20	497
Pr (ppm)	4	5	1	1	2	5	1	32
Nd (ppm)	32	35	1	4	10	29	11	209
Sm (ppm)	41	24	1	1	9	23	1	233
Eu (ppm)	1	1	1	1	1	1	1	6
Gd (ppm)	3	4	1	1	2	3	2	15
Tb (ppm)	1	1	1	1	1	1	1	1
Dy (ppm)	3	5	1	1	3	2	2	5
Ho (ppm)	1	1	1	1	1	1	1	1
Er (ppm)	2	3	1	1	2	2	1	2
Tm (ppm)	1	1	1	1	1	1	1	1
Yb (ppm)	3	3	1	1	3	2	1	1
Lu (ppm)	1	1	1	1	1	1	1	1
Hf (ppm)	2	2	1	1	3	4	1	1
Ta (ppm)	1	1	1	1	1	1	1	1
W (ppm)	2	3	2	2	2	2	2	2
Th (ppm)	7	8	1	1	4	13	2	13
U (ppm)	2	3	1	2	1	6	1	3

Table E.4B (continued)

Element	BL40-11	BL40-27	BL54-1	BL3-4	BL10-7	BL39-4	BL40-29	BL45-5
Mo (ppm)	2	1	1	1	1	2	1	1
Cu (ppm)	50	14	1	637	13	80	120	2
Pb (ppm)	2	2	2	2	5	4	2	3
Zn (ppm)	9	3	5	16	11	33	13	11
Ag (ppm)	0.2	0.1	0.2	0.2	0.1	0.2	0.1	0.2
Ni (ppm)	2	2	18	21	2	10	7	16
Co (ppm)	2	2	3	8	6	6	6	5
Mn (ppm)	2623	2221	1081	1487	3522	3454	2723	723
Fe (wt%)	1.65	1.59	2.46	3.27	1.45	4.90	1.98	2.40
As (ppm)	3	2	2	5	5	8	2	5
U (ppm)	7	5	5	6	5	5	5	5
Th (ppm)	7	1	13	8	1	3	1	10
Sr (ppm)	28	8	9	35	11	35	11	22
Cd (ppm)	1	1	1	1	1	1	1	1
Sb (ppm)	2	2	2	2	2	2	2	2
Bi (ppm)	2	2	2	2	3	2	2	2
V (ppm)	19	5	18	21	5	23	7	14
Ca (wt%)	1.41	5.96	4.50	4.47	7.72	11.40	1 7.67	5.88
P (wt%)	.04	.06	.06	.06	.02	.03	.01	.07
La (ppm)	24	3	26	6	2	9	3	14
Cr (ppm)	23	3	12	14	4	9	4	10
Mg (wt%)	5.47	2.29	3.05	3.18	3.52	5.44	3.50	3.37
Ba (ppm)	19	77	361	395	24	1189	9	52
Ti (wt%)	.01	.01	.01	.01	.01	.02	.01	.01
B (ppm)	2	2	2	2	2	2	2	2
Al (wt%)	0.40	0.03	1.16	1.32	0.04	0.39	0.30	0.77
Na (wt%)	0.07	0.04	0.03	0.04	0.04	0.05	0.05	0.04
K (wt%)	0.04	0.02	0.20	0.21	0.01	0.10	0.01	0.12
W (ppm)	1	1	1	1	1	2	1	2
Au (ppb)	1	6	1	1	4	4	2	1
Rare earth element package								
Be (ppm)	10	10	10	10	10	10	10	10
Rb (ppm)	16	11	194	113	3	46	10	99
Y (ppm)	24	4	16	15	4	20	6	17
Zr (ppm)	75	20	166	120	10	55	10	195
Nb (ppm)	11	9	15	9	2	8	7	8
Sn (ppm)	5	1	5	6	1	5	1	2
Cs (ppm)	2	2	2	2	2	2	2	2
La (ppm)	34	4	80	25	3	25	7	31
Ce (ppm)	57	9	168	46	6	47	13	51
Pr (ppm)	5	1	13	3	1	4	1	4
Nd (ppm)	30	6	95	19	3	24	5	28
Sm (ppm)	29	1	133	15	9	35	1	33
Eu (ppm)	1	1	1	1	1	1	1	1
Gd (ppm)	3	1	5	2	1	2	1	2
Tb (ppm)	1	1	1	1	1	1	1	1
Dy (ppm)	4	1	2	2	1	2	1	2
Ho (ppm)	1	1	1	1	1	1	1	1
Er (ppm)	1	1	3	2	1	1	1	2
Tm (ppm)	1	1	1	1	1	1	1	1
Yb (ppm)	2	1	2	1	1	1	1	3
Lu (ppm)	1	1	1	1	1	1	1	1
Hf (ppm)	1	1	4	4	1	1	1	4
Ta (ppm)	1	1	1	1	1	1	1	1
W (ppm	2	2	2	2	2	2	2	2
Th (ppm)	4	1	15	11	1	4	1	9
U (ppm)	2	2	2	1	1	2	1	3

Table E.4B (continued)

Element		Sample number		
	BL49-4	BL48-3	BL32-5	BL46-10
Mo (ppm)	1	1	1	1
Cu (ppm)	3	11	57	3
Pb (ppm)	2	2	2	2
Zn (ppm)	10	27	24	25
Ag (ppm)	0.1	0.3	0.1	0.2
Ni (ppm)	6	18	46	25
Co (ppm)	2	6	10	11
Mn (ppm)	2049	1282	183	401
Fe (wt%)	2.15	4.94	5.17	4.00
As (ppm)	2	9	2	5
U (ppm)	5	5	5	5
Th (ppm)	6	14	8	13
Sr (ppm)	10	19	2	11
Cd (ppm)	1	1	1	1
Sb (ppm)	2	2	2	2
Bi (ppm)	2	2	2	2
V (ppm)	12	28	70	37
Ca (wt%)	4.98	3.70	.41	1.61
P (wt%)	.04	.05	.06	.08
La (ppm)	12	38	3	44
Cr (ppm)	8	26	38	27
Mg (wt%)	3.12	3.30	3.00	4.84
Ba (ppm)	11	72	71	277
Ti (wt%)	.01	.02	.02	.02
B (ppm)	2	2	2	2
Al (ppm)	1.00	1.36	2.31	2.53
Na (wt%)	0.03	0.05	0.02	0.01
K (wt%)	0.12	0.08	0.13	0.19
W (ppm)	2	2	1	1
Au (ppb)	4	1	1	1
Rare earth element package				
Be (ppm)	10	10	10	10
Rb (ppm)	84	35	59	69
Y (ppm)	8	23	6	26
Zr (ppm)	229	142	276	177
Nb (ppm)	8	12	13	13
Sn (ppm)	3	7	6	2
Cs (ppm)	2	2	3	2
La (ppm)	13	41	5	54
Ce (ppm)	29	75	8	91
Pr (ppm)	2	6	1	8
Nd (ppm)	17	39	2	41
Sm (ppm)	1	22	5	37
Eu (ppm)	1	1	1	1
Gd (ppm)	1	4	1	3
Tb (ppm)	1	1	1	1
Dy (ppm)	1	4	1	2
Ho (ppm)	1	1	1	1
Er (ppm)	1	2	1	2
Tm (ppm)	1	1	1	1
Yb (ppm)	1	3	1	2
Lu (ppm)	1	1	1	1
Hf (ppm)	4	3	7	4
Ta (ppm)	1	1	1	1
W (ppm)	2	2	2	2
Th (ppm)	6	13	13	11
U (ppm)	2	3	3	3

Table E.5 Brief hand sample descriptions for Sample Suite 3 from the Coal Creek Inlier, southern Ogilvie Mountains, west-central Yukon Territory. This suite of 22 samples (including duplicates) was evaluated for rare earth elements by instrumental neutron activation analysis (INAA) Sample locations are shown on Map 2 (in pocket). Results are tabulated in Table E.6.

Unit	Sample No.[1] (Lat.N, Long.W)	Sample Description
1	BL33-1 (139°10.47'W, 64°54.14'N)	Banded iron formation: thinly bedded to laminated jasper with minor layers of crystalline carbonate and traces of malachite
2	BL1-1 (139°08.24'W, 64°53.09'N)	Quartet Group: interbedded grey fine grained sandstone and black argillite
6	BL27-6 (139°08.55'W, 64°54.74'N)	Multilithic conglomerate: clasts of quartzite, dolomite, pink silty dolostone, green mudstone, jasper and specularite; carbonate matrix
BM1	BL26-2 (139°07.04'W, 64°54.19'N)	Monolithic breccia: pink silty dolostone with rare green argillite clasts: matrix is carbonate
BM1	BL33-3 (139°10.28'W, 64°54.41'N)	Monolithic breccia: foliated, pink silty dolomite clasts: 1% chalcopyrite
BM1	BL54-1 (139°36.10'W, 64°50.23'N)	Monolithic breccia: chlorite- and carbonate-rich fragmental: pale siliceous dolostone fragments
BM1	TW208A(P) (139°09.12'W, 64°53.68'N)	Breccia matrix: chlorite-rich separate of matrix from monolithic breccia; pink silicified dolostone clasts
BM4	BL50-6(P) (139°12.98'W, 64°46.02'N)	Monolithic breccia: dark grey angular laminated mudstone fragments; clast supported; minor carbonate matrix
BHcb	BL18-10(P) (139°23.13'W, 64°52.46'N)	Breccia matrix: red, coarse grained carbonate from heterolithic breccia
BHcb	BL35-4 (139°09.09'W, 64°53.71'N)	Layered heterolithic breccia: clasts are silicified pink silty dolostone, purple mudstone,quartzite and mafic intrusive; matrix is carbonate-rich with lesser chlorite and hematite

Table E.5 (continued)

Unit	Sample No.[1] (Lat.N, Long.W)	Sample Description
BHcb	BL87-70 (139°16.54'W, 64°50.99'N)	Heterolithic breccia: clasts are black argillite and gray sandstone of the Quartet Group, and pink silty dolostone, pale pink-orange-white silica and green argillite; matrix is dominantly buff, medium grained crystalline carbonate
BHh	BL24-12 (139°12.89'W, 64°53.56'N)	Massive, layered, heterolithic hematite breccia: clasts are mainly pink dolostone
BHh	BL34-15 (139°17.11'W, 64°51.26'N)	Hematite-quartz breccia: traces of chalcopyrite
BHh	BL43-7(P) (139°25.25'W, 64°44.14'N)	Layered, heterolithic breccia: clasts of pink silty dolostone, hematized gritty sediments, black to gray argillite and massive hematite; matrix is composed dominantly of carbonate and hematite with minor chlorite
BHcl	BL46-10 (139°21.12'W, 64°44.89'N)	Heterolithic breccia: rounded clasts of pink silty dolostone, light green argillite and uncommon jasper; matrix is chlorite-rich with abundant accessory carbonate and minor hematite
BHcl	BL50-2 (139°14.40'W, 64°45.78'N)	Heterolithic breccia: fragments, generally smaller than 1 cm, are black to marroon argillite, and spotted pink dolostone; wavy laminated chlorite- and hematite-rich matrix; minor carbonate
CARB	MS-1I (139°18.90'W, 64°51.81'N)	White, massive coarse grained intrusive carbonate (vein) material
P-1 (STANDARD)		Coast Mountains granodiorite

1. Codes at end of sample are: (D) = duplicate sample; (P) = pulverized sample (whole rock (XRF) by Geological Survey of Canada). P-1 (STANDARD) = standard sample provided by Dick Armstrong, Geochronology Laboratory, The University of British Columbia.

Table E.6 Rare earth element (REE) and trace element data for 22 samples (including duplicates) from the Coal Creek Inlier, Ogilvie Mountains, west-central Yukon Territory (refer to Table E.5). All values are in parts per million (ppm). Analyses were by instrumental neutron activation analysis (INAA), except where noted, and detection limits and precision of data is presented Tables E.9 and E.10. The data is normalized to chondrite and upper crust (shale) in Table 4.1.

	SAMPLE NUMBER																					
ELEMENT[1]	BL33-1	BL1-1	BL27-6	BL26-2 I	BL26-2 II	BL33-3	BL54-1	TW-208A	BL50-6	BL18-10	BL35-4 I	BL35-4 II	BL87-70	BL24-12	BL34-15 I	BL34-15 II	BL43-7	BL46-10 I	BL46-10 II	BL50-2	MS-1A	P-1
Rare earth elements[2]																						
La	3.2	56.7	60.3	21.3	34.4	102	17.5	10.5	51.3	4.3	373	376	19.4	91.9	11.7	13.6	66.2	34.6	29.8	51.7	120.0	12.5
Ce	7	106	106	40	35	168	35	22	99	11	211	224	38	106	36	40	136	63	54	94	203	24
Pr	(50	(50	(50	(50	(50	(50	(50	(50	(50	(50	(50	(50	(50	(50	(50	(50	(50	(50	(50	(50	(50	(50
Nd	(10	44	45	20	18	63	18	(10	42	(10	131	129	22	26	21	26	50	28	25	41	92	14
Sm	1.5	7.8	7.2	3.1	4.5	10.6	2.6	1.6	6.6	2.5	20.8	20.7	4.1	3.1	9.2	11.1	7.9	4.6	3.8	6.3	20.7	2.8
Eu	(1	1	2	(1	(1	2	(1	(1	1	(1	6	6	1	4	4	6	3	(1	(1	2	3	(1
Gd	(200	(200	(200	(200	(200	(200	(230	(200	(210	(200	(200	(200	(200	(200	(1300	(2200	(200	(200	(200	(200	(200	(200
Tb	(1	(1	(1	(1	(1	1	(1	(1	(1	(1	2	2	(1	(1	6	7	(1	(1	(1	(1	3	(1
Dy	1	5	4	2	3	6	2	1	5	2	8	7	5	(1	32	37	4	3	2	4	17	3
Ho	(1	(1	(1	(1	(1	(1	(1	(1	(1	(1	(1	(1	(1	(1	6	7	(1	(1	(1	(1	(1	(1
Er	(100	(100	(100	(100	(100	(120	(100	(100	(100	(230	(100	(100	(100	(100	(100	(100	(100	(100	(100	(100	(100	100
Tm	(0.5	(0.5	(0.5	(0.5	(0.5	(0.5	(0.5	(0.5	(0.5	(0.5	(0.5	(0.5	(0.5	(0.5	1.1	1.0	(0.5	(0.5	(0.5	(0.5	(0.5	(0.5
Yb	(0.5	2.4	1.5	1.4	1.5	1.8	1.3	1.1	2.5	1.3	3.3	3.8	1.9	(0.5	6.5	7.9	1.9	1.6	1.4	2.1	2.4	1.9
Lu	(0.1	0.4	0.2	0.2	0.2	0.3	0.2	0.2	0.4	0.2	0.4	0.4	0.3	(0.1	0.6	0.7	0.2	0.2	0.2	0.2	0.2	0.3
TOTAL	12.7	223.3	226.2	88.0	140.5	354.7	76.8	36.4	207.8	21.3	755.5	768.9	91.7	231.0	134.1	157.3	289.2	135.0	116.2	201.3	463.3	58.5
La/Lu	)32	142	302	107	172	340	87.5	52.5	128	21.5	933	940	65	)920	19.5	19.4	431	173	149	258	600	42
La/Sm	2.1	7.3	8.4	6.9	7.6	9.6	6.3	6.6	7.8	1.7	18	18	4.7	30	1.3	1.2	11	7.5	7.8	8.2	5.8	4.5
Tb/Lu	nd	(2.5	(5.0	(5.0	(5.0	3.3	(5.0	(5.0	(2.5	(5.0	5.0	5.0	(3.3	nd	10	10	(5.0	(5.0	(5.0	(5.0	15	(3.3
Eu/Sm	(0.67	0.13	10	(0.32	(0.22	0.19	(0.36	(0.6	0.15	(0.4	15	15	0.2	1.3	0.43	0.54	15	(0.22	(0.26	0.32	0.14	(0.36
Trace elements[2]																						
Sc	1.17	13.10	13.10	5.21	6.31	7.35	14.50	16.10	15.6	14.40	21.00	20.70	11.0	1.79	0.91	1.11	9.37	10.50	10.70	11.30	0.63	10.70
Th	0.8	21.4	11.3	8.5	12.2	13.2	16.3	13.4	19.2	(0.5	8.1	7.9	8.7	1.8	(0.5	(0.5	12.5	12.4	15.0	16.1	(0.5	3.6
U	(1	4	5	3	4	3	5	2	4	2	2	2	2	3	45	60	3	3	4	3	(1	1
Co[3]	9	8	21	2	2	2	3	21	9	10	12	8	17	3	4	5	10	9	11	4	(1	5
Cu[3]	575	24	141	3	5	5910	2	19	18	14	333	344	11	494	115	172	17	4	2	3	485	87
Ba[4]	(20	460	8500	320	640	390	700	440	500	(20	910	940	350	(20	(20	(20	2100	750	360	640	30	880

1: I = first sample of a duplicate pair; II = second sample of a duplicate pair.
2: (denotes less than quoted detection limit (see also Appendix E.2).
3: Atomic absorption was used for Co and Cu analyses.
4: X-ray fluorescence was used for Ba analysis.

Table E.7 Relative precision for Suite 1 ICP data (Table E.2) based on one replicate analysis of sample BL3-5.

Element	Conc. (ppm)	Std. dev. (1 sigma)	Prec. (%)
<u>ICP analyses-set 1</u>			
Nb	4	0	0
Ba	417	3	7.2
La	34	0	0
Ce	67	1.0	1.5
Th	9.5	0.1	1.0
<u>ICP analyses-set 2</u>			
Be	1.1	0.1	9.0
Co	11	1	9.0
Cr	39	4	10
Cu	13	3	23
La	30	2	6.7
Ni	27	3	11
V	49	0	0
Yb	1.8	0.1	5.6
Zn	52	16	31

Table E.8 Lower detection limits for REE instrumental neutron activation analyses.

Element		Lower detection limit[1]
La	Lanthanum	0.5
Ce	Cerium	5
Pr	Praseodymium	50
Nd	Neodymium	10
Sm	Samarium	0.1
Eu	Europium	1
Gd	Gadolinium	200
Tb	Terbium	1
Dy	Dysprosium	1
Ho	Holmium	1
Er	Erbium	100
Tm	Thulium	0.5
Yb	Ytterbium	0.5
Lu	Lutetium	0.1
Sc	Scandium	0.05
Th	Thorium	0.5
U	Uranium	1

1 All values are in ppm

Table E.9 Relative precision of REE data from INAA (Table E.6) based on replicate analyses of four samples.

	La			Ce			Nd		
	Conc.[1]	std. dev.[2]	Prec.[3]	Conc.	std. dev.	Prec.	Conc.	std. dev.	Prec.
BL26-2	27.3	6.1	22	37	3	8.1	19	1	5.2
BL35-4	374	2	0.5	217	6	2.8	130	1	0.1
BL34-15	12.6	0.9	7.1	38	2	5.3	23	3	13
BL46-10	32.2	2.4	7.4	58	5	8.6	26	2	7.7
Relative Precision			9.3			6.2			6.5

	Sm			Eu			Tb		
	Conc.	std. dev.	Prec.	Conc.	std. dev.	Prec.	Conc.	std. dev.	Prec.
BL26-2	3.8	0.7	18	N/D			N/D		
BL35-4	20.7	0.1	0.1	6	0	0	2	0	0
BL34-15	10.1	0.9	8.9	5	1	20	6	1	17
BL46-10	4.2	0.4	9.5	N/D			N/D		
Relative Precision			9.1			10			8

	Dy			Ho			Tm		
	Conc.	std. dev.	Prec.	Conc.	std. dev.	Prec.	Conc.	std. dev.	Prec.
BL26-2	2	1	50	N/D			N/D		
BL35-4	7	1	14	N/D			N/D		
BL34-15	34	3	8.8	6	1	17	1.0	0.1	10
BL46-10	2	1	50	N/D			N/D		
Relative Precision			31			17			10

	Yb			Lu			Sc		
	Conc.	std. dev.	Prec.	Conc.	std. dev.	Prec.	Conc.	std. dev.	Prec.
BL26-2	1.4	0.1	7.1	0.2	0	0	5.76	0.55	9.5
BL35-4	3.5	0.3	8.6	0.4	0	0	20.85	0.15	0.1
BL34-15	7.2	0.7	9.7	0.6	0.1	17	1.01	0.10	10
BL46-10	1.5	0.1	6.7	0.2	0	0	10.60	0.10	0.1
Relative Precision			8.0			4.3			4.9

	Th			U		
	Conc.	std. dev.	Prec.	Conc.	std. dev.	Prec.
BL26-2	10.4	1.9	18	3	1	33
BL35-4	8.0	0.1	1.3	2	0	0
BL34-15	N/D			52	8	15
BL46-10	13.7	1.3	9.5	3	1	33
Relative Precision			9.6			20

1 Concentration (ppm) is the average of two analyses; N/D = below detection limit.
2 Standard deviation (ppm) are 1 sigma.
3 Precision is in %

Table E.10 Accuracy of REE data (INAA) based on a comparison with the geochemical standard P-1.

	P-1 (this study) single analysis	P-1 (Erdman, 1985) mean	1 sigma
La	12.5	10.5	0.28
Ce	24	-	
Nd	14	-	
Sm	2.8	2.7	0.15
Eu	-	0.6	0.06
Dy	3	-	
Yb	1.9	1.9	0.12
Lu	0.3	0.3	0.0
Sc	10.7	8.7	0.41
Th	3.6	3.7	0.18

APPENDIX F

THE DEVELOPMENT OF RARE EARTH ELEMENT CHEMISTRY AND ITS GEOLOGICAL APPLICATIONS

Natural fractionation, the concentration or depletion of rare earth elements (REE) in a rock relative to primordial material (chondritic meteorites), was discovered in 1935. Since that time REE geochemical studies have focussed on the idea that this fractionation reflects the history of the rocks in which they are found. Rare earth elements can be used as geochemical indicators of the petrogenesis of the rock and can illucidate some processes of formation (Graf, 1984).

Several geologic processes yield minerals rich in rare earths. For instance:

(1) Magma generated in CO_2 rich regions deep within the upper mantle can form carbonatites (igneous carbonate rocks). Rare earth elements readily form strong carbonate complexes in such magmas (Muecke and Moller, 1988) and may be concentrated enough to form economic REE mineral deposits of which the Mountain Pass carbonatite (Olson *et al.*, 1954) is a well known example.

(2) Granitic magmas derived from crustal material are enriched in REEs relative to their parental rock. Heavy REEs are preferentially incorporated into early forming

crystals while the liquid residue and later phases (e.g. pegmatites) are enriched in light REEs (Graf, 1977).

(3) Rare earths can also be concentrated in hydrothermal solutions. In contrast to magmatic mineral formation heavy REEs rather than light ones are preferentially concentrated in the liquid residue during crystallization (Muecke and Moller, 1988).

Apart from being enriched in heavy and/or light REEs, the processes mentioned above also result in characteristic REE patterns that can be diagnostic of the processes that formed them.

The only naturally occurring nontripositive REEs are Ce^{4+} (Piper, 1974) and Eu^{2+} (Nagasawa and Schnetzler, 1971). Because of it's divalent state, and hence greater size in comparison to trivalent REEs, europium readily substitutes for Ba^{2+} in barite and Sr^{2+} in typical calcic plagioclase and K-feldspar (Taylor and McLennan, 1985). In certain rocks this factor may produce relative europium enrichment (positive Eu anomaly) or europium depletion (negative Eu anomaly) with respect to the other REEs. Virtually all post-Archean clastic sedimentary rocks are characterized by a negative Eu anomaly of similar magnitude and no common sedimentary rock is characterized by Eu enrichment (Taylor and McLennan, 1985).

Cerium is strongly depleted in sea water because the stable Ce ion is Ce^{4+}. Chemical precipitates (sediments) that form on the ocean floor have a significant component of sea water and this is reflected in the REE pattern that show a relative depletion of Ce. Hydrothermal solutions expressed from the ocean bottom to mix with sea water prior to precipitation may also, depending on the degree of mixing, reflect the sea water component in the REE pattern. In marine carbonates, a distinct Ce depletion is common, also reflecting the Ce depletion in sea water relative to other REEs. Clastic sedimentary rocks do not share this characteristic.

Not long after natural partitioning of REEs was discovered, Goldschmidt (1954) proposed that the homogenizing effects of sedimentary processes should result in nearly constant REE distributions in sedimentary rocks. Although there are some sedimentary environments that produce rocks with a significant variability in REE distribution, REE patterns for average sediments are remarkably similar. Haskin et al. (1968) suggested that a composite of North American shales (NASC) was representative of the upper continental crust. Other such composites of European Paleozoic shales (ES; Minami, 1935; in Taylor and McLennan, 1985) and post-Archean shales from Australia (PAAS; Nance and Taylor, 1976) are remarkably similar to NASC and reflect the average REE composition of the exposed crust. The REE concentrations in quartz-rich sedimentary rocks are typically very low, because the mineral quartz harbors low amounts of REEs, but the REE pattern parallels that of typical shale.

Chondritic meteorites have total REE concentrations that are low (several ppm) and are generally thought to be undifferentiated (or weakly differentiated). Carbonatites, at the opposite end of the spectrum, have total REE concentrations that range up to several percent and are strongly differentiated.

APPENDIX G

A REVIEW OF WORLD WIDE PROTEROZOIC BRECCIAS FROM THE LITERATURE

G.1 Wernecke-type Breccia

Many details of breccias in the Wernecke Mountains (Bell, 1986; Laznicka and Gaboury, 1986; Laznicka and Edwards, 1979) are similar to **OMB**. They are described below.

An intrusive origin for the genesis of the breccias is widely held (Bell, 1986; 1982; 1978; Bell and Delaney, 1977; Delaney, 1985; 1981; Archer and Schmidt, 1978; Archer et al., 1977; and Morin, 1976), although details in their explanations differ. Some explanations have evolved over time (see for example, Bell, 1978 vs. Bell, 1986).

Breccia occurrences in the Wernecke Mountains have undergone repeated brecciation, metasomatism and faulting (Laznicka and Gaboury, 1988; Laznicka and Edwards, 1979; Laznicka, 1977). In particular the exotic-looking fragments are altered equivalents of locally derived wallrock. Two mechanisms of formation have been suggested: (1) detachment faulting, triggered by basement extension (cf. documentation in the Ogilvie Mountains by Thompson, 1986), or (2) large, underlying and unexposed intrusion (Archer *et al.*, 1977) supported by a generally high Cu and Mo geochemical response over breccias (Archer and Schmidt, 1978).

G.1.1 Steam brecciation from dykes

Laznicka and Edwards (1979) suggested that dykes played an active role in the formation of the breccias. They invoked a mechanism based upon invasion of wet, fractured zones by magma which reacted with water present in rock formations to produce flashes of steam that violently bolted toward the surface. These blasts of steam brecciated wall rock, transported fragmented material. It also resulted in metasomatism and hydrothermal alteration of all rocks in contact with the fluids.

G.1.2 Intrusive pebble-dyke or diatreme from deep-seated igneous activity

Bell (1978), Bell and Delaney (1977) and Archer *et al.* (1977) suggested that the crosscutting breccias are diatremes. They noted similarities between the cross-cutting breccias (psuedoconglomerates of Laznicka and Edwards, 1979) and pebble dykes associated porphyry copper deposits (Bryant, 1968; Bryner, 1961). Normal faulting was followed by hydraulic fracturing or stoping, resulting from ascending fluids (produced from an upper mantle source); co-intrusion of gabbroic material followed earlier developed avenues (Bell, 1978). The variety of plastic, semi-plastic and brittle features observed in the breccias (Laznicka and Edwards, 1979) may have been produced by softening and disintegration of country rocks by fluids and upward thrusting of the breccias. [Conversely these features may have been formed by the piercement of unlithified sediments.] These ascending hydrothermal fluids could also create the type of alteration (i.e. albitization, hematitization, silicification and carbonatization) characteristic of the breccias and enclosing wall rock.

Archer and Schmidt (1978) interpreted the breccias to have formed by gas streaming in combination with crustal attenuation. They suggested that explosive gas release was generated by deep-seated igneous activity. As evidence, they cited igneous characteristics (i.e. enrichments in iron, copper and molybdenum, and contact alteration [including feldspathization]). This was particularly notable in the Bonnet Plume River District breccias that look similar to breccia pipes associated with porphyry copper deposits (Johnson and Lowell, 1961; Bryner, 1961).

Bell and Delaney (1977) and Archer et al. (1977) interpreted the crosscutting breccias of the Wernecke Mountains as diatremes with offshoots that formed breccia sills. Neither these, nor breccias investigated by Laznicka and Edwards (1979) display the criteria assigned to typical diatremes by Hearn (1968).

G.1.3 Diapirism of evaporitic material

Bell (1986) speculated that the Wernecke-type breccias were emplaced by progressive intrusion or diapirism of lower density (relatively buoyant) evaporitic material during deposition of Quartet Group and Gillespie Lake Group. In the Slats Creek area of the Wernecke Mountains these are laterally extensive and appear to follow fault splays of the Richardson Fault Array. Bell outlined individual breccia blocks in excess of 6 km across. These presumably are too large to be mobilized within a breccia pipe. In this model ascending evaporite diapirs were channeled by major structures to form laterally extensive bodies. The evaporites were subsequently dissolved and the cavity was infilled with wall rock. According to this model these breccias were derived from salt-rich layers within the Fairchild Lake Group that penetrated diapirically into overlying Quartet Group and lower Gillespie Lake Group stratigraphy.

G.2 East Arm of Great Slave Lake

Exotic breccias from the East Arm of Great Slave Lake (Reinhardt, 1972) occur in Archean crystalline basement and the overlying Proterozoic sedimentary rocks. Breccia fragments were derived from basement and overlying

Proterozoic sedimentary rocks. The matrix comprises mainly finely comminuted sedimentary rocks; significant amounts of felsite occur locally. Reinhardt (1972) invoked for brecciation magmatically derived gases, which suspended and transported solid particles, as well as local felsite magma. Regional faults and a nonconformity between Archean crystalline basement and the overlying sedimentary rocks influenced the distribution of the breccias. Hydraulic fracturing could have propagated brecciation laterally along the nonconformity. Gas streaming or fluidization (Reynolds, 1954) resulted in attrition and reduction in size of entrained fragments with upward transport. Surface venting resulted in decompression and collapse of vertical conduits, and possibly in choking of columns by fragmented rock. Addition of water to the permeable zone reduced intergranular pressure and produced a slurry that was squeezed upwards like toothpaste.

These breccias differ from **OMB** in containing granitic clasts derived from Archean crystalline basement. The bulk of the breccia, however, comprises shallow marine rocks.

G.3 Bathurst Inlet

Near Bathurst Inlet, N.W.T. Cecile and Campbell (1977) described dykes, 1-20 m wide, and pipes, 0.5 to 1 km across, of breccia composed of sedimentary clasts. The clay- and silt-sized matrix contains abundant millimetre-sized euhedral growth-zoned crystals of dolomite and quartz, and smaller tourmaline crystals. Breccias commonly display "flowage layering", interpreted to have formed by movement of masses of semi-plastic material. Cecile and Campbell (1977) proposed that pressurized fluids trapped in the sedimentary rocks intruded overlying strata, transporting fragments upward.

G.4 Adeladian Province

The *Adelaidean province in Australia has numerous deposits of Proterozoic breccia. They are of special interest to this study because:

(1) they occur in a craton margin,

(2) they cross-cut mid-Proterozoic sedimentary rocks and are approximately the same age as **OMB** and Wernecke-type breccia,

(3) breccia fragments dominantly comprise the oldest lowest sedimentary strata that is locally exposed,

(4) the matrix is of clay, silt and sand sized material that is carbonate-rich,

(5) breccia bodies are surrounded by sedimentary rocks that display hematitic alteration and local quartz-chlorite, quartz-sericite, and carbonate alteration,

(6) recent studies from underground exploration at the Olympic Dam deposit indicate that they are cylindrical, intrusive bodies, and

(7) the Olympic Dam Cu-Au-U-REE breccia deposit is the largest copper-gold deposit in the world.

G.4.1 Flinders Ranges

The Flinders Range breccias (Dalgarno and Johnson, 1965; Thomson, 1965; Lemon, 1985; Bell, 1987; Laznicka, 1988) are, in many respects, much like **OMB**. They comprise *heteroclastic breccias (fragments are carbonate, siltstone, sandstone, metabasalt and gabbro in a carbonate-rich siltstone matrix [Laznicka, 1988]). Evaporite diapirism is generally accepted as the genetic process responsible for breccias of the Flinders Ranges. Flowage of the source beds (a thick sequence of thin bedded sandstone, siltstone and carbonate) was facilitated by water saturation and by its confinement during sediment loading (Dalgarno and Johnson, 1965). Evidence to suggest that evaporite sequences were originally present includes: gypsum-anhydrite psuedomorphs, salt casts in "source beds", and a shallow-water carbonate depositional setting. Vertical faults, that penetrate down to evaporitic source beds are thought to have initiated diapirism (Lemon, 1985). Subvertical faults commonly cut other diapirs in the region (Thomson, 1965). Uplift and tilting of one fault block created instability in the source beds and caused flow of the evaporitic sequence upward and toward the fault (Lemon, 1985).

G.4.2 Olympic Dam

Olympic Dam differs from Wernecke-type breccias in several critical aspects: (i) breccias comprise common granitic, as well as sedimentary rock fragments, and (ii) prominant mineralization occurs throughout.

Breccia at Olympic Dam occurs as a hematitic breccia-dyke complex within a fractured, weakly to intensely hematized Archean granite (Oreskes et al., 1989). Breccias formed as a result of hydraulic fracturing, brecciation and fluidization (Oreskes and Einaudi, 1988). Previous interpretations described Olympic Dam breccias as alluvial deposits that formed along graben margins (Roberts and Hudson, 1983); they were subsequently altered and mineralized by hydrothermal fluids.

G.5 Mud Diapirs and Volcanoes

Mud volcanoes are the surface expression of a type of diapirism that is associated with high pressure release of gas- and/or water-charged mud or shale (Freeman, 1968). Modern examples of mud volcanoes are confined to regions underlain by unconsolidated sediment such as clay and shale. Abnormal pressures occur in these sediments due to loading by overlying sediments.

Alternatively (to the mud diapir theory), possible examples of modern sub-sea fluid (water and or gas) escape structures have been identified in regions dominated by mud volcanos where large quantities of buried methane are known to be present (Brown and Westbrook, 1988). The escape of methane gas entrains clay and connate brines in a slurry (Hedberg, 1974).

A mud (or shale) diapir is driven by density and pressure disequilibrium. Plastic deformation during ascent of gas- and water-charged mud incorporating blocks of more competant units (Barber _et al._, 1986) constitute the breccia. Seismic reflection profiles of mud volcanoes in modern slope basins clearly show diapirs crosscutting several kilometers of stratigraphic thickness (Biju-Duval _et al._, 1982). The lack of exotic fragments in the breccia reflects a thick sequence of lithologically repetitive strata. Except for their disrupted and discordant attitudes, a breccia of large blocks is indistinguishable from adjacent intact strata.

Mud diapirs form where underconsolidated muds are rapidly buried, such as along continental margins and in submarine deltas. When high rates of sedimentation are combined with low permeability, the expulsion of water cannot keep pace with increasing overburden pressure (Hedberg, 1974).

Other factors that could add significantly to high fluid pressures (Hedberg, 1974) include: (i) release of bound water during diagenesis, such as occurs in clay minerals during the conversion of montmorillonite to illite,

(ii) change of gypsum to anhydrite, and (iii) metamorphic water released during regional metamorphism.

Fault and fracture zones local to units with high fluid pressure would provide avenues of release that would guide the emplacement of the diapirs. Ascending muds would incorporate fragments due to abrasion and hydrofracturing of the wall rocks.

Methane and carbon dioxide generated within the sedimentary pile by breakdown of organic (algal) material could assist in the propulsion of the muds toward the surface. Methane is generated biochemically at near surface conditions and thermochemically at depths of several kilometers (Hedberg, 1974). Carbon dioxide can be produced by the aqueous dissolution, or decarbonation, of limestone; it can also be derived magmatically (Motyka et al., 1989).

The main source of fragments is brittle wall rocks in the region of diapir initiation, or along its path of ascent (Laznicka, 1988). Vertical faults are points of weakness where sediments with high fluid pressures can escape. Densely fractured zones generate fragments that are readily incorporated into the migrating mass.

G.5.1 Barbados

The Barbados Ridge Complex is a subduction complex developed by sediment accretion (Brown and Westbrook, 1988). Sedimentary fan turbidites, rapidly deposited on the subducting plate, created high pore fluid pressures in pelagic sequences immediately beneath the fan. The underconsolidated pelagic sediments are prone to mobility. The occurrence of abundant mud diapirs is confined to this area of turbidite deposition and their distribution is controlled by imbricate thrusts, reverse faults and folds. The mud diapirs form elongate ridges and isolated mounds. They cover over 700 square km of the surface area of the complex, a region in excess of 300 km long and about 200 km wide.

The highly pressurized pelagic sediments are able to retain fluids for a substantial period of time and diapiric material may take several million years to migrate to the surface (Brown and Weatbrook, 1988).

G.5.2 Timor

Timor, in eastern Indonesia, marks where the northern margin of the Austrailian continent is colliding with the Banda Arc (Barber et al., 1986). Continental margin sediments of the Australian continent are being added to an imbricate wedge. This wedge of sediment became a foreland fold and thrust belt northward. Clay-rich breccia deposits are situated along faults. They occur as mud diapirs associated with mud volcanoes.

The Timor breccias were developed from shales with abnormally high pore fluid pressures. The Permian-Triassic shales developed high pore pressures, in part, from overthrusting that followed the Pliocene collision of the northwest margin of Australia with the Banda Arc subduction system (Barber et al., 1986). Other factors (see above) could have added to the pore fluid pressure. Faults penetrated the stacked sequence and the subsequent release of pressure caused expulsion of fluids and the undercompacted fine grained sediment. Blocks of competant units, broken up along the fault, were included in the diapir as it ascended.